Individualised radiotherapy serving reduced toxicity in breast and prostate cancer

Ph.D. Thesis

Renáta Lilla Kószó, M.D.

Supervisor:

Zoltán Varga, Ph.D.

Doctoral School of Interdisciplinary Sciences

Department of Oncotherapy

Faculty of Medicine, University of Szeged, Hungary

Szeged

2018

List of full papers that served as the basis of the Ph.D. thesis

I. **Kószó R.**, Varga L., Fodor E., Kahán Z., Cserháti A., Hideghéty K., Együd Z., Szabó C., Borzási E., Szabó D., Müllner K., Varga Z., Maráz A.
Prone positioning on a belly board decreases rectal and bowel doses in pelvic intensity-modulated radiation therapy (IMRT) for prostate cancer
Pathol Oncol Res. 2018; doi: 10.1007/s12253-018-0436-2.
IF: 1.935

II. Kahán Z., Rárosi F., Gaál S., Cserháti A., Boda K., Darázs B., **Kószó R.**, Lakosi F., Gulyban Á., Coucke PA., Varga Z.
A simple clinical method for predicting the benefit of prone *vs.* supine positioning in reducing heart exposure during left breast radiotherapy
Radiother Oncol. 2018; 126: 487–492.
IF: 4.942

III. **Kószó R.**, Kahán Z., Darázs B., Rárosi F., Varga Z.
Dosimetric comparison of 3D-CRT, sliding window IMRT and VMAT techniques for external beam accelerated partial breast irradiation
Acta Oncologica - Under review

Related articles

I. Rusz O., **Kószó R.**, Dobi Á., Csenki M., Valicsek E., Nikolényi A., Uhercsák G., Cserháti A., Kahán Z.
Clinical benefit of fulvestrant monotherapy in the multimodal treatment of hormone receptor and HER2 positive advanced breast cancer: a case series
OncoTargets and Therapy, 2018; 11: 5459-5463
IF: 2.656

II. Varga L., **Kószó R.**, Fodor E., Cserháti A., Varga Z., Darázs B., Kahán Z., Hideghéty K., Borzási E., Szabó D., Müllner K., Maráz A.

Daily setup accuracy, side-effects and quality of life during and after prone positioned prostate radiotherapy

Anticancer Res. 2018; 38: 3699.

IF: 1.865

III. Maráz A., Cserháti A., Uhercsák G., Szilágyi É., Varga Z., Révész J., **Kószó R.**, Varga L., Kahán Z.

Dose escalation can maximize therapeutic potential of sunitinib in patients with metastatic renal cell carcinoma

BMC Cancer. 2018; 18: 296.

IF: 3.288

IV. **Kószó R.**, Sántha D., Büdi L., Erfán J., Győrfy K., Horváth Z., Kocsis J., Landherr L., Hitre E., Máhr K., Pajkos G., Pápai Z., Kahán Z.

Capecitabine in combination with docetaxel in first line in HER2-negative metastatic breast cancer: an observational study

Pathol Oncol Res. 2017; 23: 505–511.

IF: 1.935

V. Valicsek E., **Kószó R.**, Dobi Á., Uhercsák G., Varga Z., Vass A., Jebelovszky É., Kahán Z.

Cardiac surveillance findings during adjuvant and palliative trastuzumab therapy in patients with breast cancer

Anticancer Res. 2015; 35: 4967–4973.

IF: 1.895

VI. **Kószó R.**, Kahán Z.

Fulvesztrantterápia eredményezte hosszú progresszió mentes időszak kiterjedt, tünetet adó áttétes emlőrák esetén

LAM 2014; 24: 203–204.

Table of contents

List of abbreviations

3D-CRT	3-dimensional conformal radiation therapy
A_{heart}	area of the heart
AIO	All in One
ANOVA	analysis of variance
AP	antero-posterior
APBI	accelerated partial breast irradiation
BMI	body mass index
BT	brachytherapy
CBCT	cone beam computed tomography
CBR	clinical benefit rate
CN	conformation number
CT	computed tomography
CTV	clinical target volume
d	distance of the geometric centre of the PTV from the body surface
D	dose
DCIS	ductal carcinoma in situ
DIBH	deep inspiration breath hold
D_{med}	shortest distance between the anterior surface of the LAD and the chest wall
DVH	Dose-volume histogram
ECOG	European Cooperative Oncology Group
EIC	extensive intraductal component
ER	estrogen receptor
GTV	gross tumour volume
H	healthy tissue conformity index
HER2	human epidermal growth factor receptor type-2
HI	homogeneity index
IGRT	image-guided radiotherapy
IMRT	intensity-modulated radiotherapy
kV	kilovolt

LAD	left anterior descending coronary artery
LSD	least significant difference
M	merit function
MD	mean dose
MRI	magnetic resonance imaging
MV	megavolt
OAR	organ at risk
P	penalty function
PBI	partial breast irradiation
P_{med}	median plane of the full series of CT scans acquired in the supine position
PR	progesterone receptor
P_{ref}	reference plane
PSA	prostate specific antigen
PTV	planning target volume
PQI	plan quality index
PQID	difference of PQIs
RCA	right coronary artery
RT	radiotherapy
SD	standard deviation
SE	standard error
V95% (%)	percentage dose covering 95% of the PTV
V_{xGy} (%)	percentage structure volume receiving *x* Gray;
VMAT	volumetric-modulated arc radiotherapy

1 Introduction

Radiotherapy is an essential component of the management of prostate and breast cancer. Most patients become long survivors; however, irradiation may increase the risk of non-cancer-related morbidities.

Pelvic irradiation including the prostate, seminal vesicles, and lymphatic regions is an integral component of high-risk [1], organ-confined, and locally advanced prostate cancer management. The tolerance of normal tissues limits dose escalation and tumour control probability and increases the incidence of gastrointestinal morbidity. One of the most important factors related to the probability of the complications is the total dose of radiotherapy (RT) delivered to the pelvic organs. The irradiated rectal and bowel volume may be reduced by using intensity modulated (IM) and image-guided RT (IGRT) and optimal patient positioning.

Radiation-induced heart damage clearly depends on the dose exposed to its different structures [2,3]. With the aim of cardiac dose sparing and avoidance, numerous new methods have been developed [3,4]. These include, among others, partial breast irradiation (PBI) (reducing the volume to be irradiated) and prone positioning (operating by separating the heart and the radiation fields). The approaches available for the implementation of PBI include among others 3-dimensional-conformal radiation therapy (3D-CRT), with multiple static photon, and/or electron fields, intensity-modulated radiotherapy (IMRT) and volumetric-modulated arc radiotherapy (VMAT). Based on confirmatory results of the efficacy and safety of most techniques, eligibility for PBI has been extended to previously medium-risk cases, and guidelines recommend the technique more widely than before [5-7]. Prone positioning has become an alternative of conventional supine positioning in some centres, providing dramatic reduction in the ipsilateral lung dose, and in many cases significantly reducing heart exposure, too.

2 Aims

2.1 To assess whether the supine or prone position (in the latter with a belly board), and the application of the IMRT technique would result in the reduction of the radiation dose to the organs at risk (OARs) such as the rectum, colon, and small intestines during pelvic RT of prostate cancer patients.

2.2 Developing a simple clinical method in a prospective study for the operation of an already validated model for the prediction of the individually preferable treatment position (prone versus supine) during left breast radiotherapy.

2.3 To implement individualized accelerated partial breast irradiation (APBI) based on optimal dose distribution and OAR protection and identify the individually most advantageous technique by considering various tumour- and patient-related factors.

3 Patients and methods

All the procedures followed were in full accordance with the ethical standards of the responsible committees on human experimentation (institutional and national) and with the Helsinki declaration. All patients gave informed consent before enrollment into the study authorized by the national and regional ethics committees.

3.1 Prone positioning on a belly board decreases rectal and bowel doses in pelvic IMRT for prostate cancer

3.1.1 Patient population

The prospective analysis included patients with a histologically confirmed, high risk [10], localized or locally advanced (2009 TNM classification [8] stage T2-4 N0-1 M0) prostate cancer graded according to the Gleason score system [9], receiving a definitive pelvic RT at the Department of Oncotherapy, University of Szeged, Hungary. The tumour stage assessment was based on the findings of thoracic computed tomography (CT), abdominal and pelvic CT and magnetic resonance imaging (MRI), and whole-body bone scintigraphy. Clinical and pathological data were extracted from the patient files.

3.1.2 Patient positioning and computed tomography scanning

Patients were positioned on the supine and prone pelvis modules of the All in One (AIO) Solution (ORFIT, Wijnegem, Belgium) system. In supine pose, the patient was positioned with bent knees, and the genitalia were distracted with extruded polystyrene blocks. In prone position, a belly board was applied to allow the abdomen to extend into its aperture, and a polystyrene wedge was placed between the buttocks. For immobilization a six-point thermoplastic mask fixation (Pelvicast system, ORFIT, Wijnegem, Belgium) was employed. All patients underwent five-millimetre slice-increment topometric CT scanning in both positions from the diaphragm to the level of 10 cm below the femoral necks, using a Somatom Emotion 6 CT Simulator (Siemens, Erlangen, Germany). CT scanning was prepared with full bladder according to our internal protocol and following an antiflatulent diet for at least 7 days prior and during RT delivery.

3.1.3 Target and critical structure delineation

The gross tumour volume (GTV), clinical target volume (CTV), planning target volume (PTV), and OARs were delineated in the ARIA Oncology Information System (Varian Oncology Systems, Palo Alto, CA, USA) in both positions by radiation oncologists and reviewed by an experienced radiologist. The prostate was contoured as GTV_p. The proximal thirds, or in case of involvement, the full extension of the seminal vesicles and pathologic lymph nodes (GTV_N), if present, were delineated considering MRI records. CTV_N included the parailiac, upper subaortic presacral and obturator lymph nodes, contoured according to the RTOG GU Radiation Oncology Specialists Reach Consensus [10]. PTV_p included GTV_p with a 10 mm margin along the supero-inferior, left–right axis, in anterior direction and 7 mm in posterior direction. PTV_{pvs} was defined as the combination of GTV_p and seminal vesicles with a safety margin of 10 mm in posterior direction and 15 mm in any other directions. PTV was determined as PTV_{pvs}, a 7 mm margin around CTV_N and 10 mm around GTV_N, if present. The rectum, large and small intestines, urinary bladder, femoral heads, and bony structures were outlined as OARs. The rectum was defined from the ischial tuberosities to the sigmoid flexure, but at least 2 cm above PTV_{pvs}. Each rectal section, the whole rectum (R), the segment at the height of the prostate (R1), and R1 + 10 mm along the supero-inferior axis (R2) were individually delineated. Large and small bowel volumes contained all identifiable segments. The bladder was delineated from the apex to the dome [11].

3.1.4 Rectal extension and rectum–prostate distance measurement

At the height of the largest antero-posterior (AP) diameter of the prostate, rectal diameters along the AP and left–right axis were defined, and perpendicular lines were created from the centre and lateral edges of the back wall of the prostate to the outer anterior rectal wall in both supine and prone positions (Figure 1). Two independent radiation oncologists performed rectum–prostate distance measurements, both of them twice.

3.1.5 IMRT planning and dosimetric analysis

IMRT planning was performed using the Eclipse treatment planning system (Varian Oncology Systems, Palo Alto, CA, USA). The prescribed doses were 45 Gy to the PTV (1.8 Gy/day, 5 days/week), 14 Gy boost to the PTV_{pvs} and 18 Gy boost to the PTV_p, both delivered in daily

2 Gy fractions, 5 days per week, boost irradiations given sequentially. OAR dose constraints were determined as the following [10]: $V_{55Gy\ (bladder)} \leq 50\%$, $V_{70Gy\ (bladder)} \leq 30\%$; $V_{50Gy\ (rectum)} \leq 50\%$, $V_{70Gy\ (rectum)} \leq 20\%$; $V_{50Gy\ (colon)} \leq 50\%$, $V_{70Gy\ (colon)} \leq 20\%$; $V_{52Gy\ (small\ intestine)} = 0\%$; $V_{50Gy\ (femoral\ heads)} < 5\%$. For the coverage of the PTV sliding window IMRT plans were designed in both positions with a seven-field beam arrangement using 6 MV photon beam quality, consisting coplanar beam directions as the following: in prone position 0°, 136.1°, 208.3°, 258.7°, 101.7°, 306.1° and 55.2°, in supine position 0°, 38.2°, 98°, 142°, 215.7°, 269.5° and 318.2°. For the PTV_{pvs} and PTV_p VMAT plans were generated in both positions using 6 MV photon beam quality, 181°–179° and 179°–181° gantry angles and 30° and 15° collimator angles, respectively. IMRT plans were created to obtain a 95% coverage of the PTV with the 95% isodose curve. The highest priority was PTV coverage, and the second one was the sparing of OARs. Planning assistant contours of the PTV, PTV_{pvs}, and PTV_p were designed with uniform margins of 15 mm, 30 mm, 40 mm, and 50 mm in both positions. Dose-volume histograms (DVHs) were calculated for all defined volumes. Data of mean volumes of the contoured structures, mean absolute volumes of the small bowel and colon receiving 20–50 Gy, mean relative volumes of the rectal segments receiving 30–75 Gy and of the bladder receiving 30–70 Gy doses and mean of doses regarding PTV D95, PTV_{pvs} D95, and PTV_p D95 were collected.

3.1.6 Radiation treatment and image-guidance

Irradiation was carried out by using a Varian TrueBeamSTx (Varian Oncology Systems, Palo Alto, CA, USA) in prone position. Image-guidance was based on daily kV-cone beam CT (CBCT) scanning of the pelvis prior to treatment, using the standard mode settings: 125 kV, 80 mA, 13 ms, and half-fan bowtie filter. An automatic match algorithm was used to match the bony structures displayed on the planning CT and the CBCT.

3.1.7 Statistical analysis

Data were reported as mean ± standard deviation (SD), mean ± standard error (SE) or median values. The difference between the volumes and doses in supine and prone position was analysed with the paired samples t-test. Intraobserver and interobserver variabilities were calculated from the mean of distances by using correlation analysis, given a correlation

coefficient (r). SPSS 20.0 for Windows (SPSS Inc., Chicago, IL, USA) was used to perform the analysis. A p value < 0.05 was considered significant.

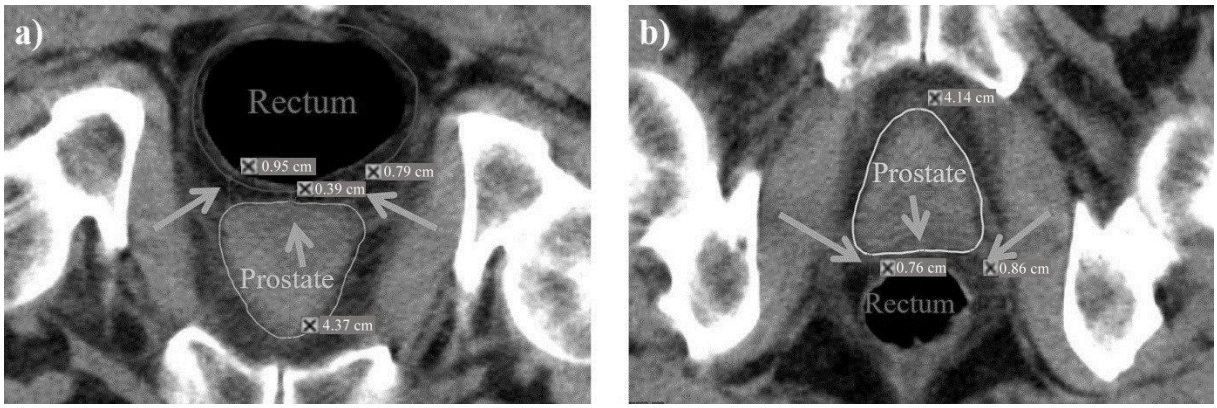

Figure 1. *Rectal extension and rectum–prostate distance measurement: At the height of the largest antero-posterior diameter of the prostate perpendiculars were created from the centre and both lateral edges of the posterior prostate wall to the anterior rectal wall in both prone (a) and supine (b) positions. Larger rectal diameters in prone, smaller in supine position in case of the same patient at the same time*

3.2 A simple clinical method for predicting the benefit of prone vs. supine positioning in reducing heart exposure during left breast radiotherapy

3.2.1 Outline of the study

First, a single CT slice image at the middle of the heart (reference plane, P_{ref}) was acquired with the help of an AP scout view in the supine position (Figure 2A). On that CT scan, the shortest distance between the anterior surface of the left anterior descending coronary artery (LAD) and the chest wall (D_{med}) and the area of the heart (A_{heart}) included in the radiation fields were measured after placing a straight line between the border of the ipsilateral latissimus dorsi muscle and the lateral edge of the sternum (Figure 2B); these data (representing the topography of the heart) were introduced to the calculator together with the patient's body mass index (BMI) (which correlated with the volumes of the breast and heart) as previously described in detail [12].

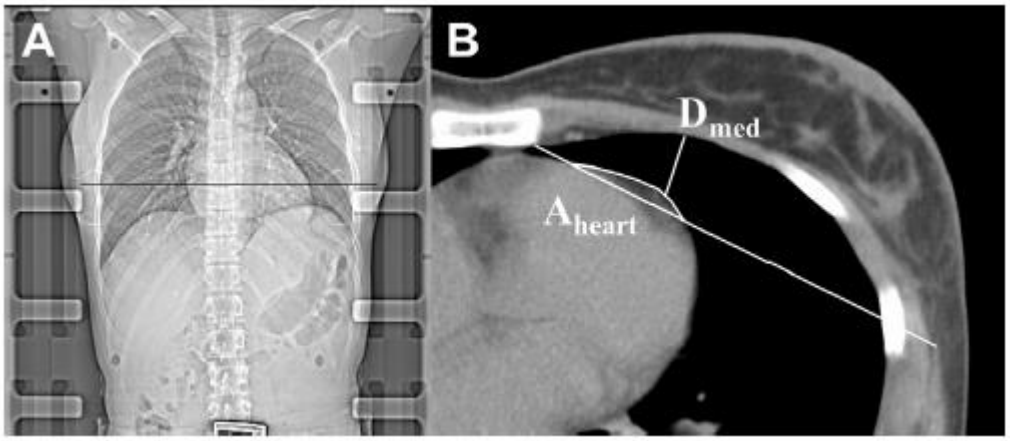

Figure 2. *The simple clinical tool generates patient-specific data to predict the benefit of prone positioning. After selecting the reference plane (P_{ref}) at the middle of the heart on the AP scout view (A), a single CT slice is acquired for the measurement of those determinants (D_{med} and A_{heart}) (B) which operate the calculator to provide estimates of the doses to the LAD or heart.*

Conformal radiation treatment plans were generated in both positions using conventional 6 MV tangential photon fields set up isocentrically and median 2 (1–3) individually weighted 6/15 MV segmental fields superimposed on the tangential fields using a multileaf collimator as described [12,13]. Wedges were used in almost all supine radiation plans. A mean dose to the PTV of 50 Gy (25 fractions) and a uniform distribution (–5% + 7%) of the prescribed dose to 95% of the PTV, were aimed at. The consistency of all contouring activities had been ensured by a chief radiation oncologist and an experienced radiologist [14]. Equivalent heart and LAD volume contouring in either setup was ensured by one author. In the next ‘‘routine clinical practice” set of 60 patients, the acquisition of a single series of CT images according to the suggestion of the calculator was aimed at, and a second CT series was taken only if any of the dose constraints approved for the specific position were not reached in the position suggested by the calculator. In this series of patients’ dose constraints were specified on the basis of previously recorded data. The upper range limits of the 90% percentile of dosimetry data in the preferred position were the following: mean LAD dose [MD_{LAD}]: 12.9 Gy and 12.5 Gy, $V_{25Gyheart}$: 2.4% and 4.7%, in the prone position and supine position, respectively. In true discordant cases, our strategy for selecting treatment position was to consider the LAD dose as a primary decisive factor.

In the validation set, data on LAD and heart dose differences between the two treatment positions were extracted from the planning system and estimated by the calculator, whereas in the ‘‘routine clinical practice” series only the estimated dose differences were available. Analyses were performed on 1. the equivalence of the P_{ref} with the median plane of the full series of CT scans acquired in the supine position (P_{med}) and 2. the effect of plane miss on the patient-related determinants and choice of preferable position. The sensitivity and specificity of this simple clinical method were evaluated based on the dosimetry data obtained using the topogram for selecting the position (n = 100). In the ‘‘routine clinical practice” series, the acceptability of the position as predicted by the calculator, the LAD and heart doses achieved without taking 2 CT series, and the need of performing a second CT series and changing position or irradiation technique were analysed.

3.2.2 External testing

The supine and prone CT series and supine topogram of patients included in the study ‘‘Individualized positioning for maximum heart and index breast protection during breast irradiation: comparative study between Prone and Supine (Approval: 26/09/2013, B707201318246) were retrospectively used for independent testing. The protocol of patient positioning, delineation and radiation treatment planning has been described [15].

First, P_{ref} was selected on the topogram. Then, the predictors BMI, D_{med}, A_{heart} as measured in P_{ref} were introduced to the calculator. As a second step, D_{med}, A_{heart} were also measured in P_{med}. LAD and heart dose differences between the two treatment positions extracted from the planning system and estimated by the calculator were analysed. Finally, the correctness of P_{ref} was evaluated.

3.2.3 Statistical methods

The calculator had been developed based on linear regression models utilizing the patients’ anatomical features, with ΔMD_{LAD} and $\Delta V_{25Gyheart}$ as dependent variables [12]. With a single cut-off point, a case was classified to prone positioning when the predicted value exceeded that value.

Thresholds were optimized based on sensitivity and specificity as calculated from previous [12] and present data (Table 1).

		Original method (double CT method, n=83)		**Simple tool (single CT method, n=100)**	
	Cut-off point	**Sensitivity (%)**	**Specificity (%)**	**Sensitivity (%)**	**Specificity (%)**
ΔMD_{LAD} (Gy)	-0.6	66.6	91.1	72.4	91.5
	-0.3	70.8	90.7	75.9	91.5
	0	74.4	90.0	75.9	91.5
	0.3	77.7	88.9	79.3	88.7
	0.6	80.7	87.5	82.8	87.3
	0.9	83.4	86.0	82.8	83.1
	1.2	85.4	83.6	86.2	81.7
	1.5	86.5	81.7	86.2	77.5
	1.8	86.8	79.9	93.1	76.1
$\Delta V_{25Gyheart}$ (%)	0	47.9	89.7	50	90.8
	0.25	56.2	88.8	58.3	89.5
	0.50	63.2	85.9	64	88
	0.75	72.4	82.4	68	85.3
	1	78.8	77.7	80	85.3
	1.25	84.0	74.0	84	81.3
	1.50	87.4	77.0	92	78.6
	1.75	89.9	62.1	96	74.6

Table 1 *Classification measures for ΔMD_{LAD} and $\Delta V_{25Gyheart}$ using a single discrimination threshold. Great consistency is seen between the original cohort [12] and the present series.*

Sensitivity and specificity were calculated with supine positioning as positive determinant in the model. For ΔMD_{LAD} a threshold of 0.6 Gy, and for $\Delta V_{25Gyheart}$ a cut-off point of 1.0% were chosen. In the definition of the cut-off points, a sensitivity of 80% at the minimum and the maximum achievable value of specificity was required.

LAD and heart dose constraints achievable by selecting the preferable position were specified by percentage estimation. Statistical analysis was performed with SPSS 22.0 for Windows.

3.3 Dosimetric comparison of 3D-CRT, sliding window IMRT and VMAT techniques for external beam accelerated partial breast radiotherapy

3.3.1 Patient population

This prospective clinical cohort trial included women after breast conserving surgery, with an age of at least 50 years, diagnosed with a unifocal and unicentric breast cancer of any invasive histological type or low risk ductal carcinoma in situ (DCIS), with any hormone receptor and human epidermal growth factor receptor-2 (HER2) status, pT1-2 (≤30 mm) tumour size removed with at least 2 mm free margin, pN0 axillary status diagnosed by sentinel lymph node biopsy or axillary block dissection, without extensive intraductal component (EIC), lymphovascular invasion or distant metastases. Excision cavity localization at surgery with titanium clips was an inclusion criterion. Exclusion criteria included relative and absolute contraindications of irradiation. All cases were discussed at a multidisciplinary tumour board. Adjuvant systemic therapy was indicated according to the institutional guidelines. Various clinical data including tumour bed situation (lateral, medial/central, upper, lower) within the breast was prospectively collected.

3.3.2 Patient positioning and CT scanning

The patients were positioned supine on an ‘All in One (AIO) Solution’ (ORFIT, Wijnegem, Belgium) breast board with the arms raised over the head. For immobilization, diagonal thermoplastic mask fixation (ORFIT, Wijnegem, Belgium) was employed. All patients underwent five-millimetre slice-increment planning CT scanning from the sternoclavicular joint to the level of 2 cm below the submammary fold, using a Somatom Emotion 6 CT Simulator (Siemens, Erlangen, Germany).

3.3.3 Target and critical structure delineation

The CTV included the excision cavity (marked with surgical clips) with a 1.5 cm margin extended in all directions, limited by 0.4 cm from the skin surface and by the outer edge of the chest wall. For compensating daily setup errors and breathing motions, a universal PTV-CTV margin of 0.5 cm was added. As OARs, the ipsilateral uninvolved breast, the contralateral breast, the lungs, the heart and the LAD [12,16] were delineated.

3.3.4 Treatment planning

In all cases, 3D-CRT, sliding window IMRT and VMAT plans were generated in the Eclipse v13.6 planning system (Varian Oncology Systems, Palo Alto, CA, USA) for a Varian TrueBeamSTx (Varian Oncology Systems, Palo Alto, CA, USA) linear accelerator with HD120 multileaf collimator. In 3D-CRT technology, two 6 MV photon fields were used, closing at an angle of approximately 120° (Figure 3A). The definition of field directions was based upon tumour location and in left-sided cases the situation of the heart and LAD in relation to the PTV. For homogeneous dose distribution, further sub-segments were employed, if necessary. Sliding window IMRT planning was carried out applying 6 MV photon energy with a five-field beam arrangement of 300°, 350°, 40°, 90° and 150° in left-sided cases and 60°, 10°, 320°, 270° and 210° in right-sided cases (Figure 3B). If the target volume was located in the medial or lateral area of the breast, an additional ±10° rotation was used, depending on laterality. The field direction range of dual arc VMAT was defined by the first and last field of the IMRT plan (Figure 3C). The isocentre was placed into the geometric centre of the PTV. For comparability purposes the same optimisation parameters were used during inverse treatment planning (IMRT, VMAT). If the shortest distance of the geometric centre of the PTV from the body surface (d) was <25 mm, in an additional plan of each technique, an 'en face' electron beam of 4-16 MeV energy was applied (Figure 3D), calculating 2/3 of the whole dose with photon and 1/3 with electron technique. For these fields Newton's metal apertures were planned to reduce normal tissue exposure. For the PTV, a total dose of 37.5 Gy was prescribed (10 fractions, 3.75 Gy/fraction, 1 fraction/day, 5 times/week), ≥99% of the PTV receiving 95% of the prescribed dose and at least 90% of the PTV receiving 100% of the prescribed dose. Ten per cent at most of the PTV was allowed to receive >107% of the prescribed dose.

3.3.5 Treatment plan evaluation

Conformity and homogeneity indexes of the PTV and dose-volume parameters of the OARs were defined in every plan.

Conformation Number (CN) [17]:

$$CN = \frac{PTV_{ref}}{V_{PTV}} \times \frac{PTV_{ref}}{V_{ref}} \quad \text{(Ideal is 1)}$$

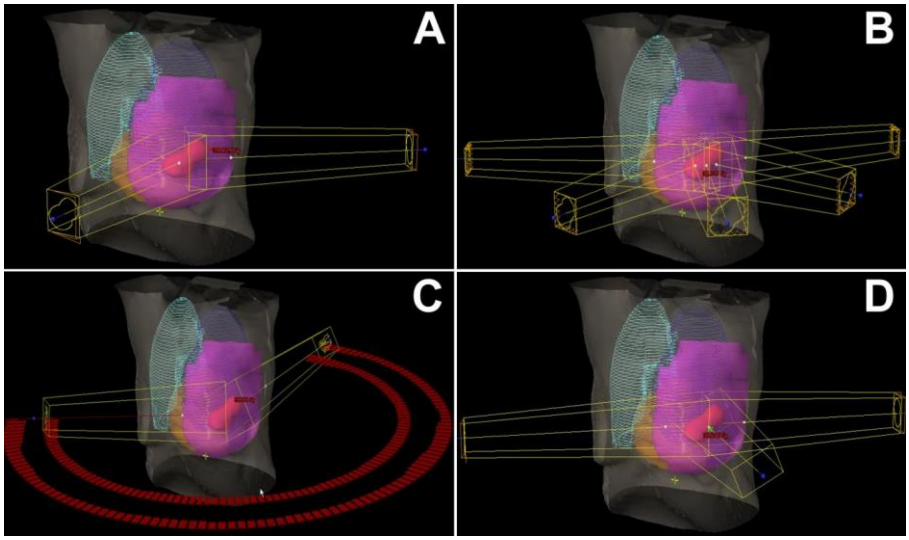

Figure 3 *Beam arrangement in 3D-CRT (A), IMRT (B), VMAT (C) radiotherapy techniques and the combination of photon fields with an 'en face' electron beam (D)*

PTV_{ref} refers to the volume of target receiving a dose equal to or greater than the reference dose, in this case the prescribed dose (37.5 Gy). V_{PTV} stands for the volume of target, and V_{ref} is the total volume that covered by the reference isodose.

Homogeneity Index (HI) [18] ($D_{2\%}$, $D_{50\%}$, $D_{98\%}$=dose received by 2%, 50% and 98% of PTV, respectively):

$$HI = \frac{D_{2\%} - D_{98\%}}{D_{50\%}} \text{ (Ideal is 0)}$$

To describe plans with a single numerical data, a Plan Quality Index (PQI) was developed based on the study of Leung et al. [19], in which the parameters (H)ealthy tissue conformity index, (M)erit and (P)enalty functions were generated as follows:

$$PQI = \sqrt{(1-H)^2 + (1-M)^2 + (1-P)^2} \text{ (Ideal is 0)}$$

The (H)ealthy tissue conformity index [20]:

$$H = \frac{PTV_{ref}}{V_{ref}} \text{ (Ideal is 1)}$$

The target volume coverage was characterized by the '(M)erit function' parameter [19], to verify the performance of hot and cold spots within the PTV. As coverage criteria differ from

prostate irradiation studied by Leung et al. [19], the following limits were applied to determine 'M'. Cold spots were defined by the percentage PTV volume covered with the 100% isodose curve (at least 90%), hot spots were defined by the percentage PTV volume receiving at least 107% of the prescribed dose (at most 10%).

$$M = \frac{\frac{V_{100\%}}{90} + \left(1 - \frac{V_{107\%}}{10}\right)}{\frac{100}{90} + 1} \text{(Ideal is 1)}$$

The relative volume of the ipsilateral healthy breast (ipsilateral breast – PTV) receiving at least 25, 50, 75 and 100% of the prescribed dose ($BreastV_{25\%, 50\%, 75\% \text{ and } 100\%}$, respectively), the mean dose to the ipsilateral lung ($Lung_{mean}$) and the relative volume of it receiving ≥40% of the prescribed dose ($LungV_{40\%}$), the mean dose to the heart ($Heart_{mean}$) and the relative volume of it receiving at least 50% of the prescribed dose ($HeartV_{50\%}$), the mean dose to the LAD (LAD_{mean}) and the relative volume of it receiving ≥20% of the prescribed dose ($LADV_{20\%}$) were collected.

For studying OAR exposure, the calculation algorithm applied by Leung et al. [19] was modified to make it suitable for the characterization of risk organ exposure during breast irradiation as follows. To describe the exposure of OARs with a single '(P)enalty function' parameter [19], specific dose parameters of four OARs compared to the 99% percentile of the respective sample population were averaged for each technique.

In right-sided cases:

$$P = \frac{\left(1 - \frac{BreastV_{25\%}}{70}\right) + \left(1 - \frac{Lung_{mean}}{10}\right) + \left(1 - \frac{Heart_{mean}}{5}\right) + \left(1 - \frac{LAD_{mean}}{5}\right)}{4} \text{(Ideal is 1)}$$

In left-sided cases:

$$P = \frac{\left(1 - \frac{BreastV_{25\%}}{70}\right) + \left(1 - \frac{Lung_{mean}}{10}\right) + \left(1 - \frac{Heart_{mean}}{10}\right) + \left(1 - \frac{LAD_{mean}}{10}\right)}{4} \text{(Ideal is 1)}$$

If the P value were negative in an extreme case (e.g. the exposure of all OARs was high), that would have been defined as 0 for further calculations.

To select the most favourable irradiation plan for a given patient, PQI values were compared. In order to determine an arbitrary threshold of PQI difference that indicates a difference in about half of the cases, we defined the PQI difference (PQID) as relevant if exceeded the value of 0.05. Each plan that reached this critical PQID level was referred to a respective 'winner method group', while that which did not was referred to the group of equality.

To study if any of the irradiation techniques would be more favourable in subgroups of patients, the effects of the volume of the PTV, its distance from the body surface (d) and the quadrant where it was situated were analysed.

3.3.6 Statistical methods

Continuous variables were expressed as mean ± SD. The means of continuous variables in the different 'winner method groups' were compared with Welch's one-way ANOVA. After significant ANOVA multiple comparisons were conducted with least significant difference (LSD) method. The dependence between two categorical variables was examined with Pearson's Chi-squared tests. The relationship between PQI components and PQI values was presented with scatter plot. Pearson correlation coefficients were calculated.

The effect of the addition of an electron beam to photon beams and treatment technique choice (3D-CRT *vs.* IMRT *vs.* VMAT) was analysed with two-way repeated measures (within subjects-within subjects) ANOVA. A $p<0.05$ was regarded as statistically significant. Statistical software IBM SPSS version 24 was used for statistical analysis.

4 Results

4.1 Prone positioning on a belly board decreases rectal and bowel doses in pelvic IMRT for prostate cancer

4.1.1 Patient population

Between October 13, 2016 and October 11, 2017, 55 patients with high risk localized or locally advanced prostate cancer were administered definitive pelvic lymph node RT. Patients belonged to the elderly age group with a median [range] age of 65.60 [53.33–83.49] years, and they were mostly overweight showing a median [range] value of body mass index of 26.96 [19.37–41.62] kg/m^2. More than three-quarters of them had a cardiovascular co-morbidity, and one-third of them were smokers. All the patients had stage T2-4 N0 M0 tumour with a Gleason score ≥ 7 and a prostate specific antigen (PSA) level at the time of the diagnosis established > 5 ng/ml. Most of the patients received a 6-month course of luteinizing hormone-releasing hormone analogue and antiandrogen (total androgen blockade, TAB) endocrine therapy, launched before the commencing of RT. The relevant patient and tumour characteristics are shown in Table 2.

4.1.2 Structure volumes and rectal extension

No significant differences were found between prone and supine positions in the volumes of the GTV_p, GTV_p+seminal vesciles, PTV, colon, small bowel, and urinary bladder. All rectal volumes (R, R1 and R2) were significantly higher in the prone position. The high SD values of mean bladder volumes in the two positioning methods might be the consequence of pre-existing urinary symptoms, such as incontinence. At the height of the largest AP level of the prostate, both the AP and the lateral rectal diameters were significantly higher in the prone position (Table 3).

4.1.3 Rectum–prostate distance

The rectum–prostate distance measured from the centre of the rear prostate wall to the outer anterior rectal wall was significantly higher in prone position. No significant differences in the

distance values measured from the left and right edges of the posterior prostate wall were found. Both intraobserver and interobserver variabilities showed close correlation (Table 4).

4.1.4 Normal tissue doses

A prone position with the additional use of a belly board led to a significant decrease in the absolute volumes receiving doses greater than 20 to 40 Gy in the small intestine and the colon; however, the difference between the volumes receiving 50 Gy was not significant (Table 5).

In dose ranges of 40 to 75 Gy, the exposure of all rectal segments was more favourable in prone position. The relative volume receiving 30 Gy dose was lower in respect of R1 segment; nonetheless, the difference was not significant. The relative exposed volume of the urinary bladder, femoral heads, and bony structures was in accordance with the dose constraints. No significant difference was found between the positioning methods (Table 6).

Tumour and patient characteristics	**Number of patients (%)**
Number of patients	55
Concurrent cardiovascular disease	44 (80.00)
History of smoking	18 (32.73)
Clinical stages	
T2	41 (74.55)
T3	12 (21.82)
T4	2 (3.64)
Gleason scores	
7	27 (48.21)
8	5 (9.09)
9	19 (33.93)
10	4 (7.14)
PSA levels on establishing the diagnosis (ng/ml)	
10>x>5	13 (23.21)
20>x≥10	9 (16.36)
≥20	33 (58.93)
Endocrine treatment	49 (89.09)

Table 2. *Patient and tumour characteristics of prostate cancer patients*

Structure	Position	Mean volume (cm^3)	Standard deviation (SD)	p value
GTV_p	Prone	130.11	49.13	0.217
	Supine	133.28	50.87	
GTV_p + seminal vesicles	Prone	188.77	58.19	0.748
	Supine	190.23	58.20	
PTV	Prone	1123.54	138.90	0.282
	Supine	1130.98	146.66	
Whole rectum (R)	Prone	155.13	105.26	<0.001
	Supine	95.61	45.89	
Rectal subsegment R1	Prone	50.32	31.84	<0.001
	Supine	34.76	23.64	
Rectal subsegment R2	Prone	74.37	41.51	<0.001
	Supine	50.78	27.64	
Colon	Prone	580.32	299.38	0.486
	Supine	604.37	337.12	
Small bowel	Prone	812.93	354.25	0.373
	Supine	772.71	353.21	
Urinary bladder	Prone	184.18	117.13	0.403
	Supine	192.40	112.56	
Rectal diameter	**Position**	**Mean diameter (mm)**	**Standard error (SE)**	**p value**
AP	Prone	50.60	2.20	<0.001
	Supine	36.70	1.50	
Lateral	Prone	43.80	2.60	0.003
	Supine	35.90	1.80	

Table 3. *Volumes of delineated structures and rectal diameters in prone and supine positions in prostate cancer patients*

4.1.5 PTV coverage

PTV coverage did not differ significantly between the two positions (PTV D95 - mean of dose 43.01 *vs.* 43.00 Gy, SD 0.26 *vs.* 0.26 in prone *vs.* supine position, respectively, p=0.782; PTV_{pvs} D95 - mean of dose 13.36 *vs.* 13.35 Gy, SD 0.07 *vs.* 0.07 in prone *vs.* supine position, respectively, p=0.591; PTV_p D95 - mean of dose 17.16 *vs.* 17.15 Gy, SD 0.09 *vs.* 0.07 in prone *vs.* supine position, respectively, p=0.435).

Distance	Position	Mean (mm)	Standard error (SE)	p value	Intraobserver variability – Correlation coefficient (r)		Interobserver variability – Correlation coefficient (r)
					Examiner 1	Examiner 2	
Left lateral	Prone	6.50	0.40	0.062	0.92	0.90	0.89
	Supine	5.70	0.40				
Medio-sagittal	Prone	2.80	0.30	0.026	0.86	0.89	0.95
	Supine	2.20	0.30				
Right lateral	Prone	5.90	0.40	0.173	0.80	0.74	0.78
	Supine	5.40	0.40				

Table 4. *Rectum–prostate distance and intraobserver and interobserver variability correlation in prone and supine positions in prostate cancer patients*

Organ At Risk	DVH parameter	Position	Mean volume (cm^3)	Standard deviation (SD)	p value
Small intestine	$V_{20\ Gy}$	Prone	79.85	89.83	<0.001
		Supine	170.34	103.62	
	$V_{30\ Gy}$	Prone	36.74	51.24	<0.001
		Supine	84.55	63.01	
	$V_{40\ Gy}$	Prone	16.99	26.08	<0.001
		Supine	32.91	31.35	
	V_{50Gy}	Prone	0.16	1.06	0.398
		Supine	0.33	1.54	
Colon	$V_{20\ Gy}$	Prone	122.43	74.52	<0.001
		Supine	181.22	109.48	
	$V_{30\ Gy}$	Prone	84.09	57.17	<0.001
		Supine	121.21	73.36	
	$V_{40\ Gy}$	Prone	53.23	44.20	0.043
		Supine	63.19	44.89	
	$V_{50\ Gy}$	Prone	2.06	4.02	0.627
		Supine	1.81	3.62	

Table 5. *Small intestine and colon exposure in prone and supine position in prostate cancer patients*

OAR	DVH parameter	Position	Mean relative V (%)	SD	p value
Whole rectum	V_{30Gy}	Prone	106.40	118.98	0.296
		Supine	89.60	7.46	
	V_{40Gy}	Prone	65.79	14.96	<0.001
		Supine	78.58	10.14	
	V_{50Gy}	Prone	35.51	13.83	<0.001
		Supine	48.38	12.29	
	V_{60Gy}	Prone	17.45	8.18	<0.001
		Supine	24.04	9.11	
	V_{70Gy}	Prone	7.57	4.10	<0.001
		Supine	10.43	4.97	
	V_{75Gy}	Prone	3.67	2.61	0.021
		Supine	4.58	3.19	
Rectal subsegment R1	$V_{30\ Gy}$	Prone	99.78	0.75	0.735
		Supine	99.80	0.61	
	V_{40Gy}	Prone	80.58	13.50	<0.001
		Supine	94.95	5.74	
	V_{50Gy}	Prone	52.25	14.18	<0.001
		Supine	68.55	10.90	
	V_{60Gy}	Prone	32.37	10.90	<0.001
		Supine	40.49	10.13	
	V_{70Gy}	Prone	16.51	5.83	<0.001
		Supine	20.74	7.14	
	V_{75Gy}	Prone	8.79	4.52	0.099
		Supine	9.97	5.67	
Rectal subsegment R2	V_{30Gy}	Prone	99.52	1.21	0.001
		Supine	98.61	1.96	
	V_{40Gy}	Prone	78.55	12.66	<0.001
		Supine	91.45	6.05	
	V_{50Gy}	Prone	49.40	13.14	<0.001
		Supine	64.83	9.89	
	V_{60Gy}	Prone	28.95	9.04	<0.001
		Supine	37.43	8.76	
	V_{70Gy}	Prone	13.52	4.75	<0.001
		Supine	17.86	5.79	
	V_{75Gy}	Prone	6.82	3.59	0.051
		Supine	7.86	4.43	
Bladder	V_{30Gy}	Prone	95.82	7.10	0.657
		Supine	95.45	5.13	
	V_{40Gy}	Prone	67.99	18.89	0.687
		Supine	68.78	16.13	
	V_{50Gy}	Prone	41.90	16.53	0.982
		Supine	41.86	14.84	
	V_{60Gy}	Prone	26.73	11.77	0.235
		Supine	25.36	10.62	
	V_{70Gy}	Prone	15.91	7.90	0.276
		Supine	14.94	7.31	

Table 6. *Exposure of rectal segments and urinary bladder in prone and supine positions in prostate cancer patients*

4.2 A simple clinical method for predicting the benefit of prone vs. supine positioning in reducing heart exposure during left breast radiotherapy

4.2.1 Validation set

In 55/100 cases, P_{ref} was the same as P_{med} while in 28 and 17 cases, P_{ref} and P_{med} differed by 1 or more planes, respectively. More among the incorrectly defined P_{ref} cases were shifted toward the caudal than the cranial direction. This resulted in smaller mean D_{med} and larger mean A_{heart} values among the plane miss cases overall (Table 7).

	All cases (n=100)		**Correct plane (n=55)**		**Plane miss (n=45)**	
	P_{ref}	**P_{med}**	**P_{ref}**	**P_{med}**	**P_{ref}**	**P_{med}**
D_{median} (cm)	1.27±0.59	1.25±0.67	1.35±0.55	1.17±0.63	1.18±0.63	1.34±0.71
A_{heart} (mm^2)	768.8±487.4	671.6±450.1	730.7±537.4	721.5±511.2	815.4±419.5	610.5±358.1

Table 7*. D_{med} and A_{heart} values (mean±SD) as measured on P_{ref} vs. P_{med} in all cases or in correctly and incorrectly specified P_{ref} cases of breast cancer patients receiving left breast irradiation; the measurements were performed on 2 CT scans at the middle of the heart either identified with the help of an AP scout view (P_{ref}) or selected from a full CT series (P_{med}).*

Within the whole series, no change in the frequency of plane misses could be detected by time. Incongruency among ΔMD_{LAD} and $\Delta V_{25Gyheart}$ in the supine and prone position as predicted by the calculator on the basis of P_{ref} *vs.* P_{med} data, was present in 14 and 18 of the cases, respectively; these were all of small numerical values (Fig. 4A, B).

When the LAD and heart dose differences predicted by the calculator based on the P_{ref} values were compared with the original dosimetric data from plans generated in both positions, the suggestion proved invalid in 14 (MD_{LAD}) and 16 ($V_{25Gyheart}$) cases (Figure 4C, D). We have compared the sensitivity and specificity of ΔMD_{LAD} and $\Delta V_{25Gyheart}$ provided by the simple method based on a single CT scan with that of the original method that indicated high

consistency [12] (Table 1). Based on these findings, the cut-off values of 0.6 Gy (ΔMD_{LAD}) and 1.0% ($\Delta V_{25Gyheart}$) have been selected for further analyses and practice.

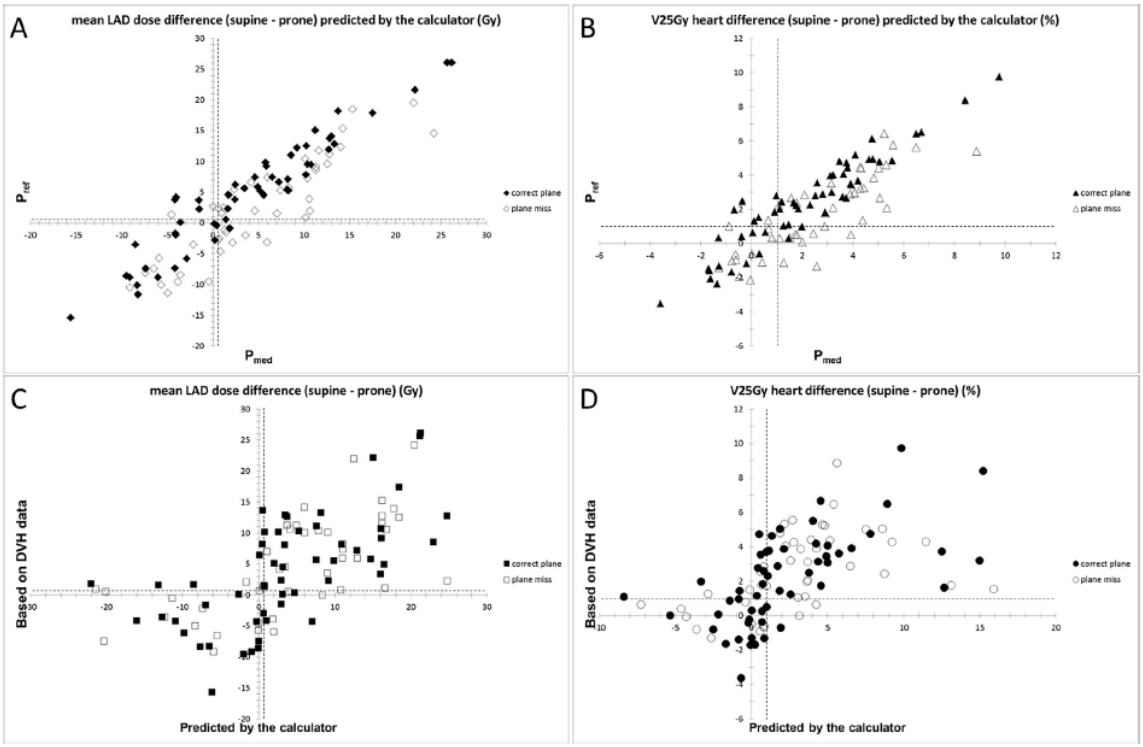

Figure 4. *Calculator suggestion of LAD (A) and heart (B) dose differences by the input of D_{med} and A_{heart} based on P_{ref} vs. P_{med}; LAD (C) and heart (D) doses according to the estimation of the simple clinical method based on a single CT scan vs. DVH data extracted from the planning system (n = 100) in breast cancer patients receiving left breast irradiation. Dashed lines indicate the cut-off values of 0.6 Gy (D_{MDLAD}) and 1.0% ($D_{V25Gyheart}$) specified by sensitivity and specificity values.*

Next, the concordance of calculator-predicted treatment position based on ΔMD_{LAD} *vs.* $\Delta V_{25Gyheart}$ and the need of intervention were analysed in the validation set. In 28 supine-predicted cases and 64 prone-predicted cases, the same treatment position was suggested by both measures (Table 8).

Among the 28 supine-predicted cases in 2, the radiotherapy plan revealed that MD_{LAD} >12.5 Gy, but only 1 could be improved by changing the treatment position. Among the 64 prone-

predicted cases in 8, the MD_{LAD} exceeded the dose constraint of 12.9 Gy; only 3 plans could be improved by applying the supine position. Among the discorcondant cases, ΔMD_{LAD} suggested prone position in 3 and supine position in 5 cases; in both groups in a single case each could the LAD dose be improved by changing the treatment position. In altogether 7 cases, a different intervention (IMRT) had to be applied (Table 8).

		$\Delta V_{25Gyheart}$							
		Supine				***Prone***			
ΔMD_{LAD}		**All**	MD_{LAD} >12.5 Gy	change position	other interven-tion	**All**	MD_{LAD} >12.9 Gy	change position	other interven-tion
	Supine	**28**	2	1/2	1/2	**5**	1/5	1/1	-
	Prone	**3**	2/3	1/2	1/2	**64**	8/64	3/8	5/8

Table 8. *Concordance of treatment position as predicted by ΔMD_{LAD} vs. $\Delta V_{25Gyheart}$, in the validation set (n=100) in breast cancer patients receiving left breast irradiation. In concordant cases the suggested position, in discordant cases the position suggested by ΔMD_{LAD} was applied unless the dose constraints were exceeded; in such cases the other treatment position or alternative techniques may be tested.*

4.2.2 „Routine practice" set

In the „routine practice" series of 60 patients, the new method proved feasible. All patients received treatment in the position suggested by the calculator except one, who had to receive a second CT in the other position due to unacceptable LAD dose. The other patients had MD_{LAD} and $V_{25Gyheart}$ values well below the predefined dose limits, and these were similar to the values calculated in the validation set (Table 9).

4.2.3 External testing

In a series of 28 breast cancer patients from Liège, the predictors BMI, D_{med} and A_{heart} significantly differed from the same parameters among the patients from Szeged. In 18/28 cases, P_{ref} was equal or close to P_{med} (≤6 mm), while in 10 cases, P_{ref} varied from P_{med} by 9-16 mm. Comparing the calculator-provided dose differences with the treatment planning data, favored treatment position was correct in 24/28 (accuracy: 85.7%) and 23/28 (accuracy: 82.1%) cases taking into account the LAD and heart doses, respectively. Sensitivity and specificity of

ΔMD_{LAD} was 83.3% and 86.4%, respectively, whereas sensitivity and specificity of $\Delta V_{25Gyheart}$ was 100.0% and 80.0%, respectively.

	Treatment position	n (%)	mean LAD dose (Gy)				V_{25Gy} heart (%)			
			mean	SD	min	max	mean	SD	min	max
Validation series	***Prone***	67 (67.0)	6.55	6.03	1.70	26.66	1.16	2.24	0.0	8.75
	Supine	33 (33.0)	6.90	3.86	1.71	13.73	1.54	1.38	0.0	4.77
"Routine practice" series	***Prone***	47 (78.3)	6.58	2.29	1.95	11.24	0.86	0.57	0.1	2.67
	Supine	13 (21.7)	7.35	3.05	2.54	15.85	1.15	0.95	0.21	3.57

Table 9. *LAD and heart doses in the validation set and the „routine practice" series in breast cancer patients receiving left breast irradiation: in the majority of cases, LAD and heart doses were well below the position-related dose constraints; for those patients who had higher than accepted doses, an alternative technique had to be applied.*

4.3 Dosimetric comparison of 3D-CRT, sliding window IMRT and VMAT techniques for external beam accelerated partial breast radiotherapy

4.3.1 Patient population

The study included 138 cases. Patients belonged to the elderly age group with a median age of 61.98 [50.11-79.71] years and the majority was postmenopausal (Table 10). In most cases breast cancer was diagnosed via breast screening, the mammographic examination showed circumscribed mass, the tumour was in the outer-upper quadrant of the breast and sentinel lymph node biopsy was carried out. Most cancers were invasive ductal carcinoma of grade 1-2, hormone receptor positive and HER2-negative. The average± SD pathologic tumour size was 11.3 ± 4.7 mm, the mean ± SD of the surgical margins was 6.8 ± 4.1 mm. The relevant patient and tumour characteristics are presented in Table 10.

4.3.2 Radiotherapy data

The tumour bed was left-sided in 78 patients (56.5%) and right-sided in 60 patients (43.5%). The mean and median PTV volume was 115.6 cm^3 and 108.5 (23.7-287.8) cm^3, respectively. The PTV volume was ≥100 cm^3 in 75 patients (54.3%). The distance of the geometric centre of the PTV from the body surface (d) was 3.6±1.6 cm (mean±SD) was less than 25 mm in 29 cases (21.0%).

In most cases, the IMRT and VMAT techniques have given superior plans based on the PQI. Parameters reflecting dose distribution within the PTV and conformity are shown in Table 11. Based on the data represented in Table 11, in most of the cases IMRT technique is the most advantageous regarding homogeneity and overdosing, however, conformity is mostly improved by VMAT plans. OAR doses according to the technique are summarized in Table 12, while OAR exposure according to the side of treatment is shown in Table 12A. OAR exposures usually show great variety, however the mean dose to the lung and heart is the lowest 3D-CRT plans. These data shown in detail in Tables 11 and 12 point to the fact that traditional plan quality indicators *per se* are not suitable to choose the optimal technique in an individual case.

The ’H’, ’M’ and ’P’ parameters and the PQI values generated are presented in Table 13.

Comparing 3D-CRT, IMRT and VMAT plans on the basis of the PQID>0.05 threshold, in the whole cohort, the three techniques were equally good in 71 cases (51.4%). VMAT technique was optimal in 45 cases (32.6%), IMRT was preferable in 13 patients (9.4%) and 3D-CRT was the best in 9 cases (6.5%).

When we analysed the 2 techniques based on inverse treatment planning separately on the basis of PQI≥0.05, the PQI was preferable using the VMAT technique in 55 cases (39.9%), while in 14 cases (10.1%) the IMRT plan was the best. VMAT and IMRT were equally good in 69 patients (50.0%).

Patient- and tumour-related characteristics	N=138	
	N	**%**
Menostatus		
Premenopausal (%)	17	12.3
Postmenopausal (%)	121	87.7
Mode of detection		
Screening (%)	109	79.0
Symptomatic (%)	29	21.0
Mammographic appearance (%)		
Circumscribed mass	71	51.4
Spiculated mass	57	41.3
Asymmetric density	7	5.1
No abnormality	1	0.7
Microcalcification (with or without a parenchymal change)	12	8.7
Axillary surgery (%)		
Sentinel lymph node biopsy	121	87.7
Axillary sampling/block dissection	17	12.3
Histological type		
Invasive ductal carcinoma not special type	116	84.1
Invasive lobular carcinoma	2	1.4
Invasive medullary carcinoma	1	0.7
Invasive tubular carcinoma	9	6.5
Invasive mucinous carcinoma	3	2.2
Invasive papillary carcinoma	2	1.4
Invasive mixed ductal/lobular carcinoma	3	2.2
Invasive apocrine carcinoma	1	0.7
Other	1	0.7
Nottingham grade (%)		
1	52	37.7
2	72	52.2
3	14	10.1
Estrogen receptor status (%)		
Positive (≥10%)	124	89.9
Negative (<10%)	14	10.1
Progesteron receptor status (%)		
Positive (≥10%)	115	83.3
Negative (<10%)	23	16.7
HER2 status (%)		
Positive	4	2.9
Negative	134	97.1
Adjuvant chemotherapy (%)	8	5.8
Adjuvant endocrine treatment (%)		
Tamoxifen	10	7.2
Aromatase inhibitor	30	21.7

Table 10. *Patient- and tumour-related characteristics of patients receiving partial breast irradiation*

	Technique	V99% (mean±SD, %)	V107% (mean±SD, %)	CN (mean±SD)	HI (mean±SD)
All cases	3D-CRT	97.27 ± 1.46	3.51 ± 1.53	0.582 ± 0.063	0.083 ± 0.018
	IMRT	97.16 ± 1.64	0.68 ± 0.73	0.833 ± 0.081	0.045 ± 0.010
	VMAT	97.71 ± 0.87	1.45 ± 1.16	0.901 ± 0.032	0.054 ± 0.010
PTV< 100 cm^3	3D-CRT	97.30 ± 1.36	3.46 ± 1.51	0.585 ± 0.061	0.082 ± 0.018
	IMRT	96.85 ± 2.27	0.66 ± 0.79	0.808 ± 0.090	0.046 ± 0.011
	VMAT	97.54 ± 1.16	1.50 ± 1.33	0.900 ± 0.035	0.054 ± 0.011
PTV≥ 100 cm^3	3D-CRT	97.26 ± 1.55	3.56 ± 1.55	0.580 ± 0.065	0.085 ± 0.017
	IMRT	97.42 ± 0.72	0.69 ± 0.67	0.853 ± 0.066	0.044 ± 0.010
	VMAT	97.86 ± 0.46	1.40 ± 1.00	0.902 ± 0.030	0.055 ± 0.009
d< 2.5 cm	3D-CRT	97.56 ± 0.75	3.86 ± 1.29	0.589 ± 0.068	0.089 ± 0.016
	3D-CRT+e	95.75 ± 2.35	4.71 ± 1.55	0.765 ± 0.071	0.082 ± 0.014
	IMRT	96.85 ± 3.20	1.07 ± 0.91	0.785 ± 0.081	0.052 ± 0.010
	IMRT+e	95.20 ± 3.42	2.87 ± 1.39	0.828 ± 0.069	0.060 ± 0.008
	VMAT	97.52 ± 1.65	2.35 ± 1.41	0.870 ± 0.037	0.064 ± 0.007
	VMAT+e	96.75 ± 2.19	3.26 ± 1.34	0.886 ± 0.048	0.065 ± 0.008

Table 11. *Partial breast irradiation according to the radiotherapy technique used: parameters reflecting dose distribution within the PTV and conformity*

Comparing the PQI values of patients for whom the 3D-CRT technique was the most advantageous to those for whom 3D-CRT was either equivalent with IMRT and VMAT, or worse, only the volume of the PTV emerged as significant variable (p=0.017) (Figure 5). The mean±SD of the PTV was 159.3±67.9 cm^3 in patients for whom the 3D-CRT plan was the optimal, 114.4±46.3 cm^3 in those for whom the IMRT technique, and 102.9±50.9 cm^3 in those for whom VMAT was the best; the PTV was 118.3±44.8 cm^3 in those patients for whom all the techniques gave similar PQI. Post hoc tests indicated that the PTVs were larger if the 3D-CRT plan was preferable (3D-CRT *vs.* IMRT: p= 0.035, 3D-CRT *vs.* VMAT: p= 0.002, 3D-CRT *vs.* IMRT/VMAT: p= 0.019).

	Technique	Ipsilateral breast				Ipsilateral lung		Heart		LAD			Contralateral breast		Body
		V100% (mean±SD, %)	V75% (mean±SD, %)	V50% (mean±SD, %)	V25% (mean±SD, %)	mean dose (mean±SD, Gy)	V40% (mean±SD, %)	mean dose (mean±SD, Gy)	V50% (mean±SD, %)	mean dose (mean±SD, Gy)	Dmax (mean±SD, Gy)	V20% (mean±SD, %)	mean dose (mean±SD, Gy)	V10% (mean±SD. %)	V10% rel to PTV (mean±SD)
All cases	3D-CRT	10.1±26.2	15.5±7.3	23.7±8.9	42.4±11.6	3.19±1.40	6.31±3.67	0.93±1.27	0.43±1.19	2.82±3.84	8.90±11.2	13.2±20.5	1.05±1.28	12.8±15.9	17.9±10.7
	IMRT	1.70±1.38	9.06±3.84	18.7±7.6	37.3±11.7	4.81±1.62	7.01±4.18	2.73±1.97	0.66±1.79	3.55±2.11	7.71±5.32	7.5±15.2	1.30±0.52	4.66±7.57	26.4±9.6
	VMAT	0.84±0.72	6.94±3.52	17.2±7.5	35.2±10.4	4.12±1.42	4.87±3.29	2.61±1.78	0.35±1.14	3.65±2.37	6.99±4.72	9.6±18.0	0.79±0.33	0.64±1.73	18.5±5.8
PTV< 100 cm^3	3D-CRT	10.5±38.6	12.0±6.1	19.8±8.2	38.1±11.7	3.23±1.43	6.52±3.51	0.95±1.36	0.39±0.96	2.86±3.75	8.11±10.5	13.5±20.6	1.25±1.33	14.4±16.1	21.6±6.5
	IMRT	1.5±1.3	7.0±2.7	14.6±5.8	31.7±10.8	4.43±1.35	6.69±3.10	2.40±1.81	0.66±1.62	3.45±2.25	7.75±5.36	8.1±15.3	1.33±0.55	6.67±8.96	33.7±8.9
	VMAT	0.5±0.4	4.9±2.3	12.8±5.7	30.8±10.2	3.71±1.13	4.41±2.13	2.29±1.64	0.31±0.91	3.48±2.14	6.80±4.54	8.7±15.7	0.80±0.33	0.65±1.15	22.3±6.0
PTV≥ 100 cm^3	3D-CRT	9.7±4.8	18.4±7.0	27.0±8.2	46.0±10.3	3.16±1.39	6.13±3.81	0.91±1.19	0.47±1.35	2.80±3.93	9.54±11.7	13.0±20.6	0.89±1.22	11.5±15.9	14.8±12.4
	IMRT	1.9±1.4	10.8±3.8	22.2±7.2	41.9±10.3	5.12±1.76	7.28±4.91	3.01±2.07	0.65±1.94	3.64±2.00	7.68±5.32	7.0±15.3	1.27±0.49	3.00±5.80	20.3±4.6
	VMAT	1.1±0.8	8.6±3.5	20.9±6.9	38.9±9.1	4.47±1.55	5.25±3.99	2.88±1.86	0.39±1.31	3.80±2.55	7.15±4.88	10.4±19.9	0.79±0.32	0.62±2.10	15.3±3.1
d< 2.5 cm	3D-CRT	6.79±4.82	12.8±7.51	17.2±9.08	39.8±12.9	2.60±1.22	6.16±3.70	1.25±1.86	0.46±1.23	2.96±3.70	9.69±12.3	15.4±21.3	1.90±1.61	21.8±18.9	17.9±10.7
	3D-CRT+e	2.59±2.28	9.06±5.44	15.1±8.34	27.0±11.8	3.41±1.74	5.96±3.68	1.24±1.33	0.47±1.10	3.44±3.28	11.1±12.5	10.0±16.6	1.28±1.08	18.0±16.3	21.9±6.6
	IMRT	1.76±1.46	7.28±3.43	14.0±6.67	29.9±11.9	4.62±1.81	7.72±4.27	2.97±2.46	0.99±2.27	3.44±2.48	8.94±6.54	10.2±17.9	1.55±0.62	11.6±11.1	26.4±9.6
	IMRT+e	1.17±0.87	6.86±3.83	11.2±5.89	22.8±10.9	4.82±2.12	6.73±4.72	2.40±1.82	0.64±1.35	3.84±3.05	10.7±9.58	17.8±21.3	1.13±0.49	2.38±3.93	24.0±7.8
	VMAT	0.82±0.61	5.42±3.10	12.5±6.81	30.5±11.9	3.85±1.52	5.44±3.27	2.94±2.19	0.62±1.42	4.01±2.61	7.92±5.51	12.7±21.4	1.02±0.42	1.62±3.05	18.5±5.8
	VMAT+e	0.74±0.72	5.63±3.47	10.1±5.68	22.0±10.4	4.31±1.97	5.54±4.26	2.38±1.66	0.49±1.01	4.16±3.05	10.1±9.24	18.7±22.6	0.70±0.28	0.44±1.41	18.8±4.3

Table 12 *Partial breast irradiation according to the radiotherapy technique used: Dose to the organs at risk*

	Technique	Heart left-sided cases		LAD left-sided cases			Heart right-sided cases		LAD right-sided cases		
		mean dose (mean±SD, Gy)	V50% (mean±SD, %)	mean dose (mean±SD, Gy)	Dmax (mean±SD, Gy)	V20% (mean±SD, %)	mean dose (mean±SD, Gy)	V50% (mean±SD, %)	mean dose (mean±SD, Gy)	Dmax (mean±SD, Gy)	V20% (mean±SD, %)
All cases	3D-CRT	1.15±1.21	0.77±1.51	4.07±4.33	13.9±12.4	16.6±19.9	0.66±1.29	0.00±0.00	1.25±2.32	2.69±4.32	9.0±20.6
	IMRT	3.45±2.23	1.08±2.16	4.57±2.17	10.5±5.8	13.5±18.3	1.82±1.05	0.12±0.96	2.27±1.10	4.33±0.73	0.00±0.00
	VMAT	3.16±2.01	0.62±1.48	4.90±2.45	9.9±4.6	17.2±21.3	1.91±1.11	0.01±0.07	2.07±0.80	3.46±1.21	0.00±0.00
PTV< 100 cm^3	3D-CRT	1.06±1.08	0.68±1.20	3.84±4.20	11.7±12.3	15.0±19.4	0.81±1.68	0.00±0.00	1.54±2.58	3.62±5.07	11.4±22.2
	IMRT	3.01±2.10	0.94±1.70	4.52±2.28	10.6±5.8	14.3±18.0	1.59±0.81	0.28±1.44	2.01±1.17	4.21±0.85	0.00±0.00
	VMAT	2.73±1.90	0.52±1.16	4.58±2.14	9.5±4.3	15.3±18.3	1.70±0.94	0.02±0.11	2.01±0.92	3.37±1.47	0.00±0.00
PTV≥ 100 cm^3	3D-CRT	1.22±1.33	0.85±1.75	4.28±4.48	15.9±12.4	17.9±20.5	0.54±0.89	0.00±0.00	1.01±2.11	1.95±3.52	7.0±19.4
	IMRT	3.84±2.28	1.19±2.51	4.61±2.09	10.4±6.0	12.8±18.8	2.01±1.19	0.00±0.00	2.47±1.02	4.43±0.62	0.00±0.00
	VMAT	3.54±2.05	0.71±1.72	5.18±2.70	10.2±4.8	19.0±23.7	2.08±1.22	0.00±0.00	2.12±0.70	3.54±0.97	0.00±0.00
d< 2.5 cm	3D-CRT	1.17±1.43	0.79±1.54	3.48±4.26	13.6±14.9	14.4±19.9	1.36±2.40	0.00±0.00	2.22±2.74	4.82±5.43	16.8±23.9
	3D-CRT+e	1.28±1.09	0.80±1.35	4.80±3.43	17.5±13.5	16.8±18.9	1.20±1.66	0.00±0.01	1.52±1.84	3.25±3.61	0.35±1.23
	IMRT	3.52±2.95	1.68±2.79	4.60±2.52	12.5±6.9	17.4±20.7	2.21±1.29	0.01±0.03	1.80±1.17	4.47±0.92	0.00±0.00
	IMRT+e	2.85±2.12	1.09±1.64	5.67±2.68	16.8±9.0	30.4±19.6	1.77±1.09	0.00±0.01	1.24±0.80	3.03±0.64	0.00±0.00
	VMAT	3.20±2.58	1.02±1.76	5.05±2.88	11.0±5.6	21.6±24.3	2.58±1.50	0.05±0.16	2.54±1.11	4.08±1.72	0.00±0.00
	VMAT+e	2.63±1.91	0.81±1.24	5.86±2.89	15.9±8.6	31.8±21.2	2.02±1.21	0.04±0.10	1.74±0.76	2.78±1.16	0.00±0.00

Table 12A *Partial breast irradiation according to the radiotherapy technique used: Dose to the organs at risk according to side of therapy*

	Technique	H (mean±SD)	M (mean±SD)	P (mean±SD)	PQI (mean±SD)
All cases	3D-CRT	0.598±0.067	0.768±0.069	0.654±0.160	0.595±0.127
	IMRT	0.857±0.087	0.902±0.032	0.544±0.131	0.497±0.126
	VMAT	0.922±0.035	0.868±0.054	0.571±0.128	0.461±0.125
PTV< 100 cm^3	3D-CRT	0.602±0.064	0.771±0.068	0.663±0.177	0.588±0.137
	IMRT	0.836±0.098	0.901±0.035	0.591±0.120	0.464±0.115
	VMAT	0.923±0.039	0.865±0.062	0.613±0.117	0.424±0.113
PTV≥ 100 cm^3	3D-CRT	0.594±0.070	0.765±0.070	0.647±0.145	0.601±0.119
	IMRT	0.876±0.072	0.903±0.030	0.505±0.127	0.524±0.129
	VMAT	0.921±0.033	0.871±0.046	0.535±0.126	0.492±0.128
d< 2.5 cm	3D-CRT	0.604±0.071	0.753±0.059	0.651±0.223	0.607±0.169
	3D-CRT+e	0.799±0.082	0.704±0.072	0.673±0.155	0.505±0.120
	IMRT	0.811±0.089	0.882±0.040	0.576±0.154	0.495±0.133
	IMRT+e	0.870±0.069	0.789±0.059	0.611±0.134	0.475±0.113
	VMAT	0.893±0.042	0.824±0.065	0.568±0.167	0.490±0.149
	VMAT+e	0.916±0.048	0.778±0.059	0.611±0.136	0.467±0.118

Table 13 *The (H)ealthy tissue conformity, the (M)erit function, the (P)enalty function and the PQI according to technique in patients receiving partial breast irradiation*

Comparing the inverse planning techniques (IMRT and VMAT) only, the use of the IMRT method gave superior plans in case of superficially located tumour beds ($p<0.001$) (Figure 6) and if the target volumes were located in the medial/central ($p<0.032$) or upper quadrants ($p<0.046$) of the breast (Table 14).

In case of superficially located PTVs (d<25 mm, 29 patients) the effect of the addition of an electron beam was analysed for all the techniques (3D-CRT, IMRT and VMAT). Two-way repeated measures ANOVA revealed that the magnitude of the effect of adding an electron beam depends on the chosen technique (significant interaction, $p<0.001$). Although the addition of an electron beam improved the PQI of all treatment plans, its extent was relevant (PQI>0.05) only in the 3D-CRT plans, but not in the IMRT or VMAT plans (Table 15, Figure 7).

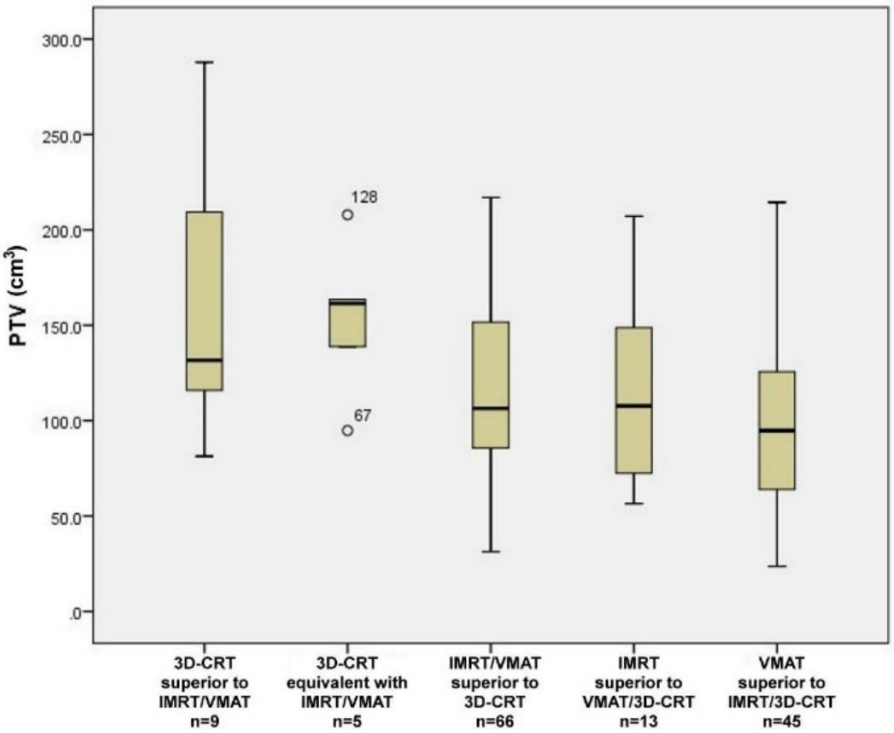

Figure 5 *Comparison of PQI values of those patients receiving partial breast irradiation for whom 3D-CRT was the most advantageous, 3D-CRT was equivalent with IMRT or VMAT, IMRT and VMAT were equivalent but superior to 3D-CRT, IMRT was the most favourable and finally VMAT was the most favourable plan, depending on the volume of the PTV*

		Radiotherapy technique [n (%)]				Radiotherapy technique [n (%)]		
		IMRT better	**Equiva-lent**	**VMAT better**		**IMRT better**	**Equiva-lent**	**VMAT better**
Quadrant	**Lateral**	4 (28.6%)	44 (63.8%)	36 (65.5%)	**Lower**	0 (0%)	21 (30.4%)	12 (21.8%)
	Medial/ central	10 (71.4%)	25 (36.2%)	19 (34.5%)	**Upper**	14 (100%)	48 (69.6%)	43 (78.2%)

Table 14 *The more advantageous radiotherapy technique in relation to the location of the target volume in patients receiving partial breast irradiation*

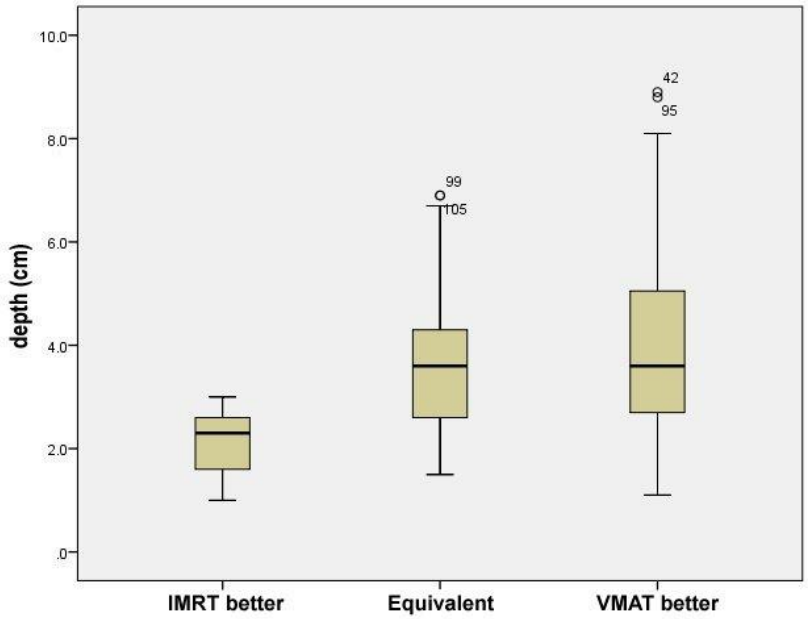

Figure 6 *PQI was superior with IMRT in cases with superficially located target volumes than with VMAT in patients receiving partial breast irradiation*

	Mean ± SD of PQI	**PQID**	**95% Confidence interval for PQID**	**p**
IMRT	0.495 ± 0.025	0.020	0.000-0.039	0.055
IMRT + electron	0.475 ± 0.021			
VMAT	0.490 ± 0.028	0.023	0.002-0.045	0.037
VMAT + electron	0.467 ± 0.022			
3D-CRT	0.607 ± 0.031	0.102	0.070-0.133	<0.001
3D-CRT + electron	0.505 ± 0.022			

Table 15 *Mean differences of PQI values regarding the effect of adding an 'en face' electron beam to photon beams using IMRT, VMAT and 3D-CRT techniques in patients receiving partial breast irradiation*

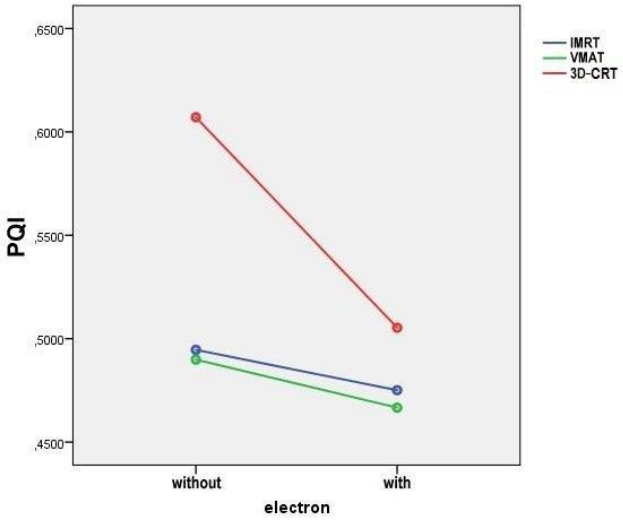

Figure 7 *The effect of adding an 'en face' electron beam to photon beams on IMRT, VMAT and 3DCRT plans in patients receiving partial breast irradiation as depicted on a profile figure*

In 67 cases with PQI differences >0.05, we analysed which components (H, M and P function) were the primary determinants of PQI according to the three radiotherapy techniques. We found that the best PQI value of a case was primarily dependent on the P function representing OAR exposure. This function was the strength of the few (n=9) 3D-CRT-preferred cases with a relatively large PTV (mean: 159.3 cm^3, range: 81.3-287.8 cm^3) (Figure 8).

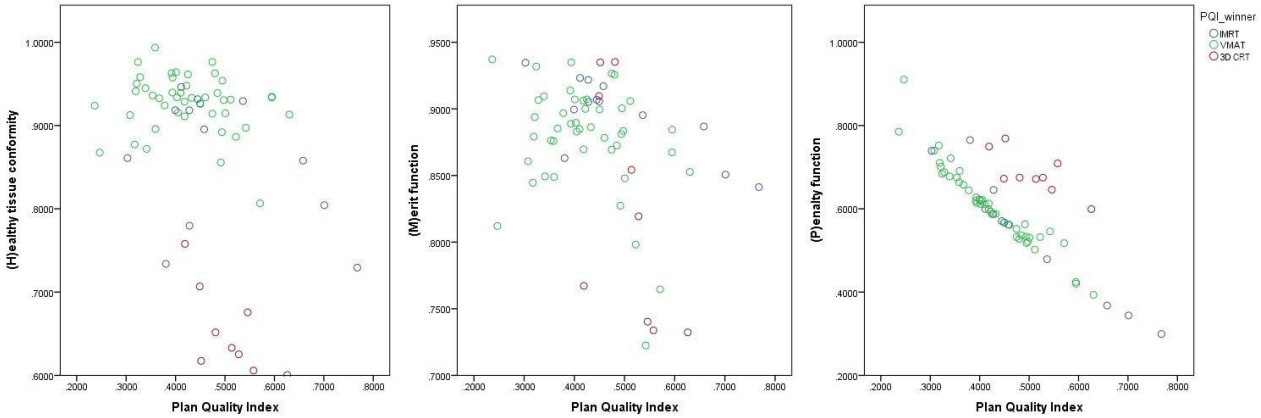

Figure 8 *Representation of the effect of the components of the PQI according to the preferable plan (IMRT, VMAT or 3D-CRT) in patients receiving partial breast irradiation*

5 Discussion

5.1 Prone positioning on a belly board decreases rectal and bowel doses in pelvic IMRT for prostate cancer

Clinically localized high-risk prostate cancer frequently shows micrometastatic spreading to the pelvic lymph nodes; therefore, RT and three years of androgen suppressing endocrine treatment are the standard of care. Dose escalation to the prostate even to 80–86.4 Gy reduces biochemical failure and the appearance of distant metastases [21]. However, survival data are controversial regarding field size [21]. There is no consensus recommendation for patient selection for pelvic RT in this population, considering the increased exposure of OARs and toxicity. 90% of patients treated with pelvic RT develop permanent alterations in bowel habits [22], 50% of them complain about adverse changes in life quality [23], and 20–40% of them assess this impact as moderate or severe [24]. The small intestine, the rectum, and to a lesser extent, the colon are dose-limiting organs, tolerating a 50–60 Gy dose at conventional fractionation [25,26]. Normal tissue complication probability (NTCP) studies suggest that the small intestine volume receiving 15 and 45 Gy (V_{15Gy} and V_{45Gy}) is a relevant parameter for GI morbidity [27,28]. According to the review of Fiorino et al. [29], keeping V_{70Gy} and V_{75Gy} to <25% and <5%, respectively, results in a decrease in the development of late rectal bleeding. Moderate dose volumes, such as V_{40Gy} and V_{50Gy} are predictive for chronic late incontinence [30] and are also important in developing rectal bleeding [29,30]. The dosimetric analysis [31] of the anatomical subregions showed that rectal bleeding is associated with V_{70Gy} of the anorectal region, fecal incontinence with V_{15Gy} of external sphincter, and V_{55Gy} of the iliococcygeal muscle, whereas stool frequency with V_{40Gy} of the levator ani and V_{45Gy} of the iliococcygeal muscle. In the prospective study of Dréan et al. [32], rectal subregions at risk have been delineated, and the authors have found that the exposure of the subprostatic anterior hemirectum and the upper part of the anal canal was 4 Gy higher in patients developing rectal bleeding.

Technological advances allowing rectal sparing include the use of endorectal balloons filled with air or water, reducing the exposure of the posterior rectal wall by moving away the prostate from it, depending on the volume of the balloons [33]. Bioabsorbable tissue spacers injected

into the retroprostatic fascia also increase the distance between the prostate and the anterior rectal wall, resulting in significant reduction in both acute and late GI toxicities [34]. Regarding patient positioning, Zelefsky et al. [35] and McLaughlin et al. [36] have described significantly lower rectal doses in the prone position, using 3D-CRT technique. The results have also been confirmed in the phase II trial of O'Neil et al. [37] and by Bajon et al. using tomotherapy [38]. Nevertheless, Baylay et al. [39] have found supine position more favourable by using larger PTV margins in prone position, and Kato et al. [40] by applying IMRT in supine and 3D-CRT in prone position. In prone position, the decreased rectal exposure is a result of the posterior retraction of the rectum and anterior displacement of the prostate; however, the accurate mechanism of it is unknown [35, 36, 40].

In 3D-CRT of rectal malignancies, the prone treatment position even without a belly board results in the reduction of the irradiated small intestine volume as compared to the supine posture [41]. In case of pelvic malignancies, a larger decrease in the small intestine exposure can be obtained by the additional use of a belly board in comparison with both prone position alone [42,43] or supine position [44,45]. The use of IMRT technique decreases bowel doses by 40–50%, as compared to 3D-CRT [46,47]. In case of gynecological and rectal tumours, a belly board-assisted prone position using IMRT results in a further reduction in the irradiated volume of the small intestine, even in the low dose areas [48,49]. The advantage of the use of a belly board is also confirmed in postoperatively irradiated patients [50,51], which might be the consequence of the significantly higher mobilization of the small intestine loops. The findings of Fu et al. [52] show that the gain of the use of a belly board is greater if the irradiated small intestine volume close to the target volume is larger. According to that study, a prone position on a belly board results in a remarkable decrease in the small bowel volume in case of gynecological malignancies but not in rectal cancer patients. A full bladder also functions as a natural spacer, transposing the small intestine loops from the pelvis to the abdomen, resulting in a reduction in the irradiated small intestine volume [50].

In rectal cancer patients treated with chemo-radiotherapy, Baglan et al. [27] have demonstrated an explicit relationship between the volume of the small bowel receiving at least 15 Gy and the degree of acute small intestinal toxicity. Robertson et al. [53] have proved that a reduction in

the small bowel volume receiving low dose results in a significant decrease in the complication rate. Both authors have delineated the single small intestinal loops. In case of gynecological cancer patients treated with pelvic IMRT, Roeske et al. [28], contouring the peritoneal cavity, have detected that the risk of acute gastrointestinal toxicity is five times as little for small bowel volume of 100 cm^3 gaining the prescribed 45 Gy dose as of 200 cm^3. According to Gunnlaugsson et al. [54], the delineation of single small intestinal loops is the recommended contouring method instead of delineating the peritoneal cavity, as they have observed strong correlation between the occurrence of early side effects and small intestinal loop exposure, and no significant connection with the peritoneal cavity.

Our study was limited by the lack of delineating the penile bulb, and the relatively small number of patients involved, which however was double the number of patients previously reported. As most papers have described larger intrafraction prostate motion in prone position [8] and literature data [55] show that a 3 mm PTV margin allows for CTV to be covered for 99% of cases when daily CBCT is used, accurate patient repositioning, daily reconstruction of the rectum, prostate safety margins, early toxicity and life quality during and after RT were also evaluated, and found to be similar to literature data of patients treated in supine position [56]. Late toxicities need further examination due to the short follow-up period.

5.2 A simple clinical method for predicting the benefit of prone vs. supine positioning in reducing heart exposure during left breast radiotherapy

According to the present study and others [12,57-60], in about 20% of the cases, prone positioning during left breast radiotherapy increases the dose to the LAD or the heart. To estimate and select the preferable positioning mode, supine CT seems the best approach to consider the patient's anatomical determinants. We have shown that a single CT scan at the middle of the heart may replace a whole CT series by providing consistent anatomical data thus avoiding extra radiation exposure to the patient and work load to the staff. Based on the outcome of the external validation of the method on an independent case series, we recommend its use after local testing.

Our validated statistical model for predicting the preferable treatment position utilizes 3 specific measures and seems the most complex predictive tool for this purpose in the literature [12]. In other studies, the in-field heart volume [61-63] and most frequently the size of the breast [3,57] have been used for selection. Increased BMI has also been related to larger heart doses [64] or consequential radiation cardiac morbidity [65], but its role in predicting benefit of prone positioning may be refined by the use of other patient-related parameters [12]. We consider the BMI in our calculator as a stable parameter while there is potential uncertainty in the specification of P_{ref} or imprecision in the actual measurement of D_{median} or A_{heart} on a given image. Nevertheless, detailed analysis indicates that accidental imprecision does not significantly influence final prediction (data not shown). The dose constraints optimized by individual positioning provides additional safety in practice. Despite the lack of full equivalence of the data extracted from the original method *vs.* the new method, the ultimate consistency still seems to qualify the developed „simple tool" for clinical application.

External validation indicated similar accuracy as the originally developed method. Despite the reassuring results of the validation on an independent series of patients in a radiotherapy centre using a slightly different protocol, the utility of the reported clinical tool could be compromised by the diversity of practice in others. PTV contouring depends on repositioning accuracy and the method of treatment verification. Interfractional differences may be especially large in the prone position [13,66]. Lakosi et al. found population systematic error values of 4.5/3.9/3.3 mm in the lateral/longitudinal/vertical directions, while the random error was 5.4/3.8/2.8 mm [15]. Among our recent prone breast radiotherapy cases, the population systematic and random error in the lateral/longitudinal/vertical directions was 3.4/2.3/2.7 mm and 7.8/4.6/6.9 mm, respectively. Only some groups study the dose to the coronary arteries [12,54,60,67-70]. The outlining of the coronary vessels shows significant inter-observer variation that may jeopardize dose verification in the selected position. [16,71]. Different approaches have been tested to improve consistency including the administration of contrast media [16,71,72]. Lee et al. developed a new protocol to outline the LAD region which included 96% of the LAD volume as delineated by 4 experienced radiation oncologists [72]. Significant impact was made by the implementation of specific guidelines [16,71,72]. Since the utility of the simple tool might be influenced by several factors, we consider essential its testing before routine use.

The benefit of positioning prone *vs.* supine may be discordant by means of LAD and heart doses [12,57,70]. We regard the LAD dose as a surrogate indicator of radiation harm due to its proven role in late cardiac morbidity [2] and because the LAD being situated on the anterior surface of the heart is a sensitive marker of danger if the heart is at all included into radiation. Our strategy for optimization in individual cases is to consider the MD_{LAD} as priority that is usually confirmed by the heart dose (as was true for 92% of cases in our series).

The radiation exposure of the heart may be significantly reduced by the use of respiration-guided techniques including the deep inspiration breath hold (DIBH) technique and respiratory gating. In the UK HeartSpare study, supine DIBH provided superior cardiac sparing than a free-breathing prone position in larger-breasted women [67]. Interestingly, the implementation of DIBH in the prone position gave the optimal heart sparing results as compared with that in the supine position or free-breathing [68]. There are some centres that due to resource limitations prioritise high cardiac dose cases for DIBH [73]. Our tool could be used for patients either not amenable for or not having access to DIBH due to patient-specific features or limited/no resources.

We think that since a linear, no-threshold association exists between the mean heart dose and coronary events [2], doses to the LAD, right coronary artery or the circumflex artery should be controlled [60]. Nevertheless, the utilization of heart dose-volume data only is a possibility if LAD contouring can not be afforded. Since good agreement exists between the mean heart dose and $V_{25Gyheart}$ (Rprone: 0.98, Rsupine: 0.99) or MD_{LAD} (Rprone and Rsupine: 0.87) in both positions ($p<0.001$ in all comparisons), the here presented tool could be adapted to practices which adher to the consideration of the mean heart dose.

5.3 Dosimetric comparison of 3D-CRT, sliding window IMRT and VMAT techniques for external beam accelerated partial breast radiotherapy

In selected early breast cancer cases, APBI is an attractive treatment alternative to whole breast irradiation by shortening the course of RT and reducing radiation exposure of healthy tissues significantly [6,74,75]. Various teletherapy techniques have been studied for APBI with

different dosimetric specialities [76-82]. Our findings indicate that IMRT, VMAT or 3D-CRT may be individually superior in at least half of the cases; by selecting the most advantageous APBI method, dose homogeneity and OAR exposure could be optimised. The here described PQI that takes into account both homogeneity, conformity and dose to various OARs may serve as a comprehensive tool for comparing teletherapy APBI plans.

Many studies analysed the dosimetry of inverse-planning techniques over standard 3D-CRT [83-88]. The use of IMRT or VMAT improved conformity in all studies, and in most of them selected OARs' exposure as well. With the use of IMRT, the reduction of the dose to the ipsilateral breast [84,85], lung and heart [85] was achieved as compared to that of 3D-CRT plans. In the study of Rusthoven et al. [85], the ipsilateral breast dose was especially more favourable with IMRT than with 3D-CRT in cases with larger PTV/breast ratio and smaller breasts. Interestingly, we found altogether 9 cases out of 138 with relatively larger PTVs, in which 3D-CRT provided the best PQI probably due to the formula's complexity. Using the VMAT technique, the dose to the lung and heart was lower than that with 3D-CRT [89]. Qiu et al. [87] performed a dosimetric analysis of 16 VMAT *vs.* IMRT *vs.* 3D-CRT plans. The dose (V_{5Gy}, V_{10Gy}) to the ipsilateral breast was significantly lower with VMAT than the other 2 techniques. Heart exposure was similar among the three techniques while lung dose was superior with IMRT and VMAT than with 3D-CRT; IMRT provided the most favourable low-dose distribution in the ipsilateral lung [87].

Stelczer et al. [88] compared the step and shoot and sliding window IMRT methods and the VMAT technique to the 3D-CRT technique based on various dosimetric parameters and the original PQI approach [19] in 10 low-risk breast cancer cases. While dose homogeneity was superior using the sliding window IMRT, in accordance with our results, ipsilateral breast exposure was significantly lower with VMAT, and the protection of the lung and heart was the best with 3DCRT [88]. $V_{50\%}$ of the ipsilateral breast was the lowest in VMAT plans (29.4%), as compared to 3D-CRT (44.1%) and sliding window IMRT (35.6%) plans. As a consequence, they recommend the use of sliding window IMRT for APBI [88].

The addition of electrons to photon beams provides more conformal but less homogenous dose distribution as compared to the photon only technique. We have found five studies dealing with

the mixed beam technique in APBI [83,90-93]. All agreed that this approach may lower the ipsilateral breast dose; lung and heart doses varied according to study, and obviously the situation of the tumour bed [92]. Clearly, the use of electrons should be reserved for tumours non-deeply located [94]. In the present study, the addition of a shaped electron field to 3D-CRT provided benefit in cases with d<25 mm. We believe that this method could be recommended if due to limitations of resources or technology 3D-CRT were utilized for APBI.

In selected cases, APBI provides similar efficacy and less toxicity versus whole breast irradiation with probably better cosmesis and acceptance by the patients [95,96]. Most prospective phase II and phase III studies utilizing 3D-CRT technique for APBI have reported favourable early and late side effect profile, good or excellent cosmetic results and quality of life comparable to that with whole breast irradiation [79,96-99]. Likewise, excellent outcome was reported in studies with IMRT [81,82]. Nevertheless, in some APBI studies implementing the IMRT [80,100] or 3D-CRT method [101,102] progressive breast fibrosis and poor cosmetic outcome was reported. In the most recently reported RAPID trial, more fibrosis and progressively deteriorating cosmetic outcome was found after APBI with 3D-CRT/IMRT than after whole breast radiotherapy [103]. All these studies applied similar doses as the other teletherapy APBI trials, but in an accelerated manner (dosing twice daily). Impaired cosmetic results following 3D-CRT or IMRT APBI could have been also due to the irradiation of larger target volumes and more extensive ipsilateral breast tissue as well. The detrimental effect of large irradiated volumes on fibrosis-related poor cosmesis had been described in the 1990s [104]. Based on our results, if ipsilateral breast dose is a concern we propose the VMAT technique, or if 3D-CRT is to be utilised, the addition of electrons.

Our study suggests that while dose coverage and acceptable homogeneity may be ensured by any of the studied techniques, the main differences may be detected in OAR exposure in about 50% of the cases. Namely the dose to the heart and LAD and the success to limit the radiation dose to the ipsilateral breast much depend on the selected method. For the evaluation of different techniques, different measures have been used in the literature. Most of the studies compared various dose-volume parameters, OAR exposure, maximum doses, coverage or more complex indexes such as conformity index, conformation number, homogeneity index or the PQI which we used [19]. All parameters carry different meanings, but if used singly,

comparisons are difficult. This is why we aimed at following a comprehensive approach which is based on the simultaneous consideration of various factors such as homogeneity, conformity and OAR protection. Since in our study conformity and homogeneity did not differ as significantly as OAR exposures in the different plans (Figure 8), PQID mainly depended on which technique ensured the best comprehensive OAR protection. The strength of our method is that we based it on a relatively large and comprehensive data set.

6 Summary, conclusions

6.1 During pelvic IMRT in prostate cancer, prone positioning on a belly board decreases the irradiated small bowel volumes even in the low dose ranges and contributes to rectal sparing. The relative dose reduction in the rectal exposure might be a consequence of the slightly increasing distance between the prostate wall and the rectal wall, and the increasing volume and diameters of the rectum generated by the displacement of rectal gases. Considering the dosimetric advantages, prone position on a belly board is recommended for pelvic IMRT in prostate cancer.

6.2 Great consistency of our method based on a validated model for the prediction of treatment position prone *vs.* supine with less heart exposure during left breast RT has been demonstrated; the simplified tool presented here omits the performance of planning CT in both positions. Based on the results of its external validation, we truly recommend its use in centres that apply prone positioning in routine practice.

6.3 PQI is a good tool to evaluate external beam APBI plans. In most cases, IMRT and especially VMAT plans give superior PQI values than 3D-CRT plans. 3D-CRT may be favourable in cases with large PTV. In superficially situated tumour beds the addition of an electron beam results in significant PQI improvement of 3D-CRT plans. Comparing the IMRT and VMAT methods, IMRT seems superior in tumours of the superior or inner quadrant of the breast. PQI is primarily dependent on OAR exposure.

7 Acknowledgements

First of all, I express my gratitude to my supervisor, Zoltán Varga, Ph.D., who has helped and encouraged me during my studies and supported me in the completion of this work.

I am very grateful to Professor Zsuzsanna Kahán, director of the Department of Oncotherapy, University of Szeged, for guiding me in all my scientific and professional activities and providing excellent working conditions for me at the institute.

I am greatly indebted to Anikó Maráz, M.D., Ph.D., Katalin Hideghéty, M.D., Ph.D., Adrienne Cserháti, M.D., Linda Varga, M.D., Zsófia Együd, M.D., Csilla Szabó, M.D., Emőke Borzási, M.D., Szilvia Gaál, M.D., Emese Fodor and Barbara Darázs, whose invaluable support significantly contributed to my scientific work.

The important instructive guidance in the field of biostatistics by Ferenc Rárosi and Krisztina Boda, Ph.D. are highly esteemed.

I greatly appreciate all the support and work of high standard provided by physician, physicist and technician colleagues of the Department of Oncotherapy, University of Szeged that helped this thesis to be born.

I would like to express my sincere gratitude to my family, husband, parents and sister for their endless love, patience and support in all my efforts.

8 References

[1] Lukka H, Warde P, Pickles T, et al; Canadian GU Radiation Oncologist Group. Controversies in prostate cancer radiotherapy: consensus development. Canadian GU Radiation Oncologist Group. Can J Urol. 2001;8:1314-1322.

[2] Darby SC, Ewertz M, McGale P, et al. Risk of ischemic heart disease in women after radiotherapy for breast cancer. N Engl J Med. 2013;368:987–998.

[3] Taylor CW, Kirby AM. Cardiac side-effects from breast cancer radiotherapy. Clin Oncol (R Coll Radiol). 2015;7:621-629.

[4] Shah C, Badiyan S, Berry S, et al. Cardiac dose sparing and avoidance techniques in breast cancer radiotherapy. Radiother Oncol. 2014;112:9-16.

[5] Shah C, Wobb J, Manyam B, et al. Accelerated partial breast irradiation utilizing brachytherapy: patient selection and workflow. J Contemp Brachytherapy. 2016;8:90-94.

[6] Polgár C, Van Limbergen E, Pötter R, et al.; GEC-ESTRO breast cancer working group. Patient selection for accelerated partial-breast irradiation (APBI) after breast-conserving surgery: Recommendations of the Groupe Européen de Curiethérapie-European Society for Therapeutic Radiology and Oncology (GEC-ESTRO) breast cancer working group based on clinical evidence (2009). Radiother Oncol. 2010;94:264-273.

[7] Correa C, Harris EE, Leonardi MC, et al. Accelerated Partial Breast Irradiation: Executive summary for the update of an ASTRO Evidence-Based Consensus Statement. Pract Radiat Oncol. 2017;7:73-79.

[8] Sobin LH, Gospodarowicz MK, Wittekind C. TNM Classification of Malignant Tumors, 7th Edition. Wiley-Blackwell; 2009.

[9] Mellinger GT, Gleason D, Bailar J 3rd. The histology and prognosis of prostatic cancer. J Urol. 1967;97:331–337.

[10] Lawton CAF, Michalski J, El-Naga I, et al. RTOG GU radiation oncology specialists reach consensus on pelvic lymph node volumes for high-risk prostate cancer. Int J Radiat Oncol Biol Phys. 2009;74:383-387.

[11] Viswanathan AN, Yorke ED, Marks LB, et al. Radiation dose-volume effects of the urinary bladder. Int J Radiat Oncol Biol Phys. 2010;76(Suppl 3):S116-122.

[12] Varga Z, Cserháti A, Rárosi F, et al. Individualized positioning for maximum heart protection during breast irradiation. Acta Oncol. 2014;53:58-64.

[13] Varga Z, Hideghéty K, Mező T, et al. Individual positioning: A comparative study of adjuvant breast radiotherapy in the prone versus supine position. Int J Radiat Oncol Biol Phys. 2009;75:94-100.

[14] Feng M, Moran JM, Koelling T, et al. Development and validation of a heart atlas to study cardiac exposure to radiation following treatment for breast cancer. Int J Radiat Oncol Biol Phys. 2011;79:10-18.

[15] Lakosi F, Gulyban A, Ben-Mustapha Simoni S, et al. Feasibility evaluation of prone breast irradiation with the Sagittilt© system including residual-intrafractional error assessment. Cancer Radiother. 2016;20:776-782.

[16] Duane F, Aznar MC, Bartlett F, et al. A cardiac contouring atlas for radiotherapy. Radiother Oncol. 2017;122:416-422.

[17] van't Riet A, Mak AC, Moerland MA, et al. A conformation number to quantify the degree of conformality in brachytherapy and external beam irradiation: Application to the prostate. Int J Radiat Oncol Biol Phys. 1997;37:731-736.

[18] Shaw E, Kline R, Gillin M, et al. Radiation Therapy Oncology Group: Radiosurgery quality assurance guidelines. Int J Radiat Oncol Biol Phys. 1993;27:1231-1239.

[19] Leung LHT, Kan MWK, Cheng ACK, et al. A new dose-volume-based Plan Quality Index for IMRT plan comparison. Radiother Oncol. 2007;85:407-417.

[20] Lomax NJ, Scheib SG. Quantifying the degree of conformity in radiosurgery treatment planning. Int J Radiat Oncol Biol Phys. 2003;55:1409-1419.

[21] Juloori A, Shah C, Stephans K, et al. Evolving paradigm of radiotherapy for high-risk prostate cancer: current consensus and continuing controversies. Prostate Cancer. 2016;2016:2420786.

[22] Olopade F, Norman A, Blake P, et al. A modified Inflammatory Bowel Disease questionnaire and the Vaizey Incontinence questionnaire are simple ways to identify patients with significant gastrointestinal symptoms after pelvic radiotherapy. Br J Cancer. 2005;92:1663-1670.

[23] Gami B, Harrington K, Blake P, et al. How patients manage gastrointestinal symptoms after pelvic radiotherapy. Aliment Pharmacol Therapeut. 2003;18:987-994.

[24] Andreyev H. Gastrointestinal symptoms after pelvic radiotherapy: a new understanding to improve management of symptomatic patients. Lancet Oncol. 2007;8:1007-1017.

[25] Letschert JGJ. The prevention of radiation-induced small bowel complications. Eur J Cancer. 1995;31:1361-1365.

[26] Michalski JM, Gay H, Jackson A, et al. Radiation dose-volume effects in radiation-induced rectal injury. Int J Radiat Oncol Biol Phys. 2010;76(Suppl 3):S123-129.

[27] Baglan KL, Frazier RC, Yan D, et al. The dose–volume relationship of acute small bowel toxicity from concurrent 5-FU-based chemotherapy and radiation therapy for rectal cancer. Int J Radiat Oncol Biol Phys. 2002;52:176–183.

[28] Roeske JC, Bonta D, Mell LK, et al. A dosimetric analysis of acute gastrointestinal toxicity in women receiving intensity-modulated whole-pelvic radiation therapy. Radiother Oncol. 2003;69:201–207.

[29] Fiorino C, Valdagni R, Rancati T, et al. Dose-volume effects for normal tissues in external radiotherapy: pelvis. Radiother Oncol. 2009;93:153–167.

[30] Peeters ST, Hoogeman MS, Heemsbergen WD, et al. Rectal bleeding, fecal incontinence, and high stool frequency after conformal radiotherapy for prostate cancer: normal tissue complication probability modeling. Int J Radiat Oncol Biol Phys. 2006;66:11–19.

[31] Schaake W, van der Schaaf A, van Dijk LV, et al. Normal tissue complication probability (NTCP) models for late rectal bleeding, stool frequency and fecal incontinence after radiotherapy in prostate cancer patients. Radiother Oncol. 2016;119:381-387.

[32] Dréan G, Acosta O, Ospina JD, et al. Identification of a rectal subregion highly predictive of rectal bleeding in prostate cancer IMRT. Radiother Oncol. 2016;119:388–397.

[33] van Lin EN, Hoffmann AL, van Kollenburg P, et al. Rectal wall sparing effect of three different endorectal balloons in 3D conformal and IMRT prostate radiotherapy. Int J Radiat Oncol Biol Phys. 2005;63:565–576.

[34] Serrano N, Kalman NS, Anscher MS. Reducing rectal injury in men receiving prostate cancer radiation therapy: current perspectives. Cancer Manag Res. 2017;9:339-350.

[35] Zelefsky MJ, Happersett L, Leibel SA, et al. The effect of treatment positioning on normal tissue dose in patients with prostate cancer treated with three-dimensional conformal radiotherapy. Int J Radiat Oncol Biol Phys. 1997;37:13-19.

[36] McLaughlin PW, Wygoda A, Sahijdak W, et al. The effect of patient position and treatment technique in conformal treatment of prostate cancer. Int J Radiat Oncol Biol Phys. 1999;45:407–413.

[37] O'Neil L, Armstrong J, Buckney S, et al. A phase II trial for the optimisation of treatment position in the radiation therapy of prostate cancer. Radiother Oncol. 2008;88:61–66.

[38] Bajon T, Piotrowski T, Antczak A, et al. Comparison of dose-volume histograms for supine and prone position in patients irradiated for prostate cancer – A preliminary study. Rep Pract Oncol Radiother. 2011;16:65-70.

[39] Bayley AJ, Catton CN, Haycocks T, et al. A randomized trial of supine vs. prone positioning in patients undergoing escalated dose conformal radiotherapy for prostate cancer. Radiother Oncol. 2003;70:37–44.

[40] Kato T, Obata Y, Kadoya N, et al. A comparison of prone three-dimensional conformal radiotherapy with supine intensity-modulated radiotherapy for prostate cancer: which technique is more effective for rectal sparing? Br J Radiol. 2009;82:654–661.

[41] Drzymala M, Hawkins MA, Henrys AJ, et al. The effect of treatment position, prone or supine, on dose–volume histograms for pelvic radiotherapy in patients with rectal cancer. Br J Radiol. 2009;82:321-327.

[42] Kim TH, Chie EK, Kim DY, et al. Comparison of the belly board device method and the distended bladder method for reducing irradiated small bowel volumes in preoperative radiotherapy of rectal cancer patients. Int J Radiat Oncol Biol Phys. 2005;62:769-775.

[43] Huh SJ, Park W, Ju SG, et al. Small-bowel displacement system for the sparing of small bowel in three-dimensional conformal radiotherapy for cervical cancer. Clin Oncol. 2004;16:467-473.

[44] Martin J, Fitzpatrick K, Horan G, et al. Treatment with a belly-board device significantly reduces the volume of small bowel irradiated and results in low acute toxicity in adjuvant radiotherapy for gynecologic cancer: results of a prospective study. Radiother Oncol. 2005;74:267-274.

[45] Pinkawa M, Gagel B, Demirel C, et al. Dose–volume histogram evaluation of prone and supine patient position in external beam radiotherapy for cervical and endometrial cancer. Radiother Oncol. 2003;69:99-105.

[46] Mundt A, Roeske J, Lujan A. Intensity-modulated radiation therapy in gynecologic malignancies. Med Dosimetry. 2002;27:131-136.

[47] Portelance L, Chao K, Grigsby P, et al. Intensity-modulated radiation therapy (IMRT) reduces small bowel, rectum, and bladder doses in patients with cervical cancer receiving pelvic and para-aortic irradiation. Int J Radiat Oncol Biol Phys. 2001;51:261-266.

[48] Stromberger C, Kom Y, Kawgan-Kagan M, et al. Intensity-modulated radiotherapy in patients with cervical cancer. An intra-individual comparison of prone and supine positioning. Radiat Oncol. 2010;5:63–68.

[49] Beriwal S, Jain SK, Heron DE, et al. Dosimetric and toxicity comparison between prone and supine position IMRT for endometrial cancer. Int J Radiat Oncol Biol Phys. 2007;67:485-489.

[50] Kim TH, Kim DY, Cho KH, et al. Comparative analysis of the effects of belly board and bladder distension in postoperative radiotherapy of rectal cancer patients. Strahlenther Onkol. 2005;9:601-605.

[51] Saynak M, Kucucuk S, Aslay I. Abdominal pillow for the sparing of small bowel in four-field conventional pelvic radiotherapy. Eur J Gynaecol Oncol. 2008;29:643-648.

[52] Fu YT, Lam JC, Tze JM. Measurement of irradiated small bowel volume in pelvic irradiation and the effect of a belly board. Clin Oncol (R Coll Radiol). 1995;7:188-192.

[53] Robertson JM, Lockman D, Yan D, et al. The dose-volume relationship of small bowel irradiation and acute grade 3 diarrhea during chemoradiotherapy for rectal cancer. Int J Radiat Oncol Biol Phys. 2008;70:413-418.

[54] Gunnlaugsson A, Kjellen E, Nilsson P, et al. Dose–volume relationships between enteritis and irradiated bowel volumes during 5-fluorouracil and oxaliplatin based chemoradiotherapy in locally advanced rectal cancer. Acta Oncol. 2007;46:937-944.

[55] Gill SK, Reddy K, Campbell N, et al. Determination of optimal PTV margin for patients receiving CBCT-guided prostate IMRT: comparative analysis based on CBCT dose calculation with four different margins. J Appl Clin Med Phys. 2015;16:252-262.

[56] Varga L, Kószó R, Fodor E, et al. Daily setup accuracy, side-effects and quality of life during and after prone positioned prostate radiotherapy. Anticancer Res. 2018;38:3699.

[57] Kirby AM, Evans PM, Donovan EM, et al. Prone versus supine positioning for whole and partial-breast radiotherapy: a comparison of non-target tissue dosimetry. Radiother Oncol. 2010;96:178-184.

[58] Lymberis SC, DeWyngaert JK, Parhar P, et al. Prospective assessment of optimal individual position (prone versus supine) for breast radiotherapy: Volumetric and dosimetric correlations in 100 patients. Int J Radiat Oncol Biol Phys 2012;84:902-909.

[59] Formenti SC, DeWyngaert JK, Jozsef G, et al. Prone vs supine positioning for breast cancer radiotherapy. JAMA. 2012;308:861-863.

[60] Würschmidt F, Stoltenberg S, Kretschmer M, et al. Incidental dose to coronary arteries is higher in prone than in supine whole breast irradiation. A dosimetric comparison in adjuvant radiotherapy of early stage breast cancer. Strahlenther Onkol. 2014;190:563-568.

[61] DeWyngaert JK, Jozsef G, Mitchell J, et al. Accelerated intensity-modulated radiotherapy to breast in prone position: dosimetric results. Int J Radiat Oncol Biol Phys. 2007;68:1251-1259.

[62] Formenti SC, Gidea-Addeo D, Goldberg JD, et al. Phase I–II trial of prone accelerated intensity modulated radiation therapy to the breast to optimally spare normal tissue. J Clin Oncol. 2007;25:2236-2242.

[63] Zhao X, Wong EK, Wang Y, et al. A support vector machine (SVM) for predicting preferred treatment position in radiotherapy of patients with breast cancer. Med Phys. 2010;37:5341-5350.

[64] Evans SB, Sioshansi S, Moran MS, et al. Prevalence of poor cardiac anatomy in carcinoma of the breast treated with whole-breast radiotherapy: Reconciling modern cardiac dosimetry with cardiac mortality data. Am J Clin Oncol. 2012;35:587–592.

[65] Evans ES, Prosnitz RG, Yu X, et al. Impact of patient-specific factors, irradiated left ventricular volume, and treatment set-up errors on the development of myocardial perfusion defects after radiation therapy for left-sided breast cancer. Int J Radiat Oncol Biol Phys. 2006;66:1125–1134.

[66] Mulliez T, Gulyban A, Vercauteren T, et al. Setup accuracy for prone and supine whole breast irradiation. Strahlenther Onkol. 2016;192:254-259.

[67] Bartlett FR, Colgan RM, Donovan EM, et al. The UK HeartSpare Study (Stage IB): randomised comparison of a voluntary breath-hold technique and prone radiotherapy after breast conserving surgery. Radiother Oncol. 2015;114:66-72.

[68] Mulliez T, Veldeman L, van Greveling A, et al. Hypofractionated whole breast irradiation for patients with large breasts: A randomized trial comparing prone and supine positions. Radiother Oncol. 2013;108:203-208.

[69] Mulliez T, Veldeman L, Speleers B, et al. Heart dose reduction by prone deep inspiration breath hold in left-sided breast irradiation. Radiother Oncol. 2015;114:79-84.

[70] Verhoeven K, Swelden C, Petillion S, et al. Breathing adapted radiation therapy in comparison with prone position to reduce the doses to the heart, left anterior descending artery and contralateral breast in whole breast radiation therapy. Pract Radiat Oncol. 2014;4:123-129.

[71] Lorenzen EL, Taylor CV, Maraldo M, et al. Inter-observer variation in delineation of the heart and left anterior descending coronary artery in radiotherapy for breast cancer: A multi-centre study from Denmark and the UK. Radiother Oncol. 2013;108:254-258.

[72] Lee J, Hua K-L, Hsu S-M, et al. Development of delineation for the left anterior descending coronary artery region in left breast cancer radiotherapy: An optimized organ at risk. Radiother Oncol. 2017;122:423-430.

[73] Tanna N, McLauchlan R, Karis S, et al. Assessment of upfront selection criteria to prioritise patients for breath-hold left-sided breast radiotherapy. Clin Oncol (R Coll Radiol). 2017;29:356-361.

[74] Veronesi U, Marubini E, Mariani L, et al. Radiotherapy after breast conserving surgery in small breast carcinoma: long-term results of a randomized trial. Ann Oncol. 2001;12:997-1003.

[75] Polgár C, Strnad V, Major T. Brachytherapy for partial breast irradiation: the European experience. Semin Radiat Oncol. 2005;15:116-122.

[76] Njeh CF, Saunders MW, Langton CM. Accelerated partial breast irradiation using external beam conformal radiation therapy: a review. Crit Rev Oncol Hematol. 2012;81:1-20.

[77] Formenti SC. External-beam partial-breast irradiation. Semin Radiat Oncol. 2005;15:92-99.

[78] Chen PY, Wallace M, Mitchell C, et al. Four-year efficacy, cosmesis and toxicity using three-dimensional conformal external beam radiation therapy to deliver accelerated partial breast irradiation. Int J Radiat Oncol Biol Phys. 2010;76:991-997.

[79] Shah C, Wilkinson JB, Lanni T, et al. Five-year outcomes and toxicities using 3-dimensional conformal external beam radiation therapy to deliver accelerated partial breast irradiation. Clin Breast Cancer. 2013;13:206-211.

[80] Liss AL, Ben-David MA, Jagsi R, et al. Decline of cosmetic outcomes following accelerated partial breast irradiation using intensity-modulated radiation therapy: Results of a single-institution prospective clinical trial. Int J Radiat Oncol Biol Phys. 2014;89:96-102.

[81] Lewin AA, Derhagopian R, Saigal K, et al. Accelerated partial breast irradiation is safe and effective using intensity-modulated radiation therapy in selected early-stage breast cancer. Int J Radiat Oncol Biol Phys. 2012;82:2104-2110.

[82] Lei RY, Leonard CE, Howell KT, et al. Four-year clinical update from a prospective trial of accelerated partial breast intensity-modulated therapy (APBIMRT). Breast Cancer Res Treat. 2013;140:119-133.

[83] El Nemr M, Heymann S, Verstraet R, et al. Mixed modality treatment planning of accelerated partial breast irradiation: to improve complex dosimetry cases. Radiat Oncol. 2011;6:154.

[84] Moon SH, Shin KH, Kim TH, et al. Dosimetric comparison of four different external beam partial breast irradiation techniques: three-dimensional conformal radiotherapy, intensity-modulated radiotherapy, helical tomotherapy, and proton beam therapy. Radiother. Oncol. 2009;90:66-73.

[85] Rusthoven KE, Carter DL, Howell K, et al. Accelerated partial-breast intensity-modulated radiotherapy results in improved dose distribution when compared with three-dimensional treatment-planning techniques. Int J Radiat Oncol Biol Phys. 2008;70:296-302.

[86] Qiu J-J, Chang Z, Wu QJ, et al. Impact of volumetric-modulated arc therapy technique on treatment with partial breast irradiation. Int J Radiat Oncol Biol Phys. 2010;78:288-296.

[87] Qiu JJ, Chang Z, Horton JK, et al. Dosimetric comparison of 3D conformal, IMRT, and V-MAT techniques for accelerated partial-breast irradiation (APBI). Med Dosim. 2014;39:152-158.

[88] Stelczer G, Major T, Mészáros N, et al. Dosimetric comparison of different techniques for external beam accelerated partial breast irradiation. Magy Onkol. 2016;60:305-311.

[89] Essers M, Osman SOS, Hol S, et al. Accelerated partial breast irradiation (APBI): are breath-hold and volumetric radiation therapy techniques useful? Acta Oncol. 2014;53:788-794.

[90] Kozak KR, Doppke KP, Katz A, et al. Dosimetric comparison of two different three-dimensional conformal external beam accelerated partial breast irradiation techniques. Int J Radiat Oncol Biol Phys. 2006;65:340-346.

[91] Recht A, Ancukiewicz M, Alm El-Din MA, et al. Lung dose-volume parameters and the risk of pneumonitis for patients treated with accelerated partial-breast irradiation using three-dimensional conformal radiotherapy. J Clin Oncol. 2009;27:3887-3893.

[92] Mydin AR, Gaffney H, Bergman A, et al. Does a three-field electron / minitangent photon technique offer dosimetric advantages to a multifield, photon-only technique for accelerated partial breast irradiation? Am. J. Clin. Oncol. 2010;33:336-340.

[93] Palma BA, Sánchez AU, Salguero FJ, et al. Combined modulated electro and photon beams planned by a Monte-Carlo-based optimization procedure for accelerated partial breast irradiation. Phys Med Biol. 2012;57:1191-1202.

[94] Fekete G, Újhidy D, Együd Z, et al. Partial breast radiotherapy with simple teletherapy techniques. Med Dosim. 2015;40:290-295.

[95] Strnad V, Ott OJ, Hildebrandt G, et al. 5-year results of accelerated partial breast irradiation using sole interstitial multicatheter brachytherapy versus whole-breast irradiation with boost after breast-conserving surgery for low-risk invasive and in-situ carcinoma of the female breast: a randomised, phase 3, non-inferiority trial. Lancet. 2016;387:229-238.

[96] Coles CE, Griffin CL, Kirby AM, et al. Partial-breast radiotherapy after breast conservation surgery for patients with early breast cancer (UK IMPORT LOW trial): 5-year results from a multicentre, randomised, controlled, phase 3, non-inferiority trial. Lancet. 2017;390:1048-1060.

[97] Mózsa E, Mészáros N, Major T, et al. Accelerated partial breast irradiation with external beam three-dimensional conformal radiotherapy. Strahlenther Onkol. 2014;190:444-450.

[98] Rodriguez N, Sanz X, Dengra J, et al. Five-year outcomes, cosmesis, and toxicity with 3-dimensional conformal external beam radiation therapy to deliver accelerated partial breast irradiation. Int J Radiat Oncol Biol Phys. 2013;87:1051-1057.

[99] Chafe S, Moughan J, McCormick B, et al. Late toxicity and patient self-assessment of breast appearance/satisfaction on RTOG0319: A phase 2 trial of 3-dimensional conformal radiation therapy-accelerated partial breast irradiation following lumpectomy for stages I and II breast cancer. Int J Radiat Oncol Biol Phys. 2013;86:854-859.

[100] Jagsi R, Ben-David MA, Moran JM, et al. Unacceptable cosmesis in a protocol investigating intensity-modulated radiotherapy with active breathing control for accelerated partial-breast irradiation. Int J Radiat Oncol Biol Phys. 2010;76:71-78.

[101] Hepel JT, Tokita M, MacAusland SG, et al. Toxicity of three-dimensional conformal radiotherapy for accelerated partial breast irradiation. Int J Radiat Oncol Biol Phys. 2009;75:1290-1296.

[102] Olivotto IA, Whelan TJ, Parpia S, et al. Interim cosmetic and toxicity results from RAPID: A randomized trial of accelerated partial breast irradiation using three-dimensional conformal external beam radiation therapy. J Clin Oncol. 2013;31:4038-4045.

[103] Whelan T, Julian J, Levine M, et al. RAPID: A randomized trial of accelerated partial breast irradiation using 3-dimensional conformal radiotherapy (3DCRT). San Antonio Breast Cancer Symposium; 2018 Dec 4-8; San Antonio, TX, USA. Abstract No GS4-03.

[104] Borger JH, Kemperman H, Smitt HS, et al. Dose and volume effects on fibrosis after breast conservation therapy. Int J Radiat Oncol Biol Phys. 1994;30:1073-1081.

9 Appendix

I.

Pathology & Oncology Research
https://doi.org/10.1007/s12253-018-0436-2

ORIGINAL ARTICLE

Prone Positioning on a Belly Board Decreases Rectal and Bowel Doses in Pelvic Intensity-Modulated Radiation Therapy (IMRT) for Prostate Cancer

Renáta Kószó[1] · Linda Varga[1] · Emese Fodor[1] · Zsuzsanna Kahán[1] · Adrienne Cserháti[1] · Katalin Hideghéty[1] · Zsófia Együd[1] · Csilla Szabó[1] · Emőke Borzási[1] · Dorottya Szabó[1,2] · Kitti Müllner[1] · Zoltán Varga[1] · Anikó Maráz[1]

Received: 1 May 2018 / Accepted: 29 May 2018

Abstract
The presence of normal tissues in the irradiated volume limits dose escalation during pelvic radiotherapy (RT) for prostate cancer. Supine and prone positions on a belly board were compared by analyzing the exposure of organs at risk (OARs) using intensity modulated RT (IMRT). The prospective trial included 55 high risk, localized or locally advanced prostate cancer patients, receiving definitive image-guided RT. Computed tomography scanning for irradiation planning was carried out in both positions. Gross tumor volume, clinical and planning target volumes (PTV) and OARs were delineated, defining subprostatic and periprostatic rectal subsegments. At the height of the largest antero-posterior (AP) diameter of the prostate, rectal diameters and distance from the posterior prostate wall were measured. IMRT plans were generated. Normal tissue exposure and structure volumes were compared between supine and prone plans using paired t-test. In the volumes of the prostate, PTV, colon and small bowel, no significant differences were found. In prone position, all rectal volumes, diameters, and rectum–prostate distance were significantly higher, the irradiated colon and small bowel volume was lower in dose ranges of 20–40 Gy, and the exposure to all rectal segments was more favorable in 40–75 Gy dose ranges. No significant difference was found in the exposure of other OARs. Prone positioning on a belly board is an appropriate positioning method aiming rectum and bowel protection during pelvic IMRT of prostate cancer. The relative reduction in rectal exposure might be a consequence of the slight departure between the prostate and rectal wall.

Keywords Prostate cancer · IMRT · Prone · Belly board · Small bowel · Rectum

Introduction

Prostate cancer is the second most common malignancy worldwide [1]. Its prognosis has improved as a result of adjuvant androgen deprivation therapy and the escalated dose, and the efficacy of radiotherapy (RT) [2]. Therefore, pelvic irradiation including the prostate, seminal vesicles, and lymphatic regions is an integral component of high-risk [3], organ-confined, and locally advanced prostate cancer management.

Although RT is getting more targeted, the tolerance of normal tissues limits dose escalation and tumor control probability, and makes the incidence of acute and chronic gastrointestinal (GI) morbidity higher, aggravating the co-existing urological, sexual, and psychological problems of the increasing number of cancer survivors [4]. The phenomena of GI injury secondary to RT are described as pelvic radiation disease (PRD) [5]. Acute PRD, occurring during or shortly after RT, presents in abdominal–anorectal pain, lack of appetite, nausea, vomiting, bloating, diarrhea, and rectal bleeding. Chronic complications developing between 1.5 and 6 years after the completion of pelvic RT may manifest as anorexia, lactose intolerance, malabsorption, fistula formation, bowel obstruction, perforation, and fecal incontinence [6]. The symptoms depend on the degree and extent of the tissue damage [7] and have a significant adverse effect on the patient's quality of life [8]. The most important factors related to the probability of the complications are the total dose of RT delivered to the pelvic organs, the applied regime, the size of the treatment fields, the presence

✉ Renáta Kószó
koszorenata@gmail.com

[1] Department of Oncotherapy, University of Szeged, Korányi Alley 12, Szeged H-6720, Hungary

[2] Oncological Center, Ferenc Csolnoky Hospital, Kórház Str.1, Veszprém 8200, Hungary

Published online: 07 June 2018

of radiation implants, concurrent chemotherapy, and the volume of the bowel irradiated [7].

The irradiated bowel volume can be minimized by surgical and non-surgical methods [9]. Surgical means include pelvic reconstruction, reperitonealization of the pelvic floor, placement of an omental sling, and the inserting of a synthetic prosthesis under the small intestine. Radiotherapeutic techniques embrace among others the use of intensity modulated (IM) and image-guided (IG) RT, adaptive irradiation, a shrinking field, modified fractionation schemes, endorectal balloons, tissue spacers, bladder distension, and optimal patient position.

The purpose of our study was to assess whether a supine or prone position on a belly board, applying IMRT technique, results in the reduction of the radiation dose to organs at risk (OARs), primarily the rectum, colon, and small intestines during pelvic RT of prostate cancer patients.

Materials and Methods

Patient Population

The prospective analysis included patients with a histologically confirmed, high risk [10], localized or locally advanced (2009 TNM classification [11] stage T2–4 N0–1 M0) prostate cancer graded according to the Gleason score system [12], receiving a definitive pelvic RT at the Department of Oncotherapy, University of Szeged, Hungary. The tumor stage assessment was based on the findings of thoracic computed tomography (CT), abdominal and pelvic CT and magnetic resonance imaging (MRI), and whole-body bone scintigraphy. Clinical and pathological data were extracted from the patient files.

Patient Positioning and Computed Tomography Scanning

Patients were positioned on the supine and prone pelvis modules of the All in One (AIO) Solution (ORFIT, Wijnegem, Belgium) system. In supine pose, the patient was positioned with bent knees, and the genitalia were distracted with extruded polystyrene blocks. In prone position, a belly board was applied to allow the abdomen to extend into its aperture, and a polystyrene wedge was placed between the buttocks. For immobilization a six-point thermoplastic mask fixation (Pelvicast system, ORFIT, Wijnegem, Belgium) was employed. All patients underwent five-millimeter slice-increment topometric CT scanning in both positions from the diaphragm to the level of 10 cm below the femoral necks, using a Somatom Emotion 6 CT Simulator (Siemens, Erlangen, Germany). CT scanning was prepared with full bladder according to our internal protocol, and following an antiflatulent diet for at least 7 days prior and during RT delivery.

Target and Critical Structure Delineation

The gross tumor volume (GTV), clinical target volume (CTV), planning target volume (PTV), and OARs were delineated in the ARIA Oncology Information System (Varian Oncology Systems, Palo Alto, CA, USA) in both positions by radiation oncologists and reviewed by an experienced radiologist. The prostate was contoured as GTV_p, the proximal thirds, or in case of involvement, the full extension of the seminal vesicles were contoured as GTV_{vs}, and pathologic lymph nodes, if present, as GTV_N, considering MRI records. CTV_N included the parailiac, upper subaortic presacral and obturator lymph nodes, contoured according to the RTOG GU Radiation Oncology Specialists Reach Consensus [13]. PTV_p included GTV_p with a 10 mm margin along the supero-inferior, left–right axis, in anterior direction and 7 mm in posterior direction. PTV_{pvs} was defined as the combination of GTV_p and GTV_{vs} with a safety margin of 10 mm and 15 mm in posterior direction and any other directions, respectively. PTV was determined as PTV_{pvs}, a 7 mm margin around CTV_N and 10 mm around GTV_N, if present. The rectum, large and small intestines, urinary bladder, femoral heads, and bony structures were outlined as OARs. The rectum was defined from the ischial tuberosities to the sigmoid flexure, but at least 2 cm above PTV_{pvs}. Each rectal section, the whole rectum (R), the segment at the height of the prostate (R1), and R1 + 10 mm along the supero-inferior axis (R2) were individually delineated. Large and small bowel volumes contained all identifiable segments. The bladder was delineated from the apex to the dome [14].

Rectal Extension and Rectum–Prostate Distance Measurement

At the height of the largest antero-posterior (AP) diameter of the prostate, rectal diameters along the AP and left–right axis were defined, and perpendicular lines were created from the center and lateral edges of the back wall of the prostate to the outer anterior rectal wall in both supine and prone positions (Fig. 1). Two independent radiation oncologists performed rectum–prostate distance measurements, both of them twice.

Intensity-Modulated Radiotherapy Planning and Dosimetric Analysis

IMRT planning was performed using the Eclipse treatment planning system (Varian Oncology Systems, Palo Alto, CA, USA). The prescribed doses were 45 Gy to the center of the PTV (1.8 Gy/day, 5 days/week), 14 Gy of the PTV_{pvs} and 18 Gy of PTV_p, both delivered in daily 2 Gy fractions, 5 days per week. OAR dose constraints were determined as the following [13]: $V_{55Gy\ (bladder)} \leq 50\%$, $V_{70Gy\ (bladder)} \leq 30\%$; $V_{50Gy\ (rectum)} \leq 50\%$, $V_{70Gy\ (rectum)} \leq 20\%$; $V_{50Gy\ (colon)} \leq 50\%$, V_{70Gy}

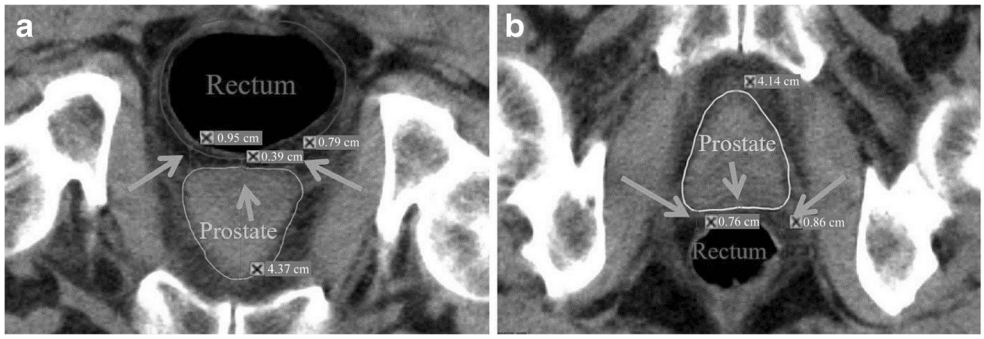

Fig. 1 Rectal extension and rectum–prostate distance measurement: At the height of the largest antero-posterior diameter of the prostate perpendiculars were created from the center and both lateral edges of the posterior prostate wall to the anterior rectal wall in both prone (**a**) and supine (**b**) positions. Larger rectal diameters in prone, smaller in supine position in case of the same patient at the same time

$_{(colon)} \leq 20\%$; $V_{52Gy\ (small\ intestine)} = 0\%$; $V_{50Gy\ (femoral\ heads)} <$ 5%. For the coverage of the PTV sliding window IMRT plans were designed in both positions with a seven-field beam arrangement using 6 MV photon beam quality, consisting coplanar beam directions as the following: in prone position 0°, 136.1°, 208.3°, 258.7°, 101.7°, 306.1° and 55.2°, in supine position 0°, 38.2°, 98°, 142°, 215.7°, 269.5° and 318.2°. For the PTV_{pvs} and PTV_p volumetric modulated arc therapy (VMAT) plans were generated in both positions using 6 MV photon beam quality, 181°–179° and 179°–181° gantry angles and 30° and 15° collimator angles, respectively. IMRT plans were created to obtain a 95% coverage of the PTV with the 95% isodose curve. The highest priority was PTV coverage, and the second one was the sparing of OARs. Planning assistant contours of the PTV, PTV_{pvs}, and PTV_p were designed with uniform margins of 15 mm, 30 mm, 40 mm, and 50 mm in both positions. Dose-volume histograms were calculated for all defined volumes. Data of mean volumes of the contoured structures, mean absolute volumes of the small bowel and colon receiving 20–50 Gy, mean relative volumes of the rectal segments receiving 30–75 Gy and of the bladder receiving 30–70 Gy doses and mean of doses regarding PTV D95, PTV_{pvs} D95, and PTV_p D95 were collected.

Radiation Treatment and Image-Guidance

Irradiation was carried out by using a Varian TrueBeamSTx (Varian Oncology Systems, Palo Alto, CA, USA) in prone position. Image-guidance was based on daily kV-cone beam CT (CBCT) scanning of the pelvis prior to treatment, using the standard mode settings: 125 kV, 80 mA, 13 ms, and half-fan bowtie filter. An automatic match algorithm was used to match the bony structures displayed on the planning CT and the CBCT.

Statistical Analysis

Data were reported as mean ± SD, mean ± SE or median values. The difference between the volumes and doses in supine and prone position was analyzed with the paired samples t-test. Intraobserver and interobserver variabilities were calculated from the mean of distances by using correlation analysis, given a correlation coefficient (r). SPSS 20.0 for Windows (SPSS Inc., Chicago, IL, USA) was used to perform the analysis. A p value <0.05 was considered significant.

Results

Patient Population

Between October 13, 2016 and October 11, 2017, 55 patients with high risk localized or locally advanced prostate cancer were administered definitive pelvic lymph node RT. Patients belonged to the elderly age group with a median [range] age of 65.60 [53.33–83.49] years, and they were mostly overweight showing a median [range] value of body mass index of 26.96 [19.37–41.62] kg/m^2. More than three-quarters of them had a cardiovascular co-morbidity, and one-third of them were smokers. All the patients had stage T2–4 N0 M0 tumor with a Gleason score ≥ 7 and a prostate specific antigen (PSA) level at the time of the diagnosis established >5 ng/ml. Most of the patients received a 6-month course of luteinizing hormone-releasing hormone analogue and antiandrogen (total androgen blockade, TAB) endocrine therapy, launched before the commencing of RT. The relevant patient and tumor characteristics are shown in Table 1.

Structure Volumes and Rectal Extension

No significant differences were found between prone and supine positions in the volumes of the GTV_p, PVS, PTV, colon, small bowel, and urinary bladder. All rectal volumes (R, R1 and R2) were significantly higher in prone position. The higher SD values of mean bladder volumes in the two positioning methods might be the consequence of pre-existing urinary symptoms, such as incontinence. At the height of the largest

Table 1 Patient and tumor characteristics

Tumor and patient characteristics	Number of patients (%)
Number of patients	55
Concurrent cardiovascular disease	44 (80.00)
History of smoking	18 (32.73)
Clinical stages	
T2	41 (74.55)
T3	12 (21.82)
T4	2 (3.64)
Gleason scores	
7	27 (48.21)
8	5 (9.09)
9	19 (33.93)
10	4 (7.14)
PSA levels on establishing the diagnosis (ng/ml)	
$10 > x > 5$	13 (23.21)
$20 > x \geq 10$	9 (16.36)
≥ 20	33 (58.93)
Endocrine treatment	49 (89.09)

AP level of the prostate, both the AP and the lateral rectal diameters were significantly higher in prone position (Table 2).

Table 2 Volumes of the delineated structures and rectal diameters in prone and supine positions

Structure	Position	Mean volume (cm^3)	Standard deviation (SD)	p value
GTV_p	Prone	130.11	49.13	0.217
	Supine	133.28	50.87	
PVS	Prone	188.77	58.19	0.748
	Supine	190.23	58.20	
PTV	Prone	1123.54	138.90	0.282
	Supine	1130.98	146.66	
Whole rectum (R)	Prone	155.13	105.26	<0.001
	Supine	95.61	45.89	
Rectal subsegment R1	Prone	50.32	31.84	<0.001
	Supine	34.76	23.64	
Rectal subsegment R2	Prone	74.37	41.51	<0.001
	Supine	50.78	27.64	
Colon	Prone	580.32	299.38	0.486
	Supine	604.37	337.12	
Small bowel	Prone	812.93	354.25	0.373
	Supine	772.71	353.21	
Urinary bladder	Prone	184.18	117.13	0.403
	Supine	192.40	112.56	
Rectal diameter	Position	Mean diameter (mm)	Standard error (SE)	p value
AP	Prone	50.60	2.20	<0.001
	Supine	36.70	1.50	
Lateral	Prone	43.80	2.60	0.003
	Supine	35.90	1.80	

Rectum–Prostate Distance

The rectum–prostate distance measured from the center of the rear prostate wall to the outer anterior rectal wall was significantly higher in prone position. No significant differences in the distance values measured from the left and right edges of the posterior prostate wall were found. Both intraobserver and interobserver variabilities showed close correlation (Table 3).

Normal Tissue Doses

A prone position with the additional use of a belly board led to a significant decrease in the absolute volumes receiving doses greater than 20 to 40 Gy in the small intestine and the colon; however, the difference between the volumes receiving 50 Gy was not significant (Table 4). In dose ranges of 40 to 75 Gy, the exposure of all rectal segments was more favorable in prone position. The relative volume receiving 30 Gy dose was lower in respect of R1 segment; nonetheless, the difference was not significant. The relative exposed volume of the urinary bladder, femoral heads, and bony structures was in accordance with the dose constraints. No significant difference was found between the positioning methods (Table 5).

Planning Target Volume Coverage

PTV coverage did not differ significantly between the two positions (PTV D95 - mean of dose 43.01 vs. 43.00 Gy, SD 0.26 vs. 0.26 in prone vs. supine position, respectively, $p = 0.782$; PTV_{pvs} D95 - mean of dose 13.36 vs. 13.35 Gy, SD 0.07 vs. 0.07 in prone vs. supine position, respectively, $p = 0.591$; PTV_p D95 - mean of dose 17.16 vs. 17.15 Gy, SD 0.09 vs. 0.07 in prone *vs.* supine position, respectively, $p = 0.435$).

Discussion

Clinically localized high-risk prostate cancer frequently shows micrometastatic spreading to the pelvic lymph nodes; therefore, RT and three years of androgen suppressing endocrine treatment are the standard of care. Dose escalation to the prostate even to 80–86.4 Gy reduces biochemical failure and the appearance of distant metastases [2]. However, survival data are controversial regarding field size [2]. There is no consensus recommendation for patient selection for pelvic RT in this population, considering the increased exposure of OARs and toxicity. 90% of patients treated with pelvic RT develop permanent alterations in bowel habits [8], 50% of them complain about adverse changes in life quality [15], and 20–40% of them assess this impact as moderate or severe [16]. The small intestine, the rectum, and to a lesser extent, the colon are dose-

Table 3 Rectum–prostate distance and intraobserver and interobserver variability correlation in prone and supine positions

Distance	Position	Mean (mm)	Standard error (SE)	p value	Intraobserver variability – Correlation coefficient (r)		Interobserver variability – Correlation coefficient (r)
					Examiner 1	Examiner 2	
Left lateral	Prone	6.50	0.40	0.062	0.92	0.90	0.89
	Supine	5.70	0.40				
Mediosagittal	Prone	2.80	0.30	0.026	0.86	0.89	0.95
	Supine	2.20	0.30				
Right lateral	Prone	5.90	0.40	0.173	0.80	0.74	0.78
	Supine	5.40	0.40				

limiting organs, tolerating a 50–60 Gy dose at conventional fractionation [17, 18]. Normal tissue complication probability (NTCP) studies suggest that the small intestine volume receiving 15 and 45 Gy (V_{15} and V_{45}) is a relevant parameter for GI morbidity [19, 20]. According to the review of Fiorino et al. [21], keeping V_{70} and V_{75} to <25 and 5%, respectively, results in a decrease in the development of late rectal bleeding. Moderate dose volumes, such as V_{40} and V_{50} are predictive for chronic late incontinence [22] and are also important in developing rectal bleeding [21]. The dosimetric analysis [23] of the anatomical subregions showed that rectal bleeding is associated with V70 of the anorectal region, fecal incontinence with V15 of external sphincter, and V55 of the iliococcygeal muscle, whereas stool frequency with V40 of the levator ani and V45 of the iliococcygeal muscle. In the prospective study of Dréan et al. [24], rectal subregions at risk have been delineated, and the authors have found that the exposure of the subprostatic anterior hemirectum and the upper part of the anal canal was 4 Gy higher in patients developing rectal bleeding.

Table 4 Small intestine and colon exposure in prone and supine position

Organ at risk	DVH parameter	Position	Mean volume (cm^3)	Standard deviation (SD)	p value
Small intestine	$V_{20\ Gy}$	Prone	79.85	89.83	<0.001
		Supine	170.34	103.62	
	$V_{30\ Gy}$	Prone	36.74	51.24	<0.001
		Supine	84.55	63.01	
	$V_{40\ Gy}$	Prone	16.99	26.08	<0.001
		Supine	32.91	31.35	
	V_{50Gy}	Prone	0.16	1.06	0.398
		Supine	0.33	1.54	
Colon	$V_{20\ Gy}$	Prone	122.43	74.52	<0.001
		Supine	181.22	109.48	
	$V_{30\ Gy}$	Prone	84.09	57.17	<0.001
		Supine	121.21	73.36	
	$V_{40\ Gy}$	Prone	53.23	44.20	0.043
		Supine	63.19	44.89	
	$V_{50\ Gy}$	Prone	2.06	4.02	0.627
		Supine	1.81	3.62	

Table 5 Exposure of rectal segments and urinary bladder in prone and supine positions

Organ at risk	DVH parameter	Position	Mean relative volume (%)	Standard deviation (SD)	p value
Whole rectum	V_{30Gy}	Prone	106.40	118.98	0.296
		Supine	89.60	7.46	
	V_{40Gy}	Prone	65.79	14.96	<0.001
		Supine	78.58	10.14	
	V_{50Gy}	Prone	35.51	13.83	<0.001
		Supine	48.38	12.29	
	V_{60Gy}	Prone	17.45	8.18	<0.001
		Supine	24.04	9.11	
	V_{70Gy}	Prone	7.57	4.10	<0.001
		Supine	10.43	4.97	
	V_{75Gy}	Prone	3.67	2.61	0.021
		Supine	4.58	3.19	
Rectal subsegment R1	$V_{30\ Gy}$	Prone	99.78	0.75	0.735
		Supine	99.80	0.61	
	V_{40Gy}	Prone	80.58	13.50	<0.001
		Supine	94.95	5.74	
	V_{50Gy}	Prone	52.25	14.18	<0.001
		Supine	68.55	10.90	
	V_{60Gy}	Prone	32.37	10.90	<0.001
		Supine	40.49	10.13	
	V_{70Gy}	Prone	16.51	5.83	<0.001
		Supine	20.74	7.14	
	V_{75Gy}	Prone	8.79	4.52	0.099
		Supine	9.97	5.67	
Rectal subsegment R2	V_{30Gy}	Prone	99.52	1.21	0.001
		Supine	98.61	1.96	
	V_{40Gy}	Prone	78.55	12.66	<0.001
		Supine	91.45	6.05	
	V_{50Gy}	Prone	49.40	13.14	<0.001
		Supine	64.83	9.89	
	V_{60Gy}	Prone	28.95	9.04	<0.001
		Supine	37.43	8.76	
	V_{70Gy}	Prone	13.52	4.75	<0.001
		Supine	17.86	5.79	
	V_{75Gy}	Prone	6.82	3.59	0.051
		Supine	7.86	4.43	
Bladder	V_{30Gy}	Prone	95.82	7.10	0.657
		Supine	95.45	5.13	
	V_{40Gy}	Prone	67.99	18.89	0.687
		Supine	68.78	16.13	
	V_{50Gy}	Prone	41.90	16.53	0.982
		Supine	41.86	14.84	
	V_{60Gy}	Prone	26.73	11.77	0.235
		Supine	25.36	10.62	
	V_{70Gy}	Prone	15.91	7.90	0.276
		Supine	14.94	7.31	

Technological advances allowing rectal sparing include endorectal balloons filled with air or water, reducing the exposure of the posterior rectal wall by moving away the prostate from it, depending on the volume of the balloons [25]. Bioabsorbable tissue spacers injected into the retroprostatic fascia also increase the distance between the prostate and the anterior rectal wall, resulting in significant reduction in both acute and late GI toxicities [26]. Regarding patient positioning, Zelefsky et al. [27] and McLaughlin et al. [28] have described significantly lower rectal doses in prone position, using 3DCRT technique. The results have also been confirmed in the phase II trial of O'Neil et al. [29] and by Bajon et al. using tomotherapy [30]. Nevertheless, Baylay et al. [31] have found supine position more favorable by using larger PTV margins in prone position, and Kato et al. [32] by applying IMRT in supine and 3DCRT in prone position. In prone position, the decreased rectal exposure is a result of the posterior retraction of the rectum and anterior displacement of the prostate; however, the accurate mechanism of it is unknown [27, 28, 32].

In the 3D-CRT of rectal malignancies, a prone treatment position without a belly board compared to a supine posture results in the reduction of the irradiated small intestine volume [33]. In case of pelvic malignancies, a larger decrease in the small intestine exposure can be obtained by the additional use of a belly board in comparison with both prone position alone [34, 35] or supine position [36, 37]. The use of IMRT technique decreases bowel doses by 40–50%, as compared to 3D-CRT [38, 39]. In case of gynecological and rectal tumors, a belly board assisted prone position using IMRT results in a further reduction in the irradiated volume of the small intestine, even in low dose areas [40, 41]. The advantage of the use of a belly board is also confirmed in postoperatively irradiated patients [42, 43], which might be the consequence of the significantly higher mobilization of the small intestine loops. The findings of Fu et al. [44] show that the gain of the use of a belly board is greater if the irradiated small intestine volume close to the target volume is larger. According to that study, a prone position on a belly board results in a remarkable decrease in the small bowel volume in case of gynecological malignancies but not in rectal cancer patients. A full bladder also functions as a natural spacer, transposing the small intestine loops from the pelvis to the abdomen, resulting in a reduction in the irradiated small intestine volume [42].

In rectal cancer patients treated with chemo-radiotherapy, Baglan et al. [19] have demonstrated an explicit relationship between the volume of the small bowel receiving at least 15 Gy and the degree of acute small intestinal toxicity. Robertson et al. [45] have proved that a reduction in the small bowel volume receiving low dose results in a significant decrease in the complication rate. Both authors have delineated the single small intestinal loops. In case of gynecological cancer patients treated with pelvic IMRT, Roeske et al. [20] have detected that drawing the abdominal space, the risk of acute GI toxicity is five times as little for small bowel volume of 100 cm^3 gaining the prescribed 45 Gy dose as of 200 cm^3. According to Gunnlaugsson et al. [46], the former technique is the recommended contouring method instead of delineating the abdominal space. Gunnlaugsson et al. have observed strong correlation between the occurrence of early side effects and small intestinal loop exposure, and no significant connection with the peritoneal cavity.

Our study was limited by the lack of delineating the penile bulb, and the relatively small number of patients involved, which however was double the number of patients previously reported. As most papers have described larger intrafraction prostate and respiratory motion in prone position [11] and literature data [47] show that a 3 mm PTV margin allows for CTV to be covered for 99% of cases when daily CBCT is used, accurate patient repositioning, daily reconstruction of the rectum, prostate safety margins, early toxicity and life quality during and after RT were also evaluated, and found to be similar to literature data of patients treated in supine position. These promising results have recently been submitted. Late toxicities need further examination due to the short follow-up period.

In conclusion, in the pelvic IMRT for prostate cancer, a prone position on a belly board decreases the irradiated small bowel volumes even in low dose ranges and contributes to rectal sparing. The relative dose reduction in the rectal exposure might be a consequence of the slight departure between the prostate wall and the rectal wall, as consistent with the literature, and the increasing volume and diameters of the rectum generated by the displacement of rectal gases. Considering the dosimetric advantages, prone position on a belly board could be recommended for the pelvic IMRT of prostate cancer.

Compliance with Ethical Standards

Conflict of Interest The authors declare that they have no conflict of interest.

Ethical Approval All procedures performed in studies involving human participants were in accordance with the ethical standards of the institutional and/or national research committee and with the 1964 Helsinki declaration and its later amendments or comparable ethical standards. The study was registered on September 19, 2016 by the Human Investigation Review Board, Regional Human Biomedical Research Ethics Committee, Albert Szent-Györgyi Health Centre, University of Szeged, Hungary, registration number: WHO 3856/2016.

Informed Consent Informed consent was obtained from all individual participants included in the study.

References

1. Ferlay J, Shin HR, Bray F, Forman D, Mathers C, Parkin DM (2010) Estimates of worldwide burden of cancer in 2008: Globocan 2008. Int J Cancer 127:2893–2917

2. Juloori A, Shah C, Stephans K, Vassil A, Tendulkar R (2016) Evolving paradigm of radiotherapy for high-risk prostate cancer: current consensus and continuing controversies. Prostate Cancer 2016:2420786
3. Lukka H, Warde P, Pickles T, Morton G, Brundage M, Souhami L, Canadian GU Radiation Oncologist Group (2001) Controversies in prostate cancer radiotherapy: consensus development. Canadian GU Radiation Oncologist Group. Can J Urol 8:1314–1322
4. Andreyev HJ (2007) Gastrointestinal problems after pelvic radiotherapy: the past, the present and the future. Clin Oncol (R Coll Radiol) 19:790–799
5. Stacey R, Green JT (2014) Radiation-induced small bowel disease: latest developments and clinical guidance. Ther Adv Chronic Dis 5: 15–29
6. Theis V, Sripadam R, Ramani V, Lal S (2010) Chronic radiation enteritis. Clin Oncol 22:70–83
7. Kennedy G, Heise C (2005) Radiation colitis and proctitis. Clin Colon Rectal Surg 20:64–72
8. Olopade F, Norman A, Blake P, Dearnaley DP, Harrington KJ, Khoo V et al (2005) A modified inflammatory bowel disease questionnaire and the Vaizey incontinence questionnaire are simple ways to identify patients with significant gastrointestinal symptoms after pelvic radiotherapy. Br J Cancer 92:1663–1670
9. Wiesendanger-Wittmer E, Sijtsema N, Muijs C, Beukema JC (2012) Systematic review of the role of a belly board device in radiotherapy delivery in patients with pelvic malignancies. Radiother Oncol 102:325–334
10. Zelefsky MJ, Cowen D, Fuks Z, Shike M, Burman C, Jackson A et al (1999) Long term tolerance of high dose three-dimensional conformal radiotherapy in patients with localized prostate carcinoma. Cancer 85:2460–2468
11. Sobin LH, Gospodarowicz MK, Wittekind C (2009) TNM classification of malignant tumors, 7th edn. Wiley-Blackwell, London
12. Mellinger GT, Gleason D, Bailar J 3rd (1967) The histology and prognosis of prostatic cancer. J Urol 97:331–337
13. Lawton CAF, Michalski J, El-Naga I, Buyyounouski MK, Lee WR, Menard C et al (2009) RTOG GU radiation oncology specialists reach consensus on pelvic lymph node volumes for high-risk prostate cancer. Int J Radiat Oncol Biol Phys 74:383–387
14. Viswanathan AN, Yorke ED, Marks LB, Eifel PJ, Shipley WU (2010) Radiation dose-volume effects of the urinary bladder. Int J Radiat Oncol Biol Phys 76(Suppl 3):S116–S122
15. Gami B, Harrington K, Blake P, Dearnaley D, Tait D, Davies J, Norman AR, Andreyev HJN (2003) How patients manage gastrointestinal symptoms after pelvic radiotherapy. Aliment Pharmacol Therapeut 18:987–994
16. Andreyev H (2007) Gastrointestinal symptoms after pelvic radiotherapy: a new understanding to improve management of symptomatic patients. Lancet Oncol 8:1007–1017
17. Letschert JGJ (1995) The prevention of radiation-induced small bowel complications. Eur J Cancer 31:1361–1365
18. Michalski JM, Gay H, Jackson A, Tucker SL, Deasy JO (2010) Radiation dose-volume effects in radiation-induced rectal injury. Int J Radiat Oncol Biol Phys 76(Suppl 3):S123–S129
19. Baglan KL, Frazier RC, Yan D, Huang RR, Martinez AA, Robertson JM (2002) The dose–volume relationship of acute small bowel toxicity from concurrent 5-FU-based chemotherapy and radiation therapy for rectal cancer. Int J Radiat Oncol Biol Phys 52: 176–183
20. Roeske JC, Bonta D, Mell LK, Lujan AE, Mundt AJ (2003) A dosimetric analysis of acute gastrointestinal toxicity in women receiving intensity-modulated whole-pelvic radiation therapy. Radiother Oncol 69:201–207
21. Fiorino C, Valdagni R, Rancati T, Sanguineti G (2009) Dose-volume effects for normal tissues in external radiotherapy: pelvis. Radiother Oncol 93:153–167
22. Peeters ST, Hoogeman MS, Heemsbergen WD, Hart AA, Koper PC, Lebesque JV (2006) Rectal bleeding, fecal incontinence, and high stool frequency after conformal radiotherapy for prostate cancer: normal tissue complication probability modeling. Int J Radiat Oncol Biol Phys 66:11–19
23. Schaake W, van der Schaaf A, van Dijk LV, Bongaerts AH, van den Bergh AC, Langendijk JA (2016) Normal tissue complication probability (NTCP) models for late rectal bleeding, stool frequency and fecal incontinence after radiotherapy in prostate cancer patients. Radiother Oncol 119:381–387
24. Dréan G, Acosta O, Ospina JD, Fargeas A, Lafond C, Corrégé G et al (2016) Identification of a rectal subregion highly predictive of rectal bleeding in prostate cancer IMRT. Radiother Oncol 119:388–397
25. van Lin EN, Hoffmann AL, van Kollenburg P, Leer JW, Visser AG (2005) Rectal wall sparing effect of three different endorectal balloons in 3D conformal and IMRT prostate radiotherapy. Int J Radiat Oncol Biol Phys 63:565–576
26. Serrano N, Kalman NS, Anscher MS (2017) Reducing rectal injury in men receiving prostate cancer radiation therapy: current perspectives. Cancer Manag Res 9:339–350
27. Zelefsky MJ, Happersett L, Leibel SA, Burman CM, Schwartz L, Dicker AP et al (1997) The effect of treatment positioning on normal tissue dose in patients with prostate cancer treated with three-dimensional conformal radiotherapy. Int J Radiat Oncol Biol Phys 37:13–19
28. McLaughlin PW, Wygoda A, Sahijdak W, Sandler HM, Marsh L, Roberson P et al (1999) The effect of patient position and treatment technique in conformal treatment of prostate cancer. Int J Radiat Oncol Biol Phys 45:407–413
29. O'Neil L, Armstrong J, Buckney S, Assiri M, Cannon M, Holmberg O (2008) A phase II trial for the optimisation of treatment position in the radiation therapy of prostate cancer. Radiother Oncol 88:61–66
30. Bajon T, Piotrowski T, Antczak A, Bąk B, Błasiak B, Kaźmierskaa J (2011) Comparison of dose-volume histograms for supine and prone position in patients irradiated for prostate cancer – a preliminary study. Rep Pract Oncol Radiother 16:65–70
31. Bayley AJ, Catton CN, Haycocks T, Kelly V, Alasti H, Bristow R et al (2003) A randomized trial of supine vs. prone positioning in patients undergoing escalated dose conformal radiotherapy for prostate cancer. Radiother Oncol 70:37–44
32. Kato T, Obata Y, Kadoya N, Fuwa N (2009) A comparison of prone three-dimensional conformal radiotherapy with supine intensity-modulated radiotherapy for prostate cancer: which technique is more effective for rectal sparing? Br J Radiol 82:654–661
33. Drzymala M, Hawkins MA, Henrys AJ, Bedford J, Norman A, Tait DM (2009) The effect of treatment position, prone or supine, on dose–volume histograms for pelvic radiotherapy in patients with rectal cancer. Br J Radiol 82:321–327
34. Kim TH, Chie EK, Kim DY, Park SY, Cho KH, Jung KH et al (2005) Comparison of the belly board device method and the distended bladder method for reducing irradiated small bowel volumes in preoperative radiotherapy of rectal cancer patients. Int J Radiat Oncol Biol Phys 62:769–775
35. Huh SJ, Park W, Ju SG, Lee JE, Han Y (2004) Small-bowel displacement system for the sparing of small bowel in three-dimensional conformal radiotherapy for cervical cancer. Clin Oncol 16:467–473
36. Martin J, Fitzpatrick K, Horan G, McCloy R, Buckney S, O'Neill L et al (2005) Treatment with a belly-board device significantly reduces the volume of small bowel irradiated and results in low acute toxicity in adjuvant radiotherapy for gynecologic cancer: results of a prospective study. Radiother Oncol 74:267–274
37. Pinkawa M, Gagel B, Demirel C, Schmachtenberg A, Asadpour B, Eble MJ (2003) Dose–volume histogram evaluation of prone and

supine patient position in external beam radiotherapy for cervical and endometrial cancer. Radiother Oncol 69:99–105
38. Mundt A, Roeske J, Lujan A (2002) Intensity-modulated radiation therapy in gynecologic malignancies. Med Dosimetry 27:131–136
39. Portelance L, Chao K, Grigsby P, Bennet H, Low D (2001) Intensity-modulated radiation therapy (IMRT) reduces small bowel, rectum, and bladder doses in patients with cervical cancer receiving pelvic and Para-aortic irradiation. Int J Radiat Oncol Biol Phys 51:261–266
40. Stromberger C, Kom Y, Kawgan-Kagan M, Mensing T, Jahn U, Schneider A et al (2010) Intensity-modulated radiotherapy in patients with cervical cancer. An intra-individual comparison of prone and supine positioning. Radiat Oncol 5:63–68
41. Beriwal S, Jain SK, Heron DE, de Andrade RS, Lin CJ, Kim H (2007) Dosimetric and toxicity comparison between prone and supine position IMRT for endometrial cancer. Int J Radiat Oncol Biol Phys 67:485–489
42. Kim TH, Kim DY, Cho KH, Kim YH, Jung KH, Ahn JB et al (2005) Comparative analysis of the effects of belly board and bladder distension in postoperative radiotherapy of rectal cancer patients. Strahlenther Onkol 181(9):601–605
43. Saynak M, Kucucuk S, Aslay I (2008) Abdominal pillow for the sparing of small bowel in four-field conventional pelvic radiotherapy. Eur J Gynaecol Oncol 29:643–648
44. Fu YT, Lam JC, Tze JM (1995) Measurement of irradiated small bowel volume in pelvic irradiation and the effect of a belly board. Clin Oncol (R Coll Radiol) 7:188–192
45. Robertson JM, Lockman D, Yan D, Wallace M (2008) The dose-volume relationship of small bowel irradiation and acute grade 3 diarrhea during chemoradiotherapy for rectal cancer. Int J Radiat Oncol Biol Phys 70:413–418
46. Gunnlaugsson A, Kjellen E, Nilsson P, Bendahl PO, Willner J, Johnsson A (2007) Dose–volume relationships between enteritis and irradiated bowel volumes during 5-fluorouracil and oxaliplatin based chemoradiotherapy in locally advanced rectal cancer. Acta Oncol 46:937–944
47. Gill SK, Reddy K, Campbell N, Chen C, Pearson D (2015) Determination of optimal PTV margin for patients receiving CBCT-guided prostate IMRT: comparative analysis based on CBCT dose calculation with four different margins. J Appl Clin Med Phys 16:252–262

II.

Radiotherapy and Oncology 126 (2018) 487–492

Contents lists available at ScienceDirect

Radiotherapy and Oncology

journal homepage: www.thegreenjournal.com

Breast radiotherapy

A simple clinical method for predicting the benefit of prone *vs.* supine positioning in reducing heart exposure during left breast radiotherapy

Zsuzsanna Kahán [a,*], Ferenc Rárosi [b], Szilvia Gaál [a], Adrienn Cserháti [a], Krisztina Boda [b], Barbara Darázs [a], Renáta Kószó [a], Ferenc Lakosi [c,d], Ákos Gulyban [c,e], Philippe A. Coucke [c], Zoltán Varga [a]

[a] *Department of Oncotherapy;* [b] *Department of Medical Informatics, University of Szeged, Hungary;* [c] *Department of Radiation Oncology, University Hospital of Liège, Belgium;* [d] *Institute of Diagnostic Imaging and Radiation Oncology, Health Center, Kaposvár University, Hungary;* [e] *Radiation Oncology Department, Europe Hospitals Brussels, Belgium*

ARTICLE INFO

Article history:
Received 26 April 2017
Received in revised form 20 December 2017
Accepted 22 December 2017
Available online 17 January 2018

Keywords:
Breast radiotherapy
Clinical tool
Heart protection
Individual positioning
LAD protection

ABSTRACT

Background and purpose: The benefit of reduced radiation heart exposure in the prone *vs.* supine position individually differs. In this prospective cohort study, the goal was to develop a simple method for the operation of a validated model for the prediction of preferable treatment position during left breast radiotherapy.

Material and methods: In 100 cases, a single CT slice was utilized for the collection of the needed patient-specific data (in addition to body mass index, the distance of the LAD from the chest wall and the area of the heart included in the radiation fields at the middle of the heart in the supine position). Outcome was analyzed in relation to the full CT series acquired in both positions and dosimetric data.

Results: Great consistency was found between the tested and original method regarding sensitivity and specificity. The prioritization of LAD dose, and the use of heart dose and position-specific dose constraints as safety measures ensure sensitivity and specificity values of 82.8% and 87.3%, respectively. In an additional "routine clinical practice" series of 60 patients the new method seemed feasible in routine clinical practice. External testing on a 28-case series indicated similar accuracy.

Conclusion: We consider this simple clinical tool appropriate for assisting individual positioning aiming at maximum heart protection during left breast irradiation.

Radiotherapy is an essential component of the management of early breast cancer. The outcome in most cases is favorable, the majority of the affected patients become long survivors. Breast radiotherapy, however, may increase the risk of non-breast cancer-related morbidities, among which heart diseases rank the first [1,2]. Radiation-induced heart damage clearly depends on the dose exposed to its different structures (3,4). While older radiotherapy practices caused more significant late hazards, heightened awareness and the use of current technical developments make this danger much lower [1,4,5]. Although the application of modern radiotherapy planning and delivery significantly improves the control of radiation dose, in many cases a part of the heart, and especially the left anterior descending artery (LAD) located to its anterior surface still receive a dose sufficient to cause long-term adverse effects. Radiogenic diffuse myocardium damage including microvasculature abnormalities, degenerative cardiomyocyte and interstitial fibrotic changes may be controlled if not extensive, but the damage of the macrovasculature indistinguishable from coronary arteriosclerosis due to other causes more likely lead to a fatal outcome [3,6–8]. The exposure of the heart and the LAD are related [9–11], and irradiation-related cardiac morbidity and mortality are considered to be consequences of late manifesting coronary artery damage. Hence the verification and control of the dose to the LAD, is of prime importance [8,9,11,12].

With the aim of cardiac dose sparing and avoidance, numerous new methods have been developed [4,5]. These include the breath-holding techniques, prone positioning (both operate by separating the heart and the radiation fields), IMRT, proton irradiation or the reduction in the volume to be irradiated, partial breast irradiation (PBI). A significant increase in the number of clinical studies [11–20], and a recent survey on clinical practice [21] suggest that prone positioning has become an alternative of conventional supine positioning in some centers. Prone positioning always provides dramatic reduction in the ipsilateral lung dose, and in many cases significantly reduces heart exposure, too. A potential disadvantage is inferior repositioning accuracy, which may be improved with experience [18] or may be compensated by online daily correction [12,22].

* Corresponding author at: Department of Oncotherapy, University of Szeged, Korányi fasor 12, H-6720 Szeged, Hungary.
E-mail address: kahan.zsuzsanna@med.u-szeged.hu (Z. Kahán).

https://doi.org/10.1016/j.radonc.2017.12.021
0167-8140/

Prone positioning was first invented for the irradiation of large-breasted women [23,24]. Indeed, since gravity pulls the breast away from the chest wall, the geometry of a pendulous breast and the tangential irradiation fields gets advantageous in the prone position [12]. Taking the overall population of breast cancer patients, however, prone positioning has such effect in 77–87% of cases only [11,14,15,19]. As a consequence, the position-dependent dose to the LAD or heart also individually differs [11,19,20]. Different approaches exist for selecting the optimal position in left breast cancer cases. Kirby et al. found that a PTV > 1000 cm^3 favors prone positioning [11]. Zhao et al. developed a two-step decision-analysis algorithm that, based on the anatomical features detected on a prone CT series, classified patients to prone radiotherapy or to a second CT in the supine position for comparison [25]. We have demonstrated that a statistical model utilizing 3 anatomical determinants (the body mass index [BMI], the distance of the LAD from the chest wall and the area of the heart included in the radiation fields at the middle of the heart in the supine position) of the patient gives accurate estimates on the benefit of one specific position over the other by means of LAD or heart doses [19]. Here we report on an original method for providing the necessary patient-specific data based on a single CT slice image representing the middle of the heart. In this prospective study, following the validation of the clinical tool, also its routine use has been tested on a separate series of cases.

Patients and methods

The study was approved by the Institutional Review Board of the University of Szeged, and all the enrolled patients gave their written informed consent to participation. Eligible patients needed postoperative left breast radiotherapy.

Outline of the study

First, a single CT slice image at the middle of the heart (reference plane, P_{ref}) was acquired with the help of an AP scout view in the supine position (Fig. 1A). On that CT scan, the shortest distance between the anterior surface of the LAD and the chest wall (D_{med}) and the area of the heart (A_{heart}) included in the radiation fields were measured after placing a straight line between the border of the ipsilateral latissimus dorsi muscle and the lateral edge of the sternum (Fig. 1B); these data (representing the topography of the heart) were introduced to the calculator together with the patient's BMI (which correlated with the volumes of the breast and heart) as previously described in detail [19]. The calculator based on a validated statistical model provided the estimated LAD and heart dose differences in the prone *vs.* supine position of the individual patient. In the first validation set of 100 patients, CT series were acquired in both the supine position and prone position. Conformal radiation treatment plans were generated in both positions using conventional 6 MV tangential photon fields set up isocentrically and median 2 (1–3) individually weighted 6/15 MV segmental fields superimposed on the tangential fields using a multileaf collimator as described [18,19]. Wedges were used in almost all supine radiation plans. A mean dose to the PTV of 50 Gy (25 fractions) and a uniform distribution (−5% + 7%) of the prescribed dose to 95% of the PTV, were aimed at. The consistency of all contouring activities had been ensured by a chief radiation oncologist (ZK) and an experienced radiologist (AC) [26]. Equivalent heart and LAD volume contouring in either setup was ensured by one author (ZK). In the next "routine clinical practice" set of 60 patients, the acquisition of a single series of CT images according to the suggestion of the calculator was aimed at, and a second CT series was taken only if any of the dose constraints approved for the specific position were not reached in the position suggested by the calculator. In this series of patients' dose constraints were specified on the basis of previously recorded data. The upper range limits of the 90% percentile of dosimetry data in the preferred position were the following: mean LAD dose [MD_{LAD}]: 12.9 Gy and 12.5 Gy, $V_{25Gyheart}$: 2.4% and 4.7%, in the prone position and supine position, respectively. In true discordant cases, our strategy for selecting treatment position was to consider the LAD dose as a primary decisive factor.

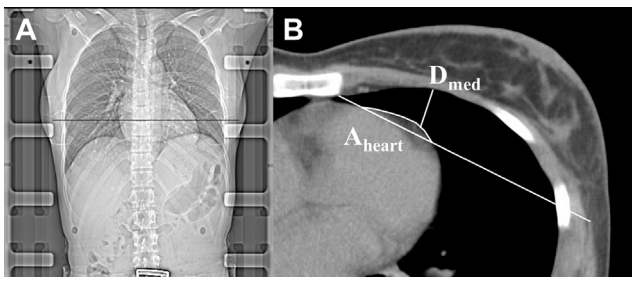

Fig. 1. The simple clinical tool generates patient-specific data to predict the benefit of prone positioning. After selecting the reference plane (P_{ref}) at the middle of the heart on the AP scout view (A), a single CT slice is acquired for the measurement of those determinants (D_{med} and A_{heart}) (B) which operate the calculator to provide estimates of the doses to the LAD or heart.

In the validation set, data on LAD and heart dose differences between the two treatment positions were extracted from the planning system and estimated by the calculator, whereas in the "routine clinical practice" series only the estimated dose differences were available. Analyses were performed on 1. the equivalence of the P_{ref} with the median plane of the full series of CT scans acquired in the supine position (P_{med}) and 2. the effect of plane miss on the patient-related determinants and choice of preferable position. The sensitivity and specificity of this simple clinical method were evaluated based on the dosimetry data obtained using the topogram for selecting the position (n = 100). In the "routine clinical practice" series, the acceptability of the position as predicted by the calculator, the LAD and heart doses achieved without taking 2 CT series, and the need of performing a second CT series and changing position or irradiation technique were analyzed.

External testing

The supine and prone CT series and supine topogram of patients included in the study "Individualized positioning for maximum heart and index breast protection during breast irradiation: comparative study between Prone and Supine (Approval: 26/09/2013, B707201318246) were retrospectively used for independent testing. The protocol of patient positioning, delineation and radiation treatment planning has been described [27].

First, P_{ref} was selected on the topogram. Then, the predictors BMI, D_{med}, A_{heart} as measured in P_{ref} were introduced to the calculator. As a second step, D_{med}, A_{heart} were also measured in $P_{med.}$ LAD and heart dose differences between the two treatment positions extracted from the planning system and estimated by the calculator were analyzed. Finally, the correctness of P_{ref} was evaluated.

Statistical methods

The calculator had been developed based on linear regression models utilizing the patients' anatomical features, with ΔMD_{LAD} and $\Delta V_{25Gyheart}$ as dependent variables [19]. With a single cut-off point, a case was classified to prone positioning when the predicted value exceeded that value. Thresholds were optimized based on sensitivity and specificity as calculated from previous

Table 1
Classification measures for ΔMD_{LAD} and $\Delta V_{25Gyheart}$ using a single discrimination threshold. Great consistency is seen between the original cohort [19] and the present series.

		Original method (double CT method, $n = 83$)		Simple tool (single CT method, $n = 100$)	
	Cut-off point	Sensitivity (%)	Specificity (%)	Sensitivity (%)	Specificity (%)
ΔMD_{LAD} (Gy)	−0.6	66.6	91.1	72.4	91.5
	−0.3	70.8	90.7	75.9	91.5
	0	74.4	90.0	75.9	91.5
	0.3	77.7	88.9	79.3	88.7
	0.6	80.7	87.5	82.8	87.3
	0.9	83.4	86.0	82.8	83.1
	1.2	85.4	83.6	86.2	81.7
	1.5	86.5	81.7	86.2	77.5
	1.8	86.8	79.9	93.1	76.1
$\Delta V_{25Gyheart}$ (%)	0	47.9	89.7	50	90.8
	0.25	56.2	88.8	58.3	89.5
	0.50	63.2	85.9	64	88
	0.75	72.4	82.4	68	85.3
	1	78.8	77.7	80	85.3
	1.25	84.0	74.0	84	81.3
	1.50	87.4	77.0	92	78.6
	1.75	89.9	62.1	96	74.6

Table 2
D_{med} and A_{heart} values (mean ± SD) as measured on P_{ref} *vs.* P_{med} in all cases or in correctly and incorrectly specified P_{ref} cases; the measurements were performed on 2 CT scans at the middle of the heart either identified with the help of an A-P scout view (P_{ref}) or selected from a full CT series (P_{med}).

	All cases ($n = 100$)		Correct plane ($n = 55$)		Plane miss ($n = 45$)	
	P_{ref}	P_{med}	P_{ref}	P_{med}	P_{ref}	P_{med}
D_{median} (cm)	1.27 ± 0.59	1.25 ± 0.67	1.35 ± 0.55	1.17 ± 0.63	1.18 ± 0.63	1.34 ± 0.71
A_{heart} (mm^2)	768.8 ± 487.4	671.6 ± 450.1	730.7 ± 537.4	721.5 ± 511.2	815.4 ± 419.5	610.5 ± 358.1

[19] and present data (Table 1). Sensitivity and specificity were calculated with supine positioning as positive determinant in the model. For ΔMD_{LAD} a threshold of 0.6 Gy, and for $\Delta V_{25Gyheart}$ a cut-off point of 1.0% were chosen. In the definition of the cut-off points, a sensitivity of 80% at the minimum and the maximum achievable value of specificity was required.

LAD and heart dose constraints achievable by selecting the preferable position were specified by percentage estimation. Statistical analysis was performed with SPSS 22.0 for Windows.

Results

Validation set

In 55/100 cases, P_{ref} was the same as P_{med} while in 28 and 17 cases, P_{ref} and P_{med} differed by 1 or more planes, respectively. More among the incorrectly defined P_{ref} cases were shifted toward the caudal than the cranial direction. This resulted in smaller mean D_{med} and larger mean A_{heart} values among the plane miss cases overall (Table 2). Within the whole series, no change in the frequency of plane misses could be detected by time. Incongruency among ΔMD_{LAD} and $\Delta V_{25Gyheart}$ in the supine and prone position as predicted by the calculator on the basis of P_{ref} *vs.* P_{med} data, was present in 14 and 18 of the cases, respectively; these were all of small numerical values (Fig. 2A, B). When the LAD and heart dose differences predicted by the calculator based on the P_{ref} values were compared with the original dosimetric data from plans generated in both positions, the suggestion proved invalid in 14 (MD_{LAD}) and 16 ($V_{25Gyheart}$) cases (Fig. 2C, D). We have compared the sensitivity and specificity of ΔMD_{LAD} and $\Delta V_{25Gyheart}$ provided by the simple method based on a single CT scan with that of the original method that indicated high consistency [19] (Table 1). Based on these findings, the cut-off values of 0.6 Gy (ΔMD_{LAD}) and 1.0% ($\Delta V_{25Gyheart}$) have been selected for further analyses and practice.

Next, the concordance of calculator-predicted treatment position based on ΔMD_{LAD} *vs.* $\Delta V_{25Gyheart}$ and the need for intervention were analyzed in the validation set. In 28 supine-predicted cases and 64 prone-predicted cases, the same treatment position was suggested by both measures (Table 3). Among the 28 supine-predicted cases in 2, the radiotherapy plan revealed that MD_{LAD} > 12.5 Gy, but only 1 could be improved by changing the treatment position. Among the 64 prone-predicted cases in 8, the MD_{LAD} exceeded the dose constraint of 12.9 Gy; only 3 plans could be improved by applying the supine position. Among the discordant cases, ΔMD_{LAD} suggested prone position in 3 and supine position in 5 cases; in both groups in a single case each could the LAD dose be improved by changing the treatment position. In altogether 7 cases, a different intervention (IMRT) had to be applied (Table 3).

"Routine clinical practice" set

In the "routine clinical practice" series of 60 patients, the new method proved feasible. All patients received treatment in the position suggested by the calculator except one, who had to receive a second CT in the other position due to unacceptable LAD dose. The other patients had MD_{LAD} and $V_{25Gyheart}$ values well below the predefined dose limits, and these were similar to the values calculated in the validation set (Table 4).

External testing

In a series of 28 breast cancer patients from Liege, the predictors BMI, D_{med} and A_{heart} significantly differed from the same parameters among the patients from Szeged. In 18/28 cases, P_{ref} was equal or close to P_{med} ($\leq$6 mm), while in 10, cases P_{ref} varied from P_{med} by 9–16 mm. Comparing the calculator-provided dose differences with the treatment planning data, favored treatment position was correct in 24/28 (accuracy: 85.7%) and 23/28 (accuracy: 82.1%) cases taking into account the LAD and heart doses,

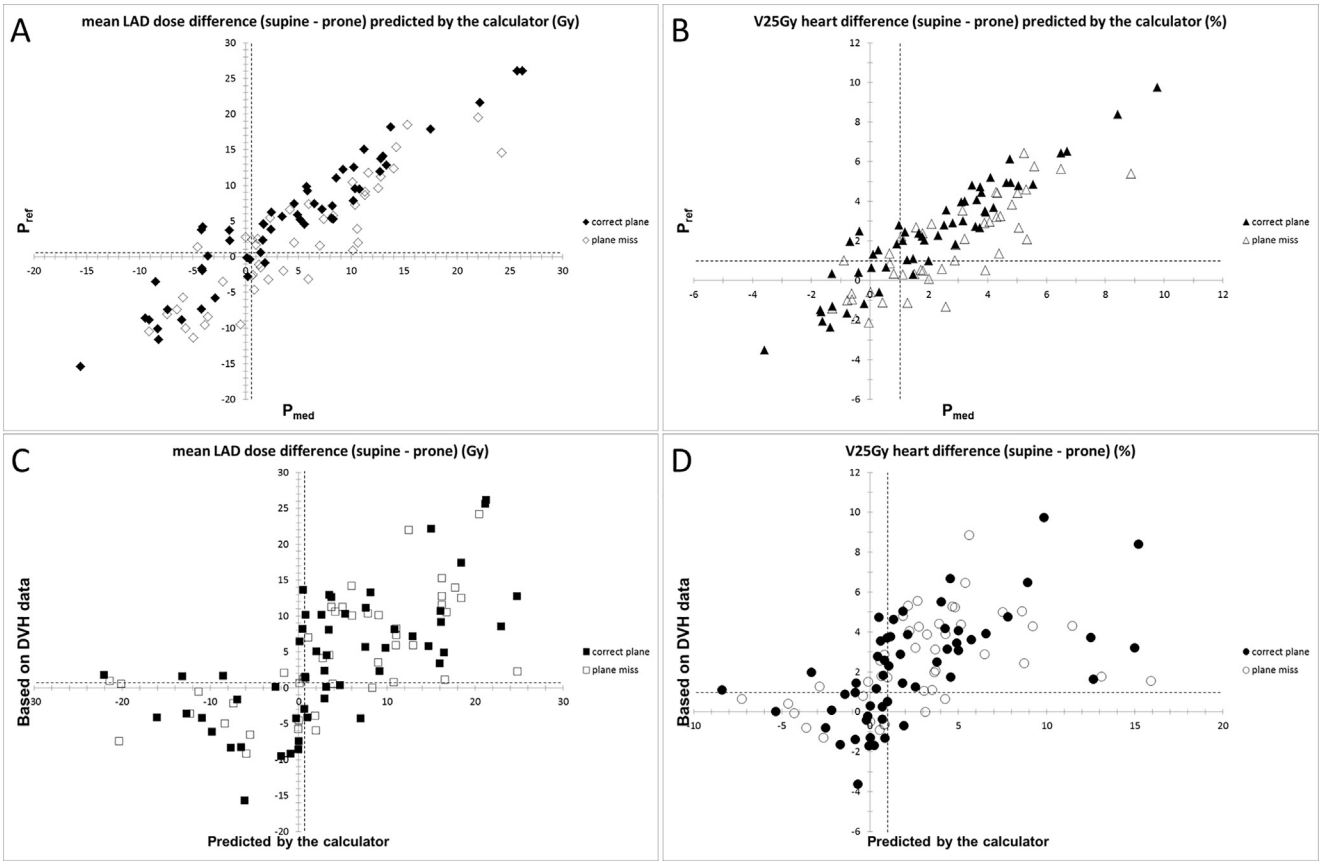

Fig. 2. Calculator suggestion of LAD (A) and heart (B) dose differences by the input of D_{med} and A_{heart} based on P_{ref} *vs.* P_{med}; LAD (C) and heart (D) doses according to the estimation of the simple clinical method based on a single CT scan *vs.* DVH data extracted from the planning system (n = 100). Dashed lines indicate the cut-off values of 0.6 Gy (ΔMD_{LAD}) and 1.0% ($\Delta V_{25Gyheart}$) specified by sensitivity and specificity values.

Table 3
Concordance of treatment position as predicted by ΔMD_{LAD} *vs.* $\Delta V_{25Gyheart}$, in the validation set (n = 100). In concordant cases the suggested position, in discordant cases the position suggested by ΔMD_{LAD} was applied unless the dose constraints were exceeded; in such cases the other treatment position or alternative techniques may be tested.

		$\Delta V_{25Gyheart}$							
		Supine				Prone			
		All	MD_{LAD} > 12.5 Gy	Change position	Other intervention	**All**	MD_{LAD} > 12.9 Gy	Change position	Other intervention
ΔMD_{LAD}	*Supine*	28	2	1/2	1/2	5	1/5	1/1	–
	Prone	3	2/3	1/2	1/2	64	8/64	3/8	5/8

Table 4
LAD and heart doses in the validation set and the "routine clinical practice" series: in the majority of cases, LAD and heart doses were well below the position-related dose constraints; for those patients who had higher than accepted doses, an alternative technique had to be applied.

	Treatment position	n (%)	Mean LAD dose (Gy)				$V_{25Gyheart}$ (%)			
			Mean	SD	Min	Max	Mean	SD	Min	Max
Validation series	*Prone*	67 (67.0)	6.55	6.03	1.70	26.66	1.16	2.24	0.0	8.75
	Supine	33 (33.0)	6.90	3.86	1.71	13.73	1.54	1.38	0.0	4.77
"Routine clinical practice" series	*Prone*	47 (78.3)	6.58	2.29	1.95	11.24	0.86	0.57	0.1	2.67
	Supine	13 (21.7)	7.35	3.05	2.54	15.85	1.15	0.95	0.21	3.57

respectively. Sensitivity and specificity of ΔMD_{LAD} was 83.3% and 86.4%, respectively, whereas sensitivity and specificity of $\Delta V_{25Gyheart}$ was 100.0% and 80.0%, respectively.

Discussion

According to the present study and others [11,14,15,19,20], in about 20% of the cases, prone positioning during left breast radiotherapy increases the dose to the LAD or the heart. To estimate and select the preferable positioning mode, supine CT seems the best approach to consider the patient's anatomical determinants. We have shown that a single CT scan at the middle of the heart may replace a whole CT series by providing consistent anatomical data thus avoiding extra radiation exposure to the patient and work load to the staff. Based on the outcome of the external implementation of the method on an independent case series, we recommend its use after local testing.

Our validated statistical model for predicting the preferable treatment position utilizes 3 specific measures, and seems the most complex predictive tool for this purpose in the literature [19]. In other studies, the in-field heart volume [16,17,25] and most frequently the size of the breast [4,11] have been used for selection. An increased BMI has also been related to larger heart doses [28] or consequential radiation cardiac morbidity [29], but its role in predicting benefit of prone positioning may be refined by the use of other patient-related parameters [19]. We consider the BMI in our calculator as a stable parameter while there is potential uncertainty in the specification of P_{ref} or imprecision in the actual measurement of D_{median} or A_{heart} on a given image. Nevertheless, detailed analysis indicates that accidental imprecision does not significantly influence final prediction (data not shown). The dose constraints optimized by individual positioning provides additional safety in practice. Despite the lack of full equivalence of the data extracted from the original method *vs.* the new method, the ultimate consistency still seems to qualify the developed "simple tool" for clinical application.

External use indicated similar accuracy as the originally developed method. Despite the reassuring results on an independent series of patients in a radiotherapy center using a slightly different protocol, the utility of the reported clinical tool could be compromised by the diversity of practice in others. PTV contouring depends on repositioning accuracy and the method of treatment verification. Interfractional differences may be especially large in the prone position [18,30]. Lakosi et al. found population systematic error values of 4.5/3.9/3.3 mm in the lateral/longitudinal/vertical directions, while the random error was 5.4/3.8/2.8 mm [27]. Among our recent breast radiotherapy cases, the population systematic and random error in the lateral/longitudinal/vertical directions was similar in the prone position *vs.* supine position (3.4/2.3/2.7 mm and 7.8/4.6/6.9 mm, respectively *vs.* 2.2/3.0/1.6 mm and 6.7/5.5/4.5 mm, respectively). Only some groups study the dose to the coronary arteries [11,12,19,20,31–34]. The outlining of the coronary vessels shows significant inter-observer variation that may jeopardize dose verification in the selected position [35,36]. Different approaches have been tested to improve consistency including the administration of contrast media [35–37]. Lee et al. developed a new protocol to outline the LAD region which included 96% of the LAD volume as delineated by 4 experienced radiation oncologists [37]. Significant impact was made by the implementation of specific guidelines [35–37]. Since the utility of the simple tool might be influenced by several factors, in addition to the use of institutional LAD contouring guidelines and study of inter-observer variation, we consider essential its testing before routine use. In the case of hypofractionated radiotherapy, the model parameters of the calculator should be re-estimated and the dose constraints should be re-defined.

The benefit of positioning prone *vs.* supine may be discordant by means of LAD and heart doses [11,19,34]. We regard the LAD dose as a surrogate indicator of radiation harm due to its proven role in late cardiac morbidity [3] and because the LAD being situated on the anterior surface of the heart is a sensitive marker of danger if the heart is at all included into radiation. Our strategy for optimization in individual cases is to consider the MD_{LAD} as priority that is usually confirmed by the heart dose (as was true for 92% of cases in our series).

The radiation exposure of the heart may be significantly reduced by the use of respiration-guided techniques including the deep inspiration breath hold (DIBH) technique and respiratory gating. In the UK HeartSpare study, supine DIBH provided superior cardiac sparing than a free-breathing prone position in large-breasted women [12]. Interestingly, the implementation of DIBH in the prone position gave the optimal heart sparing results as compared with that in the supine position or free-breathing [33]. There are some centers that due to resource limitations prioritize high cardiac dose cases for DIBH [38]. Our tool could be used for patients either not amenable for or not having access to DIBH due to patient-specific features (cardiorespiratory problems, lack of compliance) or limited/no resources, respectively.

We think that since a linear, no-threshold association exists between the mean heart dose and coronary events [3], doses to the LAD, right coronary artery or the circumflex artery should be controlled [20]. Nevertheless, the utilization of heart dose–volume data only is a possibility if LAD contouring cannot be afforded. Since good agreement exists between the mean heart dose and $V_{25Gyheart}$ (Rprone: 0.98, Rsupine: 0.99) or MD_{LAD} (Rprone and Rsupine: 0.87) in both positions ($p < 0.001$ in all comparisons), here the presented tool could be adapted to practices which adhere to the consideration of the mean heart dose.

In summary, we have demonstrated great consistency of our method based on a validated model for the prediction of treatment position prone *vs.* supine with less heart exposure during left breast radiotherapy; the simplified tool presented here omits the performance of planning CT in both positions. Based on the results of its external testing, we truly recommend its use in centers that apply prone positioning in routine clinical practice. Due to differences in populations and radiotherapy protocols, local testing is essential.

Conclusion

We consider this simple clinical tool useful for assisting individual positioning in routine clinical practice aiming at maximum heart protection during left breast irradiation.

Conflict of interest

None declared.

Acknowledgement

This work had been supported by the VKSZ 12-1-2013-0012 project. The authors are grateful to Edit Kiss and Laura Gál for their excellent technical support.

References

[1] Clarke M, Collins R, Darby S, et al. Early Breast Cancer Trialists' Collaborative Group (EBCTCG). Effects of radiotherapy and of differences in the extent of surgery for early breast cancer on local recurrence and 15-year survival: an overview of the randomised trials. Lancet 2005;366:2087–106.
[2] McGale P, Darby SC, Hall P, et al. Incidence of heart disease in 35,000 women treated with radiotherapy for breast cancer in Denmark and Sweden. Radiother Oncol 2011;100:167–75.
[3] Darby SC, Ewertz M, McGale P, et al. Risk of ischemic heart disease in women after radiotherapy for breast cancer. N Engl J Med 2013;368:987–98.
[4] Taylor CW, Kirby AM. Cardiac side-effects from breast cancer radiotherapy. Clin Oncol (R Coll Radiol) 2015;7:621–9.
[5] Shah C, Badiyan S, Berry S, et al. Cardiac dose sparing and avoidance techniques in breast cancer radiotherapy. Radiother Oncol 2014;112:9–16.
[6] Correa CR, Litt HI, Hwang WT, Ferrari VA, Solin LJ, Harris EE. Coronary artery findings after left-sided compared with right-sided radiation treatment for early-stage breast cancer. J Clin Oncol 2007;25:3031–7.
[7] Harris EE, Correa C, Hwang WT, et al. Late cardiac mortality and morbidity in early-stage breast cancer patients after breast-conservation treatment. J Clin Oncol 2006;24:4100–6.
[8] Nilsson G, Holmberg L, Garmo H, et al. Distribution of coronary artery stenosis after radiation for breast cancer. J Clin Oncol 2012;30:380–6.
[9] Nilsson G, Witt Nyström P, Isacsson U, et al. Radiation dose distribution in coronary arteries in breast cancer radiotherapy. Acta Oncol 2016;55:959–63.
[10] Becker-Schiebe M, Stockhammer M, Hoffmann W, Wetzel F, Franz H. Does mean heart dose sufficiently reflect coronary artery exposure in left-sided breast cancer radiotherapy?: influence of respiratory gating. Strahlenther Onkol 2016;192:624–31.

[11] Kirby AM, Evans PM, Donovan EM, Convery HM, Haviland JS, Yarnold JR. Prone versus supine positioning for whole and partial-breast radiotherapy: a comparison of non-target tissue dosimetry. Radiother Oncol 2010;96:178–84.
[12] Bartlett FR, Colgan RM, Donovan EM, et al. The UK HeartSpare Study (Stage IB): randomised comparison of a voluntary breath-hold technique and prone radiotherapy after breast conserving surgery. Radiother Oncol 2015;114:66–72.
[13] Griem KL, Fetherston P, Kuznetsova M, et al. Three-dimensional photon dosimetry: A comparison of treatment of the intact breast in the supine and prone position. Int J Radiat Oncol Biol Phys 2003;57:891–9.
[14] Lymberis SC, DeWyngaert JK, Parhar P, et al. Prospective assessment of optimal individual position (prone versus supine) for breast radiotherapy: volumetric and dosimetric correlations in 100 patients. Int J Radiat Oncol Biol Phys 2012;84:902–9.
[15] Formenti SC, DeWyngaert JK, Jozsef G, Goldberg JD. Prone vs supine positioning for breast cancer radiotherapy. JAMA 2012;308:861–3.
[16] DeWyngaert JK, Jozsef G, Mitchell J, Rosenstein B, Formenti SC. Accelerated intensity-modulated radiotherapy to breast in prone position: dosimetric results. Int J Radiat Oncol Biol Phys 2007;68:1251–9.
[17] Formenti SC, Gidea-Addeo D, Goldberg JD, et al. Phase I-II trial of prone accelerated intensity modulated radiation therapy to the breast to optimally spare normal tissue. J Clin Oncol 2007;25:2236–42.
[18] Varga Z, Hideghéty K, Mező T, Nikolényi A, Thurzó L, Kahán Z. Individual positioning: a comparative study of adjuvant breast radiotherapy in the prone versus supine position. Int J Radiat Oncol Biol Phys 2009;75:94–100.
[19] Varga Z, Cserháti A, Rárosi F, et al. Individualized positioning for maximum heart protection during breast irradiation. Acta Oncol. 2014;53:58–64.
[20] Würschmidt F, Stoltenberg S, Kretschmer M, Petersen C. Incidental dose to coronary arteries is higher in prone than in supine whole breast irradiation. A dosimetric comparison in adjuvant radiotherapy of early stage breast cancer. Strahlenther Onkol 2014;190:563–8.
[21] Dundas KL, Pogson EM, Batumalai V, et al. Australian survey on current practices for breast radiotherapy. J Med Imaging Radiat Oncol 2015;59:736–42.
[22] Lakosi F, Gulyban A, Janvary L, et al. Respiratory motion, anterior heart displacement and heart dosimetry: comparison between prone (Pr) and supine (Su) whole breast irradiation. Pathol Oncol Res 2015;21:1051–8.
[23] Merchant TE, McCormick B. Prone position breast irradiation. Int J Radiat Oncol Biol Phys 1994;30:197–203.
[24] Buijsen J, Jager JJ, Bovendeerd J, et al. Prone breast irradiation for pendulous breasts. Radiother Oncol 2007;82:337–40.
[25] Zhao X, Wong EK, Wang Y, et al. A support vector machine (SVM) for predicting preferred treatment position in radiotherapy of patients with breast cancer. Med Phys 2010;37:5341–50.
[26] Feng M, Moran JM, Koelling T, et al. Development and validation of a heart atlas to study cardiac exposure to radiation following treatment for breast cancer. Int J Radiat Oncol Biol Phys 2011;79:10–8.
[27] Lakosi F, Gulyban A, Ben-Mustapha Simoni S, et al. Feasibility evaluation of prone breast irradiation with the Sagittilt© system including residual-intrafractional error assessment. Cancer Radiother 2016;20:776–82.
[28] Evans SB, Sioshansi S, Moran MS, Hiatt J, Price LL, Wazer DE. Prevalence of poor cardiac anatomy in carcinoma of the breast treated with whole-breast radiotherapy: reconciling modern cardiac dosimetry with cardiac mortality data. Am J Clin Oncol 2012;35:587–92.
[29] Evans ES, Prosnitz RG, Yu X, et al. Impact of patient-specific factors, irradiated left ventricular volume, and treatment set-up errors on the development of myocardial perfusion defects after radiation therapy for left-sided breast cancer. Int J Radiat Oncol Biol Phys 2006;66:1125–34.
[30] Mulliez T, Gulyban A, Vercauteren T, et al. Setup accuracy for prone and supine whole breast irradiation. Strahlenther Onkol 2016;192:254–9.
[31] Aznar MC, Korreman SS, Pedersen AN, Persson GF, Josipovic M, Specht L. Evaluation of dose to cardiac structures during breast irradiation. Br J Radiol 2011;84:743–6.
[32] Mulliez T, Veldeman L, van Greveling A, et al. Hypofractionated whole breast irradiation for patients with large breasts: a randomized trial comparing prone and supine positions. Radiother Oncol 2013;108:203–8.
[33] Mulliez T, Veldeman L, Speleers B, et al. Heart dose reduction by prone deep inspiration breath hold in left-sided breast irradiation. Radiother Oncol 2015;114:79–84.
[34] Verhoeven K, Swelden C, Petillion S, et al. Breathing adapted radiation therapy in comparison with prone position to reduce the doses to the heart, left anterior descending artery and contralateral breast in whole breast radiation therapy. Pract Radiat Oncol 2014;4:123–9.
[35] Lorenzen EL, Taylor CV, Maraldo M, et al. Inter-observer variation in delineation of the heart and left anterior descending coronary artery in radiotherapy for breast cancer: a multi-centre study from Denmark and the UK. Radiother Oncol 2013;108:254–8.
[36] Duane F, Aznar MC, Bartlett F, et al. A cardiac contouring atlas for radiotherapy. Radiother Oncol 2017;122:416–22.
[37] Lee J, Hua K-L, Hsu S-M, et al. Development of delineation for the left anterior descending coronary artery region in left breast cancer radiotherapy: an optimized organ at risk. Radiother Oncol 2017;122:423–30.
[38] Tanna N, McLauchlan R, Karis S, Welgemoed C, Gujral DM, Cleator SJ. Assessment of upfront selection criteria to prioritise patients for breath-hold left-sided breast radiotherapy. Clin Oncol (R Coll Radiol) 2017;29:356–61.

III.

Dosimetric comparison of 3D-CRT, sliding window IMRT and VMAT techniques for external beam accelerated partial breast irradiation

Authors: Renáta Lilla Kószó[1], Zsuzsanna Kahán[1], Barbara Darázs[1], Ferenc Rárosi[2], Zoltán Varga[1]

[1]Department of Oncotherapy, [2]Department of Medical Informatics, University of Szeged, Hungary

Corresponding author: Renáta Lilla Kószó, Department of Oncotherapy, University of Szeged, Korányi fasor 12, H-6720 Szeged, Hungary. E-mail address: koszorenata@gmail.com

Running title: Dosimetric comparison of accelerated partial breast irradiation techniques

Disclosure statement: The authors report no conflicts of interest.

Abstract

Background: Our aim was to implement individualized accelerated partial breast irradiation (APBI) based on optimal dose distribution and organ at risk (OAR) protection and identify the individually most advantageous technique by considering various tumour- and patient-related factors.

Material and methods: This prospective cohort study included 138 low-risk breast cancer patients needing postoperative radiotherapy (RT). APBI plans were generated with 3-dimensional conformal RT (3D-CRT), sliding window intensity-modulated RT (IMRT) and volumetric-modulated arc radiotherapy (VMAT) techniques. If the distance of the centre of the planning target volume (PTV) from the body surface was <25 mm, additional plans were completed with an electron beam. The prescribed dose to the PTV was 37.5 Gy/10 fractions, 1 fraction/day. A Plan Quality Index (PQI) adapted for APBI served as a basis for comparisons.

Results: IMRT plans provided the best homogeneity. Conformity was improved by VMAT the most. Mean lung and heart doses were the lowest in 3D-CRT plans. PQI was the most favourable in 45 (32.6%) VMAT, 13 (9.4%) IMRT and 9 (6.5%) 3D-CRT plans, while PQIs were similar in the rest of the cases. 3D-CRT plans were preferable in patients with large PTV volumes. The addition of an electron beam improved the PQI of 3D-CRT plans but had no relevant effect on that of IMRT and VMAT. IMRT plans were more often superior than VMAT plans if the PTV was superficial ($p<0.001$), or was situated in the medial ($p=0.032$) and upper quadrants ($p=0.046$).

Conclusions: Based on a comprehensive analysis using a PQI adapted for APBI, while IMRT and VMAT plans give superior results as compared to 3D-CRT in general, the latter technique still may be preferable in a few cases with large PTV. In superficially located tumour beds, the addition of an electron beam to 3D-CRT fields or the use of IMRT seem preferable.

Keywords: accelerated partial breast irradiation (APBI); conformal radiotherapy; dosimetry; electron irradiation; IMRT; Plan Quality Index (PQI); VMAT

Introduction

Breast cancer is the most common non-skin cancer among women in the developed countries. Thanks to breast cancer screening, more and more patients are diagnosed with an early stage disease enabling breast conserving treatment involving surgery and radiotherapy [1,2]. Accelerated partial breast irradiation (APBI) proved an adequate therapeutic method in certain low-risk cases and has been introduced into practice a decade ago [2-5]. Recently, based on confirmatory results of the efficacy and safety of most techniques, eligibility for APBI has been extended to cases previously considered as medium-risk cases [4-7].

The traditional method of APBI has been brachytherapy delivered with interstitial needles, or later with innovative balloon-based brachytherapy devices [2,3,6]. Since breast brachytherapy needs special infrastructure and expertise, due to the increasing number of patients in the need of APBI later, conformal external beam radiation techniques such as 3D-conformal radiation therapy (3D-CRT) applying multiple static photon and/or electron fields, intensity-modulated radiotherapy (IMRT), tomotherapy, volumetric-modulated arc radiotherapy (VMAT) and proton beam therapy were utilized [8-11]. The combination of photon and an 'en face' electron field aims at improving planning target volume (PTV) coverage and risk organ exposure [10-14]. IMRT applies complex structure-based planning techniques and variable intensity beam fluencies to optimize dose delivery resulting in the reduction of dose inhomogeneity within the target volume and of high dose irradiation to normal tissues, producing excellent dosimetric results. However, the use of multiple beams could result in a substantial volume of normal tissue receiving low or moderate doses. The VMAT technique may further improve the previously mentioned indicators by gantry rotation and dynamic multileaf collimation [8,9]. Regarding the quality of the radiotherapy (RT) plan, there may be differences among the various techniques that differ at the individual patient level. Nevertheless, the comprehensive analysis is not trivial. Several indicators describing conformity, homogeneity, target volume coverage and organ at risk (OAR) exposure exist [15-17], however, all of these characterize a plan only from one point of view.

The aim of our study was to implement individualized APBI techniques based on both optimal dose distribution and risk organ protection. We intended to identify those tumour- and patient-

related factors which may help to select the individually most advantageous technique among 3D-CRT, IMRT, VMAT or photon-electron mixed beam RT. With the aim of comparing different RT plans in complex manner, and for selecting the most appropriate plan for an individual patient, we adapted an already existing method originally developed for evaluating IMRT plans [18] for the special need of evaluating APBI plans.

Material and methods

All the procedures followed were in full accordance with the ethical standards of the appropriate institutional and national committees on human experimentation and with the 1964 Helsinki declaration and its later amendments. The prospective study was registered by the Human Investigation Review Board, Regional Human Biomedical Research Ethics Committee, Albert Szent-Györgyi Health Centre, University of Szeged, Hungary (registration number: 74/2015-SZTE). The enrolled patients gave their written informed consent before being registered in the study.

Patient population

This prospective clinical cohort trial included women after breast conserving surgery, with an age of at least 50 years, diagnosed with a unifocal and unicentric breast cancer of any invasive histological type or low risk ductal carcinoma in situ (DCIS), with any hormone receptor and human epidermal growth factor receptor-2 (HER2) status, pT1-2 (≤30 mm) tumour size removed with at least 2 mm free margin, pN0 axillary status diagnosed by sentinel lymph node biopsy or axillary block dissection, without extensive intraductal component (EIC), lymphovascular invasion or distant metastases. Excision cavity localization at surgery with titanium clips was an inclusion criterion. Exclusion criteria included relative and absolute contraindications of irradiation. All cases were discussed at a multidisciplinary tumour board. Adjuvant systemic therapy was indicated according to the institutional guidelines. Various clinical data including tumour bed situation (lateral, medial/central, upper, lower) within the breast was prospectively collected.

Patient positioning and CT scanning

The patients were positioned supine on an 'All in One (AIO) Solution' (ORFIT, Wijnegem, Belgium) breast board with the arms raised over the head. For immobilization, diagonal thermoplastic mask fixation (ORFIT, Wijnegem, Belgium) was employed. All patients underwent five-millimetre slice-increment planning computed tomography (CT) scanning from the sternoclavicular joint to the level of 2 cm below the submammary fold, using a Somatom Emotion 6 CT Simulator (Siemens, Erlangen, Germany).

Target and critical structure delineation

The clinical target volume (CTV) included the excision cavity (marked with surgical clips) with a 1.5 cm margin extended in all directions, limited by 0.4 cm from the skin surface and by the outer edge of the chest wall. For compensating daily setup errors and breathing motions, a universal planning target volume (PTV)-CTV margin of 0.5 cm was added. As OARs, the ipsilateral uninvolved breast, the contralateral breast, the lungs, the heart and the left descending coronary artery (LAD) [19,20] were delineated.

Treatment planning

In all cases, 3D-CRT, sliding window IMRT and VMAT plans were generated in the Eclipse v13.6 planning system (Varian Oncology Systems, Palo Alto, CA, USA) for a Varian TrueBeamSTx (Varian Oncology Systems, Palo Alto, CA, USA) linear accelerator with HD120 multileaf collimator. In 3D-CRT technology, two 6 MV photon fields were used, closing at an angle of approximately 120° (Figure 1A). The definition of field directions was based upon tumour location and in left-sided cases the situation of the heart and LAD in relation to the PTV. For homogeneous dose distribution, further sub-segments were employed, if necessary. Sliding window IMRT planning was carried out applying 6 MV photon energy with a five-field beam arrangement of 300°, 350°, 40°, 90° and 150° in left-sided cases and 60°, 10°, 320°, 270° and 210° in right-sided cases (Figure 1B). If the target volume was located in the medial or lateral area of the breast, an additional ±10° rotation was used, depending on laterality. The field direction range of dual arc VMAT was defined by the first and last field of the IMRT plan (Figure 1C). The isocentre was placed into the geometric centre of the PTV. For comparability

purposes the same optimisation parameters were used during inverse treatment planning (IMRT, VMAT). If the shortest distance of the geometric centre of the PTV from the body surface (d) was <25 mm, in an additional plan of each technique, an ‘en face’ electron beam of 4-16 MeV energy was applied (Figure 1D), calculating 2/3 of the whole dose with photon and 1/3 with electron technique. For these fields Newton’s metal apertures were planned to reduce normal tissue exposure. For the PTV, a total dose of 37.5 Gy was prescribed (10 fractions, 3.75 Gy/fraction, 1 fraction/day, 5 times/week), ≥99% of the PTV receiving 95% of the prescribed dose and at least 90% of the PTV receiving 100% of the prescribed dose. Ten per cent at most of the PTV was allowed to receive >107% of the prescribed dose.

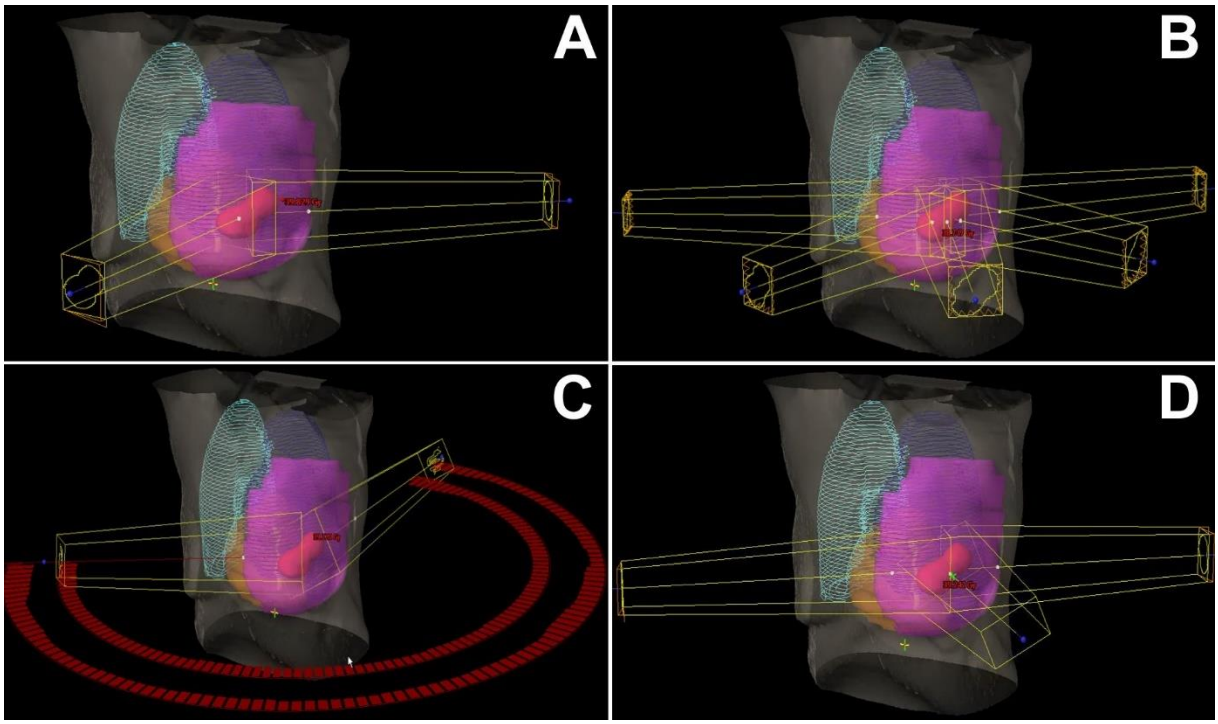

Figure 1 Beam arrangement in 3-dimensional conformal (A), intensity-modulated (B), volumetric-modulated arc (C) radiotherapy techniques and the combination of photon fields with an ‘en face’ electron beam (D)

Treatment plan evaluation

Conformity and homogeneity indexes of the PTV and dose-volume parameters of the OARs were defined in every plan.

Conformation Number (CN) [15]:

$$CN = \frac{PTV_{ref}}{V_{PTV}} \times \frac{PTV_{ref}}{V_{ref}} \quad \text{(Ideal is 1)} \tag{1}$$

PTV_{ref} refers to the volume of target receiving a dose equal to or greater than the reference dose, in this case the prescribed dose (37.5 Gy). V_{PTV} stands for the volume of target, and V_{ref} is the total volume that covered by the reference isodose.

Homogeneity Index (HI) [16] ($D_{2\%}$, $D_{50\%}$, $D_{98\%}$=dose received by 2%, 50% and 98% of PTV, respectively):

$$HI = \frac{D_{2\%} - D_{98\%}}{D_{50\%}} \text{ (Ideal is 0)} \tag{2}$$

To describe plans with a single numerical data, a Plan Quality Index (PQI) was developed based on the study of Leung et al. [18], in which the parameters (H)ealthy tissue conformity index, (M)erit and (P)enalty functions were generated as follows:

$$PQI = \sqrt{(1-H)^2 + (1-M)^2 + (1-P)^2} \text{ (Ideal is 0)} \tag{3}$$

The (H)ealthy tissue conformity index [17]:

$$H = \frac{PTV_{ref}}{V_{ref}} \text{ (Ideal is 1)} \tag{4}$$

The target volume coverage was characterized by the '(M)erit function' parameter [18], to verify the performance of hot and cold spots within the PTV. As coverage criteria differ from prostate irradiation studied by Leung et al. [18], the following limits were applied to determine 'M'. Cold spots were defined by the percentage PTV volume covered with the 100% isodose

curve (at least 90%), hot spots were defined by the percentage PTV volume receiving at least 107% of the prescribed dose (at most 10%).

$$M = \frac{\frac{V_{100\%}}{90} + \left(1 - \frac{V_{107\%}}{10}\right)}{\frac{100}{90} + 1} \text{(Ideal is 1)} \tag{5}$$

The relative volume of the ipsilateral healthy breast (ipsilateral breast – PTV) receiving at least 25, 50, 75 and 100% of the prescribed dose ($BreastV_{25\%, 50\%, 75\% \text{ and } 100\%}$, respectively), the mean dose to the ipsilateral lung ($Lung_{mean}$) and the relative volume of it receiving ≥40% of the prescribed dose ($LungV_{40\%}$), the mean dose to the heart ($Heart_{mean}$) and the relative volume of it receiving at least 50% of the prescribed dose ($HeartV_{50\%}$), the mean dose to the LAD (LAD_{mean}) and the relative volume of it receiving ≥20% of the prescribed dose ($LADV_{20\%}$) were collected.

For studying OAR exposure, the calculation algorithm applied by Leung et al. [18] was modified to make it suitable for the characterization of risk organ exposure during breast irradiation as follows. To describe the exposure of OARs with a single '(P)enalty function' parameter [18], specific dose parameters of four OARs compared to the 99% percentile of the respective sample population were averaged for each technique.

In right-sided cases:

$$P = \frac{\left(1 - \frac{BreastV_{25\%}}{70}\right) + \left(1 - \frac{Lung_{mean}}{10}\right) + \left(1 - \frac{Heart_{mean}}{5}\right) + \left(1 - \frac{LAD_{mean}}{5}\right)}{4} \text{(Ideal is 1)} \tag{6}$$

In left-sided cases:

$$P = \frac{\left(1 - \frac{BreastV_{25\%}}{70}\right) + \left(1 - \frac{Lung_{mean}}{10}\right) + \left(1 - \frac{Heart_{mean}}{10}\right) + \left(1 - \frac{LAD_{mean}}{10}\right)}{4} \text{(Ideal is 1)} \tag{7}$$

If the P value were negative in an extreme case (e.g. the exposure of all OARs was high), that would have been defined as 0 for further calculations.

To select the most favourable irradiation plan for a given patient, PQI values were compared. In order to determine an arbitrary threshold of PQI difference that indicates a difference in about half of the cases, we defined the PQI difference (PQID) as relevant if exceeded the value of 0.05. Each plan that reached this critical PQID level was referred to a respective 'winner method group', while that which did not was referred to the group of equality.

To study if any of the irradiation techniques would be more favourable in subgroups of patients, the effects of the volume of the PTV, its distance from the body surface (d) and the quadrant where it was situated were analysed.

Statistical methods

Continuous variables were expressed as mean ±standard deviation (SD). The means of continuous variables in the different 'winner method groups' were compared with Welch's one-way ANOVA. After significant ANOVA multiple comparisons were conducted with least significant difference (LSD) method. The dependence between two categorical variables was examined with Pearson's Chi-squared tests. The relationship between PQI components and PQI values was presented with scatter plot. Pearson correlation coefficients were calculated.

The effect of the addition of an electron beam to photon beams and treatment technique choice (3D-CRT *vs.* IMRT *vs.* VMAT) was analysed with two-way repeated measures (within subjects-within subjects) ANOVA. A $p<0.05$ was regarded as statistically significant. Statistical software IBM SPSS version 24 was used for statistical analysis.

Results

Patient population

The study included 138 cases. Patients belonged to the elderly age group with a median age of 62.0 (50.1-79.7) years and the majority was postmenopausal (Table 1). In most cases breast cancer was diagnosed via breast screening, the mammographic examination showed

circumscribed mass, the tumour was in the outer-upper quadrant of the breast and sentinel lymph node biopsy was carried out. Most cancers were invasive ductal carcinoma of grade 1-2, hormone receptor positive and HER2-negative. The average± SD pathologic tumour size was 11.3 ± 4.7 mm, the mean ± SD of the surgical margins was 6.8 ± 4.1 mm. The relevant patient and tumour characteristics are presented in Table 1.

Radiotherapy data

The tumour bed was left-sided in 78 patients (56.5%) and right-sided in 60 patients (43.5%). The mean and median PTV volume was 115.6 cm^3 and 108.5 (23.7-287.8) cm^3, respectively. The PTV volume was ≥100 cm^3 in 75 patients (54.3%). The distance of the geometric centre of the PTV from the body surface (d) was 3.6±1.6 cm (mean±SD) was <25 mm in 29 cases (21.0%).

In most cases, the IMRT and VMAT techniques gave superior plans based on the PQI. Parameters reflecting dose distribution within the PTV and conformity are shown in Table 2. Based on the data represented in Table 2, in most of the cases IMRT technique is the most advantageous regarding homogeneity and avoidance of overdosing, however, conformity is mostly improved by VMAT plans. OAR doses according to the technique are summarized in Table 3, while OAR exposure according to the side of treatment is shown in Table 3A. OAR exposures usually show great variety, however the mean dose to the lung and heart is the lowest in 3D-CRT plans. These data shown in detail in Tables 2 and 3 point to the fact that traditional plan quality indicators *per se* are not suitable to choose the optimal technique in an individual case.

The 'H', 'M' and 'P' parameters and the PQI values generated are presented in Table 4.

Comparing 3D-CRT, IMRT and VMAT plans on the basis of the PQID>0.05 threshold, in the whole cohort, the three techniques were equally good in 71 cases (51.4%). VMAT technique was optimal in 45 cases (32.6%), IMRT was preferable in 13 patients (9.4%) and 3D-CRT was the best in 9 cases (6.5%).

When we analysed the 2 techniques based on inverse treatment planning separately based on PQID≥0.05, the PQI was preferable using the VMAT technique in 55 cases (39.9%), while in 14 cases (10.1%) the IMRT plan was the best. VMAT and IMRT were equally good in 69 patients (50.0%).

Comparing the PQI values of patients for whom the 3D-CRT technique was the most advantageous to those for whom 3D-CRT was either equivalent with IMRT and VMAT, or worse, only the volume of the PTV emerged as significant variable (p=0.017) (Figure 2). The mean±SD of the PTV was 159.3±67.9 cm^3 in patients for whom the 3D-CRT plan was the optimal, 114.4±46.3 cm^3 in those for whom the IMRT technique, and 102.9±50.9 cm^3 in those for whom VMAT was the best; the PTV was 118.3±44.8 cm^3 in those patients for whom all the techniques gave similar PQI. Post hoc tests indicated that the PTVs were larger if the 3D-CRT plan was preferable (3D-CRT *vs.* IMRT: p= 0.035, 3D-CRT *vs.* VMAT: p= 0.002, 3D-CRT *vs.* IMRT/VMAT: p= 0.019).

Comparing the inverse planning techniques (IMRT and VMAT) only, the use of the IMRT method gave superior plans in case of superficially located tumour beds (p<0.001) (Figure 3) and if the target volumes were located in the medial/central (p<0.032) or upper quadrants (p<0.046) of the breast (Table 5).

In case of superficially located PTVs (d<25 mm, 29 patients) the effect of the addition of an electron beam was analysed for all the techniques (3D-CRT, IMRT and VMAT). Two-way repeated measures ANOVA revealed that the magnitude of the effect of adding an electron beam depends on the chosen technique (significant interaction, p<0.001). Although the addition of an electron beam improved the PQI of all treatment plans, its extent was relevant (PQI>0.05) only in the 3D-CRT plans, but not in the IMRT or VMAT plans (Table 6, Figure 4).

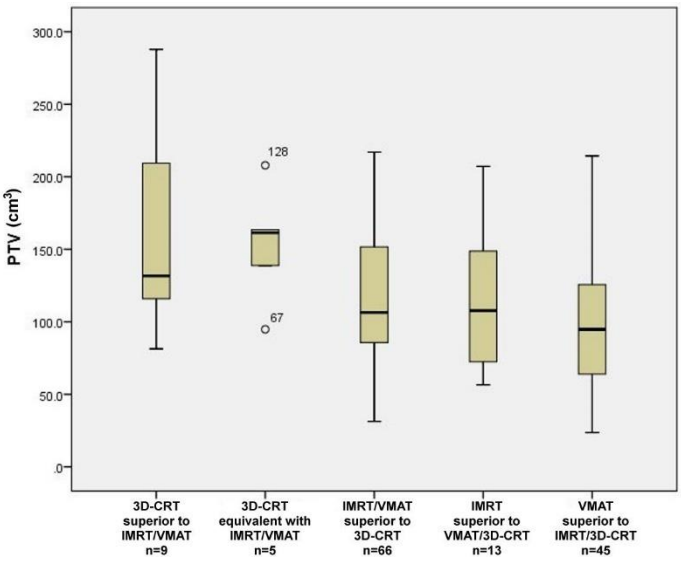

Figure 2 Comparison of Plan Quality Index values of those patients for whom 3D-CRT was the most advantageous, 3D-CRT was equivalent with IMRT or VMAT, IMRT and VMAT were equivalent but superior to 3D-CRT, IMRT was the most favourable and finally VMAT was the most favourable plan, depending on the volume of the Planning Target Volume (3D=3-dimensional conformal radiotherapy, IMRT=intensity-modulated radiotherapy, VMAT=volumetric-modulated arc radiotherapy)

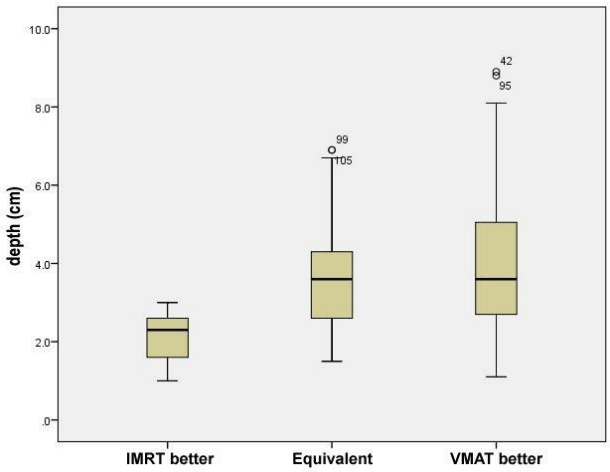

Figure 3 Plan Quality Index (PQI) was superior with intensity-modulated radiotherapy (IMRT) in cases with superficially located target volumes than with volumetric-modulated arc radiotherapy (VMAT)

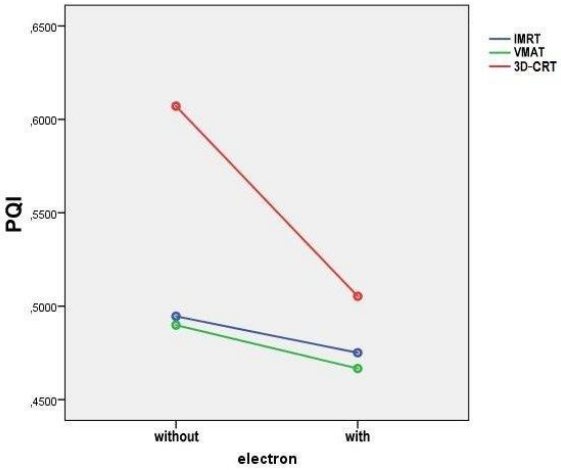

Figure 4 The effect of adding an 'en face' electron beam to photon beams on intensity-modulated radiotherapy (IMRT), volumetric-modulated arc radiotherapy (VMAT) and 3-dimensional conformal radiotherapy (3DCRT) plans as depicted on a profile figure

In 67 cases with PQI differences >0.05, we analysed which components (H, M and P function) were the primary determinants of PQI according to the three RT techniques. We found that the best PQI value of a case was primarily dependent on the P function representing OAR exposure. This function was the strength of the few (n=9) 3D-CRT-preferred cases with a relatively large PTV (mean: 159.3 cm^3, range: 81.3-287.8 cm^3) as well (Figure 5).

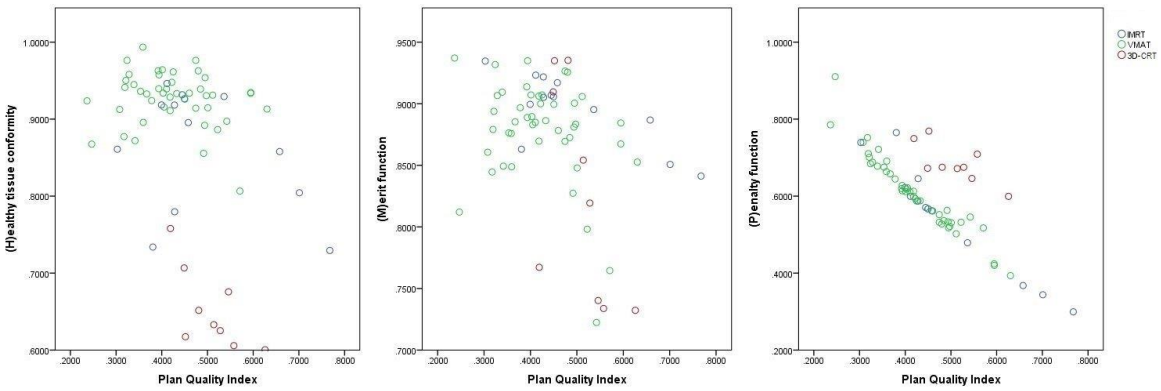

Figure 5 Representation of the effect of the components of the PQI according to the preferable plan (IMRT, VMAT or 3D-CRT)

Discussion

In selected early breast cancer cases, APBI is an attractive treatment alternative to whole breast irradiation by shortening the course of RT and reducing radiation exposure of healthy tissues significantly [1,3,4]. Various teletherapy techniques have been studied for APBI with different dosimetric specialities [8,9,21-25]. Our findings indicate that IMRT, VMAT or 3D-CRT may be individually superior in at least half of the cases; by selecting the most advantageous APBI method, dose homogeneity and OAR exposure could be optimised. The here described PQI that takes into account both homogeneity, conformity and dose to various OARs may serve as a comprehensive tool for comparing teletherapy APBI plans.

Many studies analysed the dosimetry of inverse-planning techniques over standard 3D-CRT [12,26-30]. The use of IMRT or VMAT improved conformity in all studies, and in most of them selected OARs' exposure as well. With the use of IMRT, the reduction of the dose to the ipsilateral breast [26,27], lung and heart [27] was achieved as compared to that of 3D-CRT plans. In the study of Rusthoven et al. [27], the ipsilateral breast dose was especially more favourable with IMRT than with 3D-CRT in cases with larger PTV/breast ratio and smaller breasts. Interestingly, we found altogether 9 cases out of 138 with relatively larger PTVs, in which 3D-CRT provided the best PQI probably due to the formula's complexity. Using the VMAT technique, the dose to the lung and heart was lower than that with 3D-CRT [31]. Qiu et al. [29] performed a dosimetric analysis of 16 VMAT *vs.* IMRT *vs.* 3D-CRT plans. The dose (V_{5Gy}, V_{10Gy}) to the ipsilateral breast was significantly lower with VMAT than the other 2 techniques. Heart exposure was similar among the three techniques while lung dose was superior with IMRT and VMAT than with 3D-CRT; IMRT provided the most favourable low-dose distribution in the ipsilateral lung [29].

Stelczer et al. [30] compared the step and shoot and sliding window IMRT methods and the VMAT technique to the 3D-CRT technique based on various dosimetric parameters and the original PQI approach [18] in 10 low-risk breast cancer cases. While dose homogeneity was superior using the sliding window IMRT, in accordance with our results, ipsilateral breast exposure was significantly lower with VMAT, and the protection of the lung and heart was the best with 3DCRT [30]. $V_{50\%}$ of the ipsilateral breast was the lowest in VMAT plans (29.4%),

as compared to 3D-CRT (44.1%) and sliding window IMRT (35.6%) plans. As a consequence, they recommend the use of sliding window IMRT for APBI [30].

The addition of electrons to photon beams provides more conformal but less homogenous dose distribution as compared to the photon only technique. We have found five studies dealing with the mixed beam technique in APBI [11-14,32]. All agreed that this approach may lower the ipsilateral breast dose; lung and heart doses varied according to study, and obviously the situation of the tumour bed [14]. Clearly, the use of electrons should be reserved for tumours non-deeply located [10]. In the present study, the addition of a shaped electron field to 3D-CRT provided benefit in cases with d<25 mm. We believe that this method could be recommended if due to limitations of resources or technology 3D-CRT were utilized for APBI.

In selected cases, APBI provides similar efficacy and less toxicity versus whole breast irradiation with probably better cosmesis and acceptance by the patients [33,34]. Most prospective phase II and phase III studies utilizing 3D-CRT technique for APBI have reported favourable early and late side effect profile, good or excellent cosmetic results and quality of life comparable to that with whole breast irradiation [22,34-37]. Likewise, excellent outcome was reported in studies with IMRT [24,25]. Nevertheless, in some APBI studies implementing the IMRT [23,38] or 3D-CRT method [39,40] progressive breast fibrosis and poor cosmetic outcome was reported. In the most recently reported RAPID trial, more fibrosis and progressively deteriorating cosmetic outcome was found after APBI with 3D-CRT/IMRT than after whole breast RT [41]. All these studies applied similar doses as the other teletherapy APBI trials, but in an accelerated manner (dosing twice daily). Impaired cosmetic results following 3D-CRT or IMRT APBI could have been also due to the irradiation of larger target volumes and more extensive ipsilateral breast tissue as well. The detrimental effect of large irradiated volumes on fibrosis-related poor cosmesis had been described in the 1990s [42]. Based on our results, if ipsilateral breast dose is a concern we propose the VMAT technique, or if 3D-CRT is to be utilised, the addition of electrons.

Our study suggests that while dose coverage and acceptable homogeneity may be ensured by any of the studied techniques, the main differences may be detected in OAR exposure in about 50% of the cases. Namely the dose to the heart and LAD and the success to limit the radiation

dose to the ipsilateral breast much depend on the selected method. For the evaluation of different techniques, different measures have been used in the literature. Most of the studies compared various dose-volume parameters, OAR exposure, maximum doses, coverage or more complex indexes such as conformity index, conformation number, homogeneity index or the PQI which we used [18]. All parameters carry different meanings, but if used singly, comparisons are difficult. This is why we aimed at following a comprehensive approach which is based on the simultaneous consideration of various factors such as homogeneity, conformity and OAR protection. Since in our study conformity and homogeneity did not differ as significantly as OAR exposures in the different plans (Figure 5), PQID mainly depended on which technique ensured the best comprehensive OAR protection. The strength of our method is that we based it on a relatively large and comprehensive data set.

In conclusion, we find PQI a good tool to evaluate external beam APBI plans. In most cases, IMRT and especially VMAT plans give superior PQI values than 3D-CRT plans. 3D-CRT may be favourable in cases with large PTV. In superficially situated tumour beds the addition of an electron beam results in significant PQI improvement of 3D-CRT plans. Comparing the IMRT and VMAT methods, IMRT seems superior in tumours of the superior or inner quadrant of the breast. PQI is primarily dependent on OAR exposure.

References

[1] Veronesi U, Marubini E, Mariani L, et al. Radiotherapy after breast conserving surgery in small breast carcinoma: long-term results of a randomized trial. Ann Oncol. 2001;12(7):997-1003.

[2] Vicini FA, Arthur DW. Breast brachytherapy: North American experience. Semin Radiat Oncol. 2005;15(2):108-115.

[3] Polgár C, Strnad V, Major T. Brachytherapy for partial breast irradiation: the European experience. Semin Radiat Oncol. 2005;15(2):116-122.

[4] Polgár C, Van Limbergen E, Pötter R, et al; GEC-ESTRO breast cancer working group. Patient selection for accelerated partial-breast irradiation (APBI) after breast-conserving surgery: Recommendations of the Groupe Européen de Curiethérapie-European Society for Therapeutic Radiology and Oncology (GEC-ESTRO) breast cancer working group based on clinical evidence (2009). Radiother Oncol. 2010;94(3):264-273.

[5] Smith BD, Arthur DW, Buchholz TA, et al. Accelerated partial breast irradiation consensus statement from the American Society for Radiation Oncology (ASTRO). Int J Radiat Oncol Biol Phys. 2009;74(4):987-1001.

[6] Shah C, Wobb J, Manyam B, et al. Accelerated partial breast irradiation utilizing brachytherapy: patient selection and workflow. J Contemp Brachytherapy. 2016;8(1):90-94.

[7] Correa C, Harris EE, Leonardi MC, et al. Accelerated Partial Breast Irradiation: Executive summary for the update of an ASTRO Evidence-Based Consensus Statement. Pract Radiat Oncol. 2017;7(2):73-79.

[8] Njeh CF, Saunders MW, Langton CM. Accelerated partial breast irradiation using external beam conformal radiation therapy: a review. Crit Rev Oncol Hematol. 2012;81(1):1-20.

[9] Formenti SC. External-beam partial-breast irradiation. Semin Radiat Oncol. 2005;15(2):92-99.

[10] Fekete G, Újhidy D, Együd Z, et al. Partial breast radiotherapy with simple teletherapy techniques. Med Dosim. 2015;40(4):290-295.

[11] Kozak KR, Doppke KP, Katz A, et al. Dosimetric comparison of two different three-dimensional conformal external beam accelerated partial breast irradiation techniques. Int J Radiat Oncol Biol Phys. 2006;65(2):340-346.

[12] El Nemr M, Heymann S, Verstraet R, et al. Mixed modality treatment planning of accelerated partial breast irradiation: to improve complex dosimetry cases. Radiat Oncol. 2011;6:154.
[13] Recht A, Ancukiewicz M, Alm El-Din MA, et al. Lung dose-volume parameters and the risk of pneumonitis for patients treated with accelerated partial-breast irradiation using three-dimensional conformal radiotherapy. J Clin Oncol. 2009;27(24):3887-3893.
[14] Mydin AR, Gaffney H, Bergman A, et al. Does a three-field electron / minitangent photon technique offer dosimetric advantages to a multifield, photon-only technique for accelerated partial breast irradiation? Am. J. Clin. Oncol. 2010;33(4):336-340.
[15] van't Riet A, Mak AC, Moerland MA, et al. A conformation number to quantify the degree of conformality in brachytherapy and external beam irradiation: Application to the prostate. Int J Radiat Oncol Biol Phys. 1997;37:731-736.
[16] Shaw E, Kline R, Gillin M, et al. Radiation Therapy Oncology Group: Radiosurgery quality assurance guidelines. Int J Radiat Oncol Biol Phys. 1993;27:1231-1239.
[17] Lomax NJ, Scheib SG. Quantifying the degree of conformity in radiosurgery treatment planning. Int J Radiat Oncol Biol Phys. 2003;55:1409-1419.
[18] Leung LHT, Kan MWK, Cheng ACK, et al. A new dose-volume-based Plan Quality Index for IMRT plan comparison. Radiother Oncol. 2007;85:407-417.
[19] Duane F, Aznar MC, Bartlett F, et al. A cardiac contouring atlas for radiotherapy. Radiother Oncol. 2017;122(3):416-422.
[20] Varga Z, Cserháti A, Rárosi F, et al. Individualized positioning for maximum heart protection during breast irradiation. Acta Oncol. 2014;53(1):58-64.
[21] Chen PY, Wallace M, Mitchell C, et al. Four-year efficacy, cosmesis and toxicity using three-dimensional conformal external beam radiation therapy to deliver accelerated partial breast irradiation. Int J Radiat Oncol Biol Phys. 2010;76(4):991-997.
[22] Shah C, Wilkinson JB, Lanni T, et al. Five-year outcomes and toxicities using 3-dimensional conformal external beam radiation therapy to deliver accelerated partial breast irradiation. Clin Breast Cancer.2013;13(3):206-211.
[23] Liss AL, Ben-David MA, Jagsi R, et al. Decline of cosmetic outcomes following accelerated partial breast irradiation using intensity-modulated radiation therapy: Results of a single-institution prospective clinical trial. Int J Radiat Oncol Biol Phys. 2014;89(1):96-102.

[24] Lewin AA, Derhagopian R, Saigal K, et al. Accelerated partial breast irradiation is safe and effective using intensity-modulated radiation therapy in selected early-stage breast cancer. Int J Radiat Oncol Biol Phys. 2012;82(5):2104-2110.
[25] Lei RY, Leonard CE, Howell KT, et al. Four-year clinical update from a prospective trial of accelerated partial breast intensity-modulated therapy (APBIMRT). Breast Cancer Res Treat. 2013;140(1):119-133.
[26] Moon SH, Shin KH, Kim TH, et al. Dosimetric comparison of four different external beam partial breast irradiation techniques: three-dimensional conformal radiotherapy, intensity-modulated radiotherapy, helical tomotherapy, and proton beam therapy. Radiother. Oncol. 2009;90(1):66-73.
[27] Rusthoven KE, Carter DL, Howell K, et al. Accelerated partial-breast intensity-modulated radiotherapy results in improved dose distribution when compared with three-dimensional treatment-planning techniques. Int J Radiat Oncol Biol Phys. 2008;70(1):296-302.
[28] Qiu J-J, Chang Z, Wu QJ, et al. Impact of volumetric-modulated arc therapy technique on treatment with partial breast irradiation. Int J Radiat Oncol Biol Phys. 2010;78(1):288-296.
[29] Qiu JJ, Chang Z, Horton JK, et al. Dosimetric comparison of 3D conformal, IMRT, and V-MAT techniques for accelerated partial-breast irradiation (APBI). Med Dosim. 2014;39(2):152-158.
[30] Stelczer G, Major T, Mészáros N, et al. Dosimetric comparison of different techniques for external beam accelerated partial breast irradiation. Magy Onkol. 2016;60(4):305-311.
[31] Essers M, Osman SOS, Hol S, et al. Accelerated partial breast irradiation (APBI): are breath-hold and volumetric radiation therapy techniques useful? Acta Oncol. 2014;53(6):788-794.
[32] Palma BA, Sánchez AU, Salguero FJ, et al. Combined modulated electro and photon beams planned by a Monte-Carlo-based optimization procedure for accelerated partial breast irradiation. Phys Med Biol. 2012;57(5):1191-1202.
[33] Strnad V, Ott OJ, Hildebrandt G, et al. 5-year results of accelerated partial breast irradiation using sole interstitial multicatheter brachytherapy versus whole-breast irradiation with boost after breast-conserving surgery for low-risk invasive and in-situ carcinoma of the female breast: a randomised, phase 3, non-inferiority trial. Lancet. 2016;387(10015):229-238.

[34] Coles CE, Griffin CL, Kirby AM, et al. Partial-breast radiotherapy after breast conservation surgery for patients with early breast cancer (UK IMPORT LOW trial): 5-year results from a multicentre, randomised, controlled, phase 3, non-inferiority trial. Lancet. 2017;390(10099):1048-1060.

[35] Mózsa E, Mészáros N, Major T, et al. Accelerated partial breast irradiation with external beam three-dimensional conformal radiotherapy. Strahlenther Onkol. 2014;190(5):444-450.

[36] Rodriguez N, Sanz X, Dengra J, et al. Five-year outcomes, cosmesis, and toxicity with 3-dimensional conformal external beam radiation therapy to deliver accelerated partial breast irradiation. Int J Radiat Oncol Biol Phys. 2013;87(5):1051-1057.

[37] Chafe S, Moughan J, McCormick B, et al. Late toxicity and patient self-assessment of breast appearance/satisfaction on RTOG0319: A phase 2 trial of 3-dimensional conformal radiation therapy-accelerated partial breast irradiation following lumpectomy for stages I and II breast cancer. Int J Radiat Oncol Biol Phys. 2013;86(5):854-859.

[38] Jagsi R, Ben-David MA, Moran JM, et al. Unacceptable cosmesis in a protocol investigating intensity-modulated radiotherapy with active breathing control for accelerated partial-breast irradiation. Int J Radiat Oncol Biol Phys. 2010;76(1):71-78.

[39] Hepel JT, Tokita M, MacAusland SG, et al. Toxicity of three-dimensional conformal radiotherapy for accelerated partial breast irradiation. Int J Radiat Oncol Biol Phys. 2009;75(5):1290-1296.

[40] Olivotto IA, Whelan TJ, Parpia S, et al. Interim cosmetic and toxicity results from RAPID: A randomized trial of accelerated partial breast irradiation using three-dimensional conformal external beam radiation therapy. J Clin Oncol. 2013;31(32):4038-4045.

[41] Whelan T, Julian J, Levine M, et al. RAPID: A randomized trial of accelerated partial breast irradiation using 3-dimensional conformal radiotherapy (3DCRT). Presented at: San Antonio Breast Cancer Symposium; 2018 Dec 4-8; San Antonio, TX, USA. Abstract No GS4-03.

[42] Borger JH, Kemperman H, Smitt HS, et al. Dose and volume effects on fibrosis after breast conservation therapy. Int J Radiat Oncol Biol Phys. 1994;30(5):1073-1081.

Patient- and tumour-related characteristics	N=138	
	N	%
Menostatus		
Premenopausal (%)	17	12.3
Postmenopausal (%)	121	87.7
Mode of detection		
Screening (%)	109	79.0
Symptomatic (%)	29	21.0
Mammographic appearance (%)		
Circumscribed mass	71	51.4
Spiculated mass	57	41.3
Asymmetric density	7	5.1
No abnormality	1	0.7
Microcalcification (with or without a parenchymal change)	12	8.7
Axillary surgery (%)		
Sentinel lymph node biopsy	121	87.7
Axillary sampling/block dissection	17	12.3
Histological type		
Invasive ductal carcinoma not special type	116	84.1
Invasive lobular carcinoma	2	1.4
Invasive medullary carcinoma	1	0.7
Invasive tubular carcinoma	9	6.5
Invasive mucinous carcinoma	3	2.2
Invasive papillary carcinoma	2	1.4
Invasive mixed ductal/lobular carcinoma	3	2.2
Invasive apocrine carcinoma	1	0.7
Other	1	0.7
Nottingham grade (%)		
1	52	37.7
2	72	52.2
3	14	10.1
Estrogen receptor status (%)		
Positive (≥10%)	124	89.9
Negative (<10%)	14	10.1
Progesteron receptor status (%)		
Positive (≥10%)	115	83.3
Negative (<10%)	23	16.7
HER2 status (%)		
Positive	4	2.9
Negative	134	97.1
Adjuvant chemotherapy (%)	8	5.8
Adjuvant endocrine treatment (%)		
Tamoxifen	10	7.2
Aromatase inhibitor	30	21.7

Table 1 Patient- and tumour-related characteristics

	Technique	V99% (mean±SD, %)	V107% (mean±SD, %)	CN (mean±SD)	HI (mean±SD)
All cases	3D-CRT	97.27 ± 1.46	3.51 ± 1.53	0.582 ± 0.063	0.083 ± 0.018
	IMRT	97.16 ± 1.64	0.68 ± 0.73	0.833 ± 0.081	0.045 ± 0.010
	VMAT	97.71 ± 0.87	1.45 ± 1.16	0.901 ± 0.032	0.054 ± 0.010
PTV< 100 cm^3	3D-CRT	97.30 ± 1.36	3.46 ± 1.51	0.585 ± 0.061	0.082 ± 0.018
	IMRT	96.85 ± 2.27	0.66 ± 0.79	0.808 ± 0.090	0.046 ± 0.011
	VMAT	97.54 ± 1.16	1.50 ± 1.33	0.900 ± 0.035	0.054 ± 0.011
PTV≥ 100 cm^3	3D-CRT	97.26 ± 1.55	3.56 ± 1.55	0.580 ± 0.065	0.085 ± 0.017
	IMRT	97.42 ± 0.72	0.69 ± 0.67	0.853 ± 0.066	0.044 ± 0.010
	VMAT	97.86 ± 0.46	1.40 ± 1.00	0.902 ± 0.030	0.055 ± 0.009
d< 2.5 cm	3D-CRT	97.56 ± 0.75	3.86 ± 1.29	0.589 ± 0.068	0.089 ± 0.016
	3D-CRT+e	95.75 ± 2.35	4.71 ± 1.55	0.765 ± 0.071	0.082 ± 0.014
	IMRT	96.85 ± 3.20	1.07 ± 0.91	0.785 ± 0.081	0.052 ± 0.010
	IMRT+e	95.20 ± 3.42	2.87 ± 1.39	0.828 ± 0.069	0.060 ± 0.008
	VMAT	97.52 ± 1.65	2.35 ± 1.41	0.870 ± 0.037	0.064 ± 0.007
	VMAT+e	96.75 ± 2.19	3.26 ± 1.34	0.886 ± 0.048	0.065 ± 0.008

Table 2 Partial breast irradiation according to the radiotherapy technique used: parameters reflecting dose distribution within the PTV and conformity

3D-CRT=3-dimensional conformal radiotherapy, CN=conformation number, d=distance of the centre of the PTV from the body surface, e=electron beam added, HI=homogeneity index, IMRT=intensity-modulated radiotherapy, PTV=planning target volume, SD=standard deviation, VMAT=volumetric-modulated arc radiotherapy, Vx%=relative volume of the PTV receiving x% of the prescribed dose

	Technique	Ipsilateral breast				Ipsilateral lung		Heart		LAD			Contralateral breast		Body
		V100% (mean±SD, %)	V75% (mean±SD, %)	V50% (mean±SD, %)	V25% (mean±SD, %)	mean dose (mean±SD, Gy)	V40% (mean±SD, %)	mean dose (mean±SD, Gy)	V50% (mean±SD, %)	mean dose (mean±SD, Gy)	Dmax (mean±SD, Gy)	V20% (mean±SD, %)	mean dose (mean±SD, Gy)	V10% (mean±SD. %)	V10% rel to PTV (mean±SD)
All cases	3D-CRT	10.1±26.2	15.5±7.3	23.7±8.9	42.4±11.6	3.19±1.40	6.31±3.67	0.93±1.27	0.43±1.19	2.82±3.84	8.90±11.2	13.2±20.5	1.05±1.28	12.8±15.9	17.9±10.7
	IMRT	1.70±1.38	9.06±3.84	18.7±7.6	37.3±11.7	4.81±1.62	7.01±4.18	2.73±1.97	0.66±1.79	3.55±2.11	7.71±5.32	7.5±15.2	1.30±0.52	4.66±7.57	26.4±9.6
	VMAT	0.84±0.72	6.94±3.52	17.2±7.5	35.2±10.4	4.12±1.42	4.87±3.29	2.61±1.78	0.35±1.14	3.65±2.37	6.99±4.72	9.6±18.0	0.79±0.33	0.64±1.73	18.5±5.8
PTV< 100 cm^3	3D-CRT	10.5±38.6	12.0±6.1	19.8±8.2	38.1±11.7	3.23±1.43	6.52±3.51	0.95±1.36	0.39±0.96	2.86±3.75	8.11±10.5	13.5±20.6	1.25±1.33	14.4±16.1	21.6±6.5
	IMRT	1.5±1.3	7.0±2.7	14.6±5.8	31.7±10.8	4.43±1.35	6.69±3.10	2.40±1.81	0.66±1.62	3.45±2.25	7.75±5.36	8.1±15.3	1.33±0.55	6.67±8.96	33.7±8.9
	VMAT	0.5±0.4	4.9±2.3	12.8±5.7	30.8±10.2	3.71±1.13	4.41±2.13	2.29±1.64	0.31±0.91	3.48±2.14	6.80±4.54	8.7±15.7	0.80±0.33	0.65±1.15	22.3±6.0
PTV≥ 100 cm^3	3D-CRT	9.7±4.8	18.4±7.0	27.0±8.2	46.0±10.3	3.16±1.39	6.13±3.81	0.91±1.19	0.47±1.35	2.80±3.93	9.54±11.7	13.0±20.6	0.89±1.22	11.5±15.9	14.8±12.4
	IMRT	1.9±1.4	10.8±3.8	22.2±7.2	41.9±10.3	5.12±1.76	7.28±4.91	3.01±2.07	0.65±1.94	3.64±2.00	7.68±5.32	7.0±15.3	1.27±0.49	3.00±5.80	20.3±4.6
	VMAT	1.1±0.8	8.6±3.5	20.9±6.9	38.9±9.1	4.47±1.55	5.25±3.99	2.88±1.86	0.39±1.31	3.80±2.55	7.15±4.88	10.4±19.9	0.79±0.32	0.62±2.10	15.3±3.1
d< 2.5 cm	3D-CRT	6.79±4.82	12.8±7.51	17.2±9.08	39.8±12.9	2.60±1.22	6.16±3.70	1.25±1.86	0.46±1.23	2.96±3.70	9.69±12.3	15.4±21.3	1.90±1.61	21.8±18.9	17.9±10.7
	3D-CRT+e	2.59±2.28	9.06±5.44	15.1±8.34	27.0±11.8	3.41±1.74	5.96±3.68	1.24±1.33	0.47±1.10	3.44±3.28	11.1±12.5	10.0±16.6	1.28±1.08	18.0±16.3	21.9±6.6
	IMRT	1.76±1.46	7.28±3.43	14.0±6.67	29.9±11.9	4.62±1.81	7.72±4.27	2.97±2.46	0.99±2.27	3.44±2.48	8.94±6.54	10.2±17.9	1.55±0.62	11.6±11.1	26.4±9.6
	IMRT+e	1.17±0.87	6.86±3.83	11.2±5.89	22.8±10.9	4.82±2.12	6.73±4.72	2.40±1.82	0.64±1.35	3.84±3.05	10.7±9.58	17.8±21.3	1.13±0.49	2.38±3.93	24.0±7.8
	VMAT	0.82±0.61	5.42±3.10	12.5±6.81	30.5±11.9	3.85±1.52	5.44±3.27	2.94±2.19	0.62±1.42	4.01±2.61	7.92±5.51	12.7±21.4	1.02±0.42	1.62±3.05	18.5±5.8
	VMAT+e	0.74±0.72	5.63±3.47	10.1±5.68	22.0±10.4	4.31±1.97	5.54±4.26	2.38±1.66	0.49±1.01	4.16±3.05	10.1±9.24	18.7±22.6	0.70±0.28	0.44±1.41	18.8±4.3

Table 3 Partial breast irradiation according to the radiotherapy technique used: Dose to the organs at risk

(3D-CRT=3-dimensional conformal radiotherapy, d=distance of the centre of the PTV from the body surface, e=electron beam added, IMRT=intensity-modulated radiotherapy, PTV=planning target volume, SD=standard deviation, VMAT=volumetric-modulated arc radiotherapy, Vx%=relative volume of the structure receiving x% of the prescribed dose)

	Technique	Heart left-sided cases		LAD left-sided cases			Heart right-sided cases		LAD right-sided cases		
		mean dose (mean±SD, Gy)	V50% (mean±SD, %)	mean dose (mean±SD, Gy)	Dmax (mean±SD, Gy)	V20% (mean±SD, %)	mean dose (mean±SD, Gy)	V50% (mean±SD, %)	mean dose (mean±SD, Gy)	Dmax (mean±SD, Gy)	V20% (mean±SD, %)
All cases	3D-CRT	1.15±1.21	0.77±1.51	4.07±4.33	13.9±12.4	16.6±19.9	0.66±1.29	0.00±0.00	1.25±2.32	2.69±4.32	9.0±20.6
	IMRT	3.45±2.23	1.08±2.16	4.57±2.17	10.5±5.8	13.5±18.3	1.82±1.05	0.12±0.96	2.27±1.10	4.33±0.73	0.00±0.00
	VMAT	3.16±2.01	0.62±1.48	4.90±2.45	9.9±4.6	17.2±21.3	1.91±1.11	0.01±0.07	2.07±0.80	3.46±1.21	0.00±0.00
PTV< 100 cm^3	3D-CRT	1.06±1.08	0.68±1.20	3.84±4.20	11.7±12.3	15.0±19.4	0.81±1.68	0.00±0.00	1.54±2.58	3.62±5.07	11.4±22.2
	IMRT	3.01±2.10	0.94±1.70	4.52±2.28	10.6±5.8	14.3±18.0	1.59±0.81	0.28±1.44	2.01±1.17	4.21±0.85	0.00±0.00
	VMAT	2.73±1.90	0.52±1.16	4.58±2.14	9.5±4.3	15.3±18.3	1.70±0.94	0.02±0.11	2.01±0.92	3.37±1.47	0.00±0.00
PTV≥ 100 cm^3	3D-CRT	1.22±1.33	0.85±1.75	4.28±4.48	15.9±12.4	17.9±20.5	0.54±0.89	0.00±0.00	1.01±2.11	1.95±3.52	7.0±19.4
	IMRT	3.84±2.28	1.19±2.51	4.61±2.09	10.4±6.0	12.8±18.8	2.01±1.19	0.00±0.00	2.47±1.02	4.43±0.62	0.00±0.00
	VMAT	3.54±2.05	0.71±1.72	5.18±2.70	10.2±4.8	19.0±23.7	2.08±1.22	0.00±0.00	2.12±0.70	3.54±0.97	0.00±0.00
d< 2.5 cm	3D-CRT	1.17±1.43	0.79±1.54	3.48±4.26	13.6±14.9	14.4±19.9	1.36±2.40	0.00±0.00	2.22±2.74	4.82±5.43	16.8±23.9
	3D-CRT+e	1.28±1.09	0.80±1.35	4.80±3.43	17.5±13.5	16.8±18.9	1.20±1.66	0.00±0.01	1.52±1.84	3.25±3.61	0.35±1.23
	IMRT	3.52±2.95	1.68±2.79	4.60±2.52	12.5±6.9	17.4±20.7	2.21±1.29	0.01±0.03	1.80±1.17	4.47±0.92	0.00±0.00
	IMRT+e	2.85±2.12	1.09±1.64	5.67±2.68	16.8±9.0	30.4±19.6	1.77±1.09	0.00±0.01	1.24±0.80	3.03±0.64	0.00±0.00
	VMAT	3.20±2.58	1.02±1.76	5.05±2.88	11.0±5.6	21.6±24.3	2.58±1.50	0.05±0.16	2.54±1.11	4.08±1.72	0.00±0.00
	VMAT+e	2.63±1.91	0.81±1.24	5.86±2.89	15.9±8.6	31.8±21.2	2.02±1.21	0.04±0.10	1.74±0.76	2.78±1.16	0.00±0.00

Table 3A Partial breast irradiation according to the radiotherapy technique used: Dose to the organs at risk according to the side of the radiotherapy

(3D-CRT=3-dimensional conformal radiotherapy, d=distance of the centre of the PTV from the body surface, Dmax=maximum dose, e=electron beam added, IMRT=intensity-modulated radiotherapy, LAD=left anterior descending coronary artery, SD=standard deviation, PTV=planning target volume, VMAT=volumetric-modulated arc radiotherapy, Vx%=relative volume of the structure receiving x% of the prescribed dose)

	Technique	H (mean±SD)	M (mean±SD)	P (mean±SD)	PQI (mean±SD)
All cases	3D-CRT	0.598±0.067	0.768±0.069	0.654±0.160	0.595±0.127
	IMRT	0.857±0.087	0.902±0.032	0.544±0.131	0.497±0.126
	VMAT	0.922±0.035	0.868±0.054	0.571±0.128	0.461±0.125
PTV< 100 cm^3	3D-CRT	0.602±0.064	0.771±0.068	0.663±0.177	0.588±0.137
	IMRT	0.836±0.098	0.901±0.035	0.591±0.120	0.464±0.115
	VMAT	0.923±0.039	0.865±0.062	0.613±0.117	0.424±0.113
PTV≥ 100 cm^3	3D-CRT	0.594±0.070	0.765±0.070	0.647±0.145	0.601±0.119
	IMRT	0.876±0.072	0.903±0.030	0.505±0.127	0.524±0.129
	VMAT	0.921±0.033	0.871±0.046	0.535±0.126	0.492±0.128
d< 2.5 cm	3D-CRT	0.604±0.071	0.753±0.059	0.651±0.223	0.607±0.169
	3D-CRT+e	0.799±0.082	0.704±0.072	0.673±0.155	0.505±0.120
	IMRT	0.811±0.089	0.882±0.040	0.576±0.154	0.495±0.133
	IMRT+e	0.870±0.069	0.789±0.059	0.611±0.134	0.475±0.113
	VMAT	0.893±0.042	0.824±0.065	0.568±0.167	0.490±0.149
	VMAT+e	0.916±0.048	0.778±0.059	0.611±0.136	0.467±0.118

Table 4 The (H)ealthy tissue conformity, the (M)erit function, the (P)enalty function and the Plan Quality Index (PQI) according to technique

3D-CRT=3-dimensional conformal radiotherapy, d=distance of the centre of the PTV from the body surface, e=electron beam added, IMRT=intensity-modulated radiotherapy, PTV=planning target volume, SD=standard deviation, VMAT=volumetric-modulated arc radiotherapy

		Radiotherapy technique [n (%)]				Radiotherapy technique [n (%)]		
		IMRT better	**Equiva-lent**	**VMAT better**		**IMRT better**	**Equiva-lent**	**VMAT better**
Quadrant	**Lateral**	4 (28.6%)	44 (63.8%)	36 (65.5%)	**Lower**	0 (0%)	21 (30.4%)	12 (21.8%)
	Medial/ central	10 (71.4%)	25 (36.2%)	19 (34.5%)	**Upper**	14 (100%)	48 (69.6%)	43 (78.2%)

Table 5 The more advantageous radiotherapy technique in relation to the location of the target volume

IMRT = intensity-modulated radiotherapy, VMAT = volumetric-modulated arc radiotherapy

	Mean ± SD of PQI	**PQID**	**95% Confidence interval for PQID**	**p**
IMRT	0.495 ± 0.025	0.020	0.000-0.039	0.055
IMRT + electron	0.475 ± 0.021			
VMAT	0.490 ± 0.028	0.023	0.002-0.045	0.037
VMAT + electron	0.467 ± 0.022			
3D-CRT	0.607 ± 0.031	0.102	0.070-0.133	<0.001
3D-CRT + electron	0.505 ± 0.022			

Table 6 Mean differences of PQI values regarding the effect of adding an ‘en face’ electron beam to photon beams using IMRT, VMAT and 3D-CRT techniques

3D-CRT=3-dimensional conformal radiotherapy, IMRT=intensity-modulated radiotherapy, PQI=plan quality index, PQID=difference of PQIs, VMAT=volumetric-modulated arc radiotherapy